3-10-2010

Disturbance Observer: Design and Flight Test of a Large Envelope Flight Controller

Donevan A. Rein

DISTURBANCE OBSERVER: DESIGN AND FLIGHT TEST OF A LARGE ENVELOPE FLIGHT CONTROLLER

THESIS

Donevan A. Rein, Major, USAF

AFIT/GAE/ENY/10-M18

DEPARTMENT OF THE AIR FORCE
AIR UNIVERSITY

AIR FORCE INSTITUTE OF TECHNOLOGY

Wright-Patterson Air Force Base, Ohio

AFIT/GAE/ENY/10-M18

DISTURBANCE OBSERVER: DESIGN AND FLIGHT TEST OF A LARGE ENVELOPE FLIGHT CONTROLLER

THESIS

Presented to the Faculty

Department of Aeronautics and Astronautics

Graduate School of Engineering and Management

Air Force Institute of Technology

Air University

Air Education and Training Command

In Partial Fulfillment of the Requirements for the

Degree of Master of Science in Aeronautical Engineering

Donevan A. Rein, BS

Major, USAF

March 2010

AFIT/GAE/ ENY/10-M18

DISTURBANCE OBSERVER: DESIGN AND FLIGHT TEST OF A LARGE ENVELOPE FLIGHT CONTROLLER

Donevan A. Rein, BS

Major, USAF

Approved:

_____//SIGNED//_____	3 March 2010
Paul A. Blue, Lt Col, USAF (Co-Chairman)	Date
_____//SIGNED//_____	3 March 2010
Donald L. Kunz, (Co-Chairman)	Date
_____//SIGNED//_____	3 March 2010
Timothy R. Jorris, Lt Col, USAF (Member)	Date
_____//SIGNED//_____	3 March 2010
Bradley S. Liebst (Member)	Date

AFIT/GAE/ ENY/10-M18

Abstract

A new flight controller was evaluated through piloted simulation and flight test conducted at the USAF Test Pilot School. The controller, commonly called a disturbance observer, uses inertial sensor feedback routed through a simple control architecture that acts to force the desired response while rejecting sensor noise and atmospheric disturbances. The investigation included both handling qualities testing in the Octonian simulator at the Air Force Research Laboratories Air Vehicle Directorate, and initial flight test conducted as part of a Test Management Project at the USAF TPS.

Simulation produced positive results with desired performance throughout a wide flight envelope. In addition, the desired response of the aircraft was easily modified by changing variables within the controller.

Flight test was conducted on the Variable-stability In-flight Simulator and Test Aircraft (VISTA). Twelve test sorties totaling 16.4 flight hours were conducted and culminated in multiple landings at Edwards AFB, CA. Time delay inherent in the VISTA resulted in the requirement to gain down the control surface command signal. Sensor noise was amplified and caused a control surface 'buzz." Flying qualities exhibited lower damping and frequency than 'desired' yet were consistent throughout a larger flight envelope. Post flight analysis resulted in the determination of ways to reduce the noise causing the 'buzz' and improve the flying qualities by adjusting the controller's 'desired dynamics.'

To my amazing wife and children

for their endless support and encouragement!

Acknowledgments

I would like to thank my thesis co-advisor Lt Col Paul Blue for the technical guidance and support provided despite having moved to a new job prior to me taking on this project. His professionalism and dedication to research and knowledge is unmatched and greatly appreciated.

I would also like to thank my academic and thesis co-advisor Dr. Donald Kunz for providing me the latitude to change directions midcourse and pursue a topic that I found interesting and useful.

This project would not have made it off the ground without the technical expertise and dedication of Mr. Jay Kemper of the Calspan Corporation. His efforts were critical in allowing the project to move forward to flight test.

The folks that run the Simulation Branch, Air Vehicles Directorate, Air Force Research Laboratories provided hours of support in setting up and running simulation tests in the Octonian simulator. Special thanks to Jeff Slutz, Brian Birkmire, Amy Burns, Mike Coy, and Deryck Beard.

Finally, to my TMP team, Major Jeff Kennedy, Major Shlomi Lachs, and Captain Derek Dwyer who's efforts made project Have MURDOC a complete success in meeting all test objectives.

Donevan A. Rein

Table of Contents

Page

List of Figures

Page

Page

Page

Page

List of Tables

Page

DISTURBANCE OBSERVER: DESIGN AND FLIGHT TEST OF A LARGE ENVELOPE FLIGHT CONTROLLER

I. Introduction

Motivation

Most modern aircraft employ complex flight control systems to produce seamless and consistent flying and handling qualities throughout a large flight envelope. Designing these flight control systems is difficult and tedious. It involves designing compensators that optimize performance and handling around several points throughout the flight envelope then meshing those points through the use of a gain schedule. Gain scheduling is highly dependent on the accurate measurement of aircraft states including velocity, altitude, temperature, and angle of attack. When air data system failures occur, the ability to properly gain schedule degrades and handling qualities can significantly suffer. This is a potentially fatal problem as witnessed when, in 2008, the United States Air Force lost a B-2 Stealth Bomber and nearly lost the crew upon initial takeoff due to an air data system malfunction.

Problem Statement

The purpose of this effort is to continue the research of a new and relatively simple method for flight control commonly known as a disturbance observer. Conclusions are drawn as to its potential for use in future aircraft. The controller uses aircraft inertial rate sensor feedback to generate control surface commands that produce desired flying qualities throughout a large flight envelope. The goal of this work is to

validate the controller theory by conducting simulation and flight test to assess the feasibility for use in future aircraft.

Research Objectives

The disturbance observer that is the focus of this effort was originally developed by Lt Col Paul Blue and consisted of a pitch-axis only design [Blue et al, 2002]. Research continued with the design of the lateral and directional axes by Maj Matthew Coldsnow [Coldsnow, 2009]. The overall objective of this effort is to validate disturbance observer theory through piloted simulation and flight test. Along the way, improvements are made to the lateral and directional axes designs. In addition, conclusions and recommendations are made for future research and controller potential.

Improve the Lateral and Direction Axes Disturbance Observer

While the pitch axis disturbance observer was designed using robust control theory and practice, the lateral and directional axes proved more difficult to design. For one, the pitch axis is approximated by a second order response that can be de-coupled from the other aircraft axes. The lateral axis, on the other hand, is approximated by a first order response and is coupled to the directional axis. The directional axis dutch roll mode is approximated as second order and is highly coupled to the lateral axis. Initial attempts at applying a disturbance observer to the lateral and directional axes met with some success; however, simulation resulted in marginal performance when compared to the pitch axis [Coldsnow, 2009]. This effort improves the lateral and directional designs and validates performance claims through simulation and flight testing.

Piloted Simulation and Handling Qualities

The three axis disturbance observer will be evaluated during piloted simulation to validate handling qualities performance and compare results to those obtained using an F-16 simulator.

Flight Test

The pitch axis disturbance observer will be evaluated using the Variable stability In-flight Simulator and Test Aircraft (VISTA) at the United States Air Force Test Pilot School. The goal of flight test is to validate that the disturbance observer can be used to generate controlled flight with favorable handling qualities. Thus, controller performance will be determined and handling qualities assessed.

Approach

This effort began by understanding the current state of disturbance observer design and determining areas of improvement. The pitch axis design was well established and assumed adequate for simulation and flight evaluation. The lateral and directional axes, though designed using the same techniques as the pitch axis, provided less consistent performance and room for improvement existed [Coldsnow, 2009].

Once the three axis controller design was established, piloted simulation was conducted to validate controller theory by assessing pilot performance and generating handling qualities ratings. Ratings and performance were compared to results generated with a Block 40 F-16 model using the same flying tasks. The Block 40 F-16 model was the same model used by operational F-16 pilots during simulator training and was treated as the 'experimental control' for the purposes of the study.

The final step in evaluating the disturbance observer was to implement the controller on an aircraft and conduct flight test to validate controller theory. Programmable test inputs (PTI) designed to generate clean response data were conducted allowing comparison of flight results to simulation predictions. In addition, handling qualities evaluations were conducted and compared to predictions based on the programmable test input results.

Preview of Results and Implications

Simulation and flight test results clearly demonstrate potential for disturbance observer use on future aircraft. Flight test culminated in the disturbance observer controlling the VISTA to several successful runway touchdowns. Testing produced issues observed during flight, however, that generated room for improvement and future areas for research are discussed.

Lateral and directional design improvements were made and consistent performance was generated throughout the simulation flight envelope. Piloted simulation verified controller theory by producing predicted and consistent performance throughout the flight envelope. Pilots produced better task performance and pilot ratings using the disturbance observer controlled F-16 than the default Block 40 F-16. Simulation limitations, however, were noted and discussed.

Flight test was ultimately successful as the disturbance observer controlled the pitch axis of the VISTA during twelve test sorties that included PTIs, aerobatics, formation flight, and landings. Implementation of the disturbance observer on the VISTA led to the first lesson learned due to an issue that wasn't modeled during

disturbance observer design. A time delay inherent in the VISTA implementation resulted in the requirement to apply a command signal gain to prevent instabilities. The change was implemented in a simple manner and simulation resulted in slightly reduced performance. The reduced performance translated to flight test, and damping ratios were consistently lower than predicted. This led to diminished, yet acceptable, handling qualities.

Flight test also resulted in a high frequency elevator actuator 'buzz' that was due to an amplified sensor noise signal. Noise amplification was reproduced when applying sensor noise to simulation and a preliminary investigation into solving the noise problem is discussed.

Conclusions generated from this research show the disturbance observer has potential for use in aircraft. First, since the controller uses only rate sensor feedback to generate control inputs, it could be used as a backup control method in the case of air data computer failure or malfunction. In addition, for designers of stealth aircraft, the disturbance observer could be the primary control method allowing for reduced radar cross-section by removing the pitot-static probes and ports. Finally, the disturbance observer, in its current state, is capable of providing educational value when used as a flying qualities demonstrator in simulation or on a variable stability aircraft such as the VISTA or Calspan Corporation's variable stability Learjet. The USAF Test Pilot School (TPS) curriculum currently dedicates a large portion of time demonstrating the effects of different flying qualities on aircraft handling. The disturbance observer allows the user to easily change the aircraft flying qualities by adjusting the desired short period response and would be a valuable addition to the TPS curriculum.

Thesis Overview

This thesis presents the theory, design, piloted simulation results and flight test results of the disturbance observer flight controller. Chapter 2 discusses the disturbance observer theory as well as provides a background into feedback flight control systems and handling qualities testing and ratings. The theories and concepts discussed are applied to the specific disturbance observer design and presented in Chapter 3. Chapters 4 and 5 presents piloted simulation and flight test methodology and results respectively. Conclusions and future research directions and applications are discussed in Chapter 6.

II. Background

Chapter Overview

The purpose of this chapter is to build a foundation of the basic theory behind an aircraft's modes of motion and how feedback flight control systems, specifically the disturbance observer, are used to augment and enhance their dynamics. The chapter discusses key terms pertaining to the theory as well as presents discussion of pilot ratings scales.

Aircraft Modes of motion

The aircraft modes of motion of interest for this thesis can be modeled by a second order differential equation. The properties of a second order differential equation can be illustrated by examining the motion of a mechanical system composed of a mass, a spring, and a damping device [Nelson, 1998]. Figure 1 represents the system with forces acting on it.

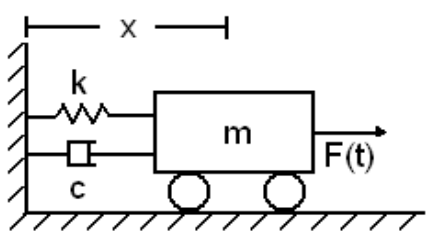

Figure 1: Mass Spring Damper System

The differential equation for the system can be written as

$$m\ddot{x} + c\dot{x} + kx = F(t) \tag{1}$$

or:

$$\ddot{x} + \frac{c}{m}\dot{x} + \frac{k}{m}x = \frac{1}{m}F(t) \tag{2}$$

The constant coefficients are the spring stiffness (k), damping constant (c), and the mass (m). They are defined by the physical characteristics of the system. If the forcing function, $F(t)$, is zero, then the rest of the equation represents the free response of the system [Nelson, 1998]. When we look at only the free response of the system and attempt to find the solution to the differential equation with constant coefficients, we let $x = Ae^{\lambda t}$. The characteristic equation becomes:

$$\lambda^2 + \frac{c}{m}\lambda + \frac{k}{m} = 0 \tag{3}$$

The roots, or eigenvalues of the system are then:

$$\lambda_{1,2} = -\frac{c}{2m} \pm \sqrt{\left(\frac{c}{2m}\right)^2 - \frac{k}{m}} \tag{4}$$

The solution of the differential equation is now:

$$x(t) = C_1 e^{\lambda_1 t} + C_2 e^{\lambda_2 t} \tag{5}$$

where C_1 and C_2 are constants determined from the initial conditions of the system [Nelson, 1998]. There are three cases that exist for a stable system response and are dependent on the eigenvalues which in turn are dependent on the physical properties of

the system. For the stable system the roots are negative and can be either real (overdamped response), imaginary (oscillatory response), or equal and real (critically damped response). For the critically damped case, when solving for the damping constant, you can define the critical damping constant as:

$$c_{cr} = 2\sqrt{km} \tag{6}$$

With the oscillatory case, the damping constant can be defined in terms of the critical damping constant.

$$c = \zeta c_{cr} \tag{7}$$

Where ζ is called the damping ratio.

$$\zeta = \frac{c}{c_{cr}} \tag{8}$$

For an undamped system where $c = 0$ and $\zeta = 0$, the frequency at which the system oscillates is called the undamped natural frequency and when referring to our system is defined as:

$$\omega_n = \sqrt{\frac{k}{m}} \tag{9}$$

The characteristic equation 3 can now be written in terms of ζ and ω_n and is known as the standard form of a second-order differential equation [Nelson, 1998].

$$\lambda^2 + 2\zeta\omega_n\lambda + \omega_n^2 = 0 \tag{10}$$

Though equation 10 was derived using a mass-spring-damper system, it can be applied to any number of systems, including aircraft.

An aircraft's equations of motion are highly complex and non-linear, however, simplifications can be made that allow us to treat the most common modes of motion as a second order response that can be analyzed using the characteristic equation 10 above. For instance, the initial response of an aircraft to a pitch disturbance or command is known as the 'short period' and is approximated by the second order differential equation with frequency ω_n and damping ratio ζ. The initial aircraft response (first few seconds) to a pure directional axis disturbance or command can also be approximated and described as second order with frequency and damping. The directional axis short period equivalent mode is commonly known as the 'dutch roll.'

Previous discussion focused on the second order differential equation and its relationship to pure pitch and yaw modes of motion. The lateral, or roll axis, however, is characterized by a first order response defined not by damping and frequency but rather a time constant (T) that represents how quickly a steady state roll rate is reached. T is essentially the inverse of the roll damping derivative of the aircraft and is a small number if the aircraft has a rapid roll response.

Flying Qualities

"The flying qualities of an air vehicle are defined as the stability and control characteristics that have an important bearing on the safety of flight and on the pilots' impressions of the ease of flying the air vehicle in steady flight and in maneuvers [DoD, 2006]." Stability and control is directly related to the frequency and damping

characteristics previously discussed and in turn are related to the aircraft's physical characteristics. Historical simulation and flight test data have led to the development of flying qualities specifications defined in the MIL-STD-1797B, *Flying Qualities of Piloted Aircraft*. The DoD standard defines aircraft classifications (Class I thru IV) and flight phase categories (Category A thru C) to acknowledge the handling requirement differences between aircraft and mission types. For instance, good flying qualities associated with heavy transport aircraft during long range cruise flight is dramatically different than those associated with a high performance dog-fight.

Flying qualities are specified in terms of the three levels below[DoD, 2006].

- **Level 1:** Satisfactory - Flying qualities clearly adequate for the mission Flight Phase. Desired performance is achievable with no more than minimal pilot compensation.

- **Level 2:** Tolerable - Flying qualities adequate to accomplish the mission Flight Phase, but some increase in pilot workload or degradation in mission effectiveness, or both, exists.

- **Level 3:** Controllable - Flying qualities such that the air vehicle can be controlled in the context of the mission Flight Phase, even though pilot workload is excessive or mission effectiveness is inadequate, or both. The pilot can transition from Category A Flight Phase tasks to Category B or C Flight Phases, and Category B and C Flight Phase tasks can be completed.

The goal of aircraft designers is to produce aircraft flying qualities that meet level 1 specifications. If the aircraft meets level 1 specifications, then the aircraft will most likely receive good pilot opinion ratings.

Handling Qualities

Flying qualities refer to the characteristics of the aircraft's stability and control with the pilot out of the control loop. Handling qualities, however, refer to the combined pilot plus aircraft handling. The MIL-STD-1797B define handling qualities as "Those qualities or characteristics of an air vehicle that govern the ease and precision with which a pilot is able to perform the tasks required in support of the air vehicle's role [DoD, 2006]." It is important to note that the handling qualities are related to the pilot's ability to perform a specific "role" or mission. The flying qualities of an aircraft can be predicted through modeling and wind tunnel testing, however, the handling qualities can be much more difficult to predict. This is primarily due to the inability to fully understand and model pilot behavior. Therefore, in order to determine an aircraft's handling qualities, one is forced to rely on the subjective nature of pilot opinion. Unfortunately, pilot opinion can be widely varied based on countless factors. In addition, to generate useful handling qualities data, the aircraft must already be built and flying, a point in development at which deficiencies are expensive to correct.

Handling Qualities Ratings Scales

Handling qualities data are critical in determining an aircraft's ability to, when combined with the pilot, perform the mission. Handling qualities data consists primarily of pilot comments and ratings. The two most common ratings scales used during handling qualities evaluations are the Cooper-Harper (CH) rating scale (Figure 2) and the Pilot-in-the-Loop Oscillation (PIO) rating scale (Figure 3).

Cooper-Harper Rating Scale

The Cooper-Harper rating scale is widely accepted in the flight test community and is used by pilots to assign a number to an aircraft's handling during a defined task. Assigning a number allows a measure of standardization and comparison. The MIL-STD-1797B, in fact, models flying qualities specifications after the levels of the Cooper-Harper rating scale, where a CH rating of 1-3 typically corresponds to an aircraft with level 1 flying qualities [DoD, 2006]. A version of the scale is depicted below.

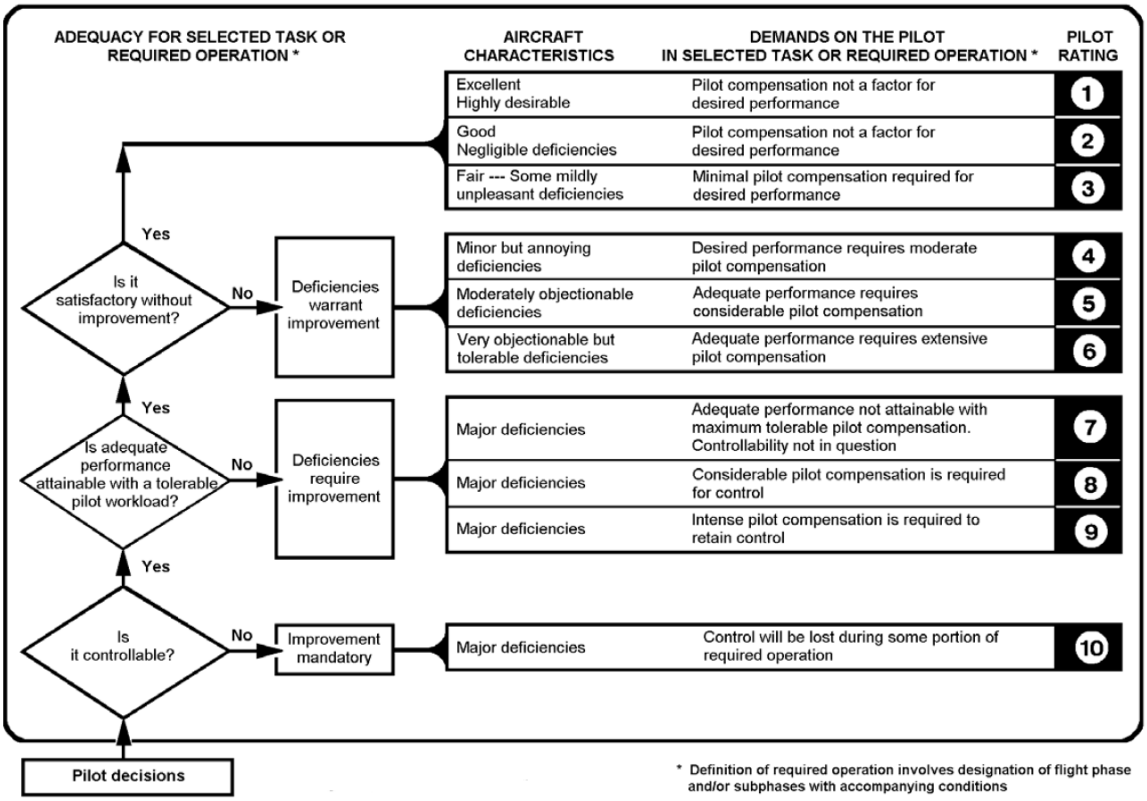

Figure 2: Cooper-Harper Rating Scale [Cooper and Harper, 1989]

To assign a CH rating, the pilot works through the decision tree while assessing task performance and pilot workload. There are many techniques on how to implement the CH scale, however, the intent is to standardize ratings as a measure of comparison.

Difficulties lie in designing tasks and assigning performance criteria that allow for a good evaluation. For instance, if the task doesn't allow for adequate performance regardless of the workload, then an otherwise level 1 or 2 aircraft will be assigned a level 3 rating. Like all subjective ratings scales, the CH rating scale has its flaws, however, its widespread use makes it the current standard for evaluating aircraft handling qualities.

Pilot-in-the-Loop Oscillation Rating Scale

The Pilot-in-the-Loop Oscillation rating scale is another tool used during handling qualities evaluations that allows pilots to assign numerical ratings to an aircraft's tendency to produce unwanted motion when controlled by the pilot. PIO is a situation where the pilot's control inputs are out of phase with the natural oscillations of the airplane and act to add to the oscillation rather than correct it [Nelson, 1998]. "Pilot-in-the-loop oscillations are associated with abrupt maneuvers and precise tracking… aggressive pilot control action will tend to bring on any PIO tendency [DoD, 2006]." There are many factors known to make aircraft prone to PIO. A few of the most common factors include time delay, control stick sensitivity, and nonlinearities such as dead band, rate limiting, and hysteresis. The PIO rating scale below is used, like the CH rating scale, to attempt to quantify the handling qualities of aircraft.

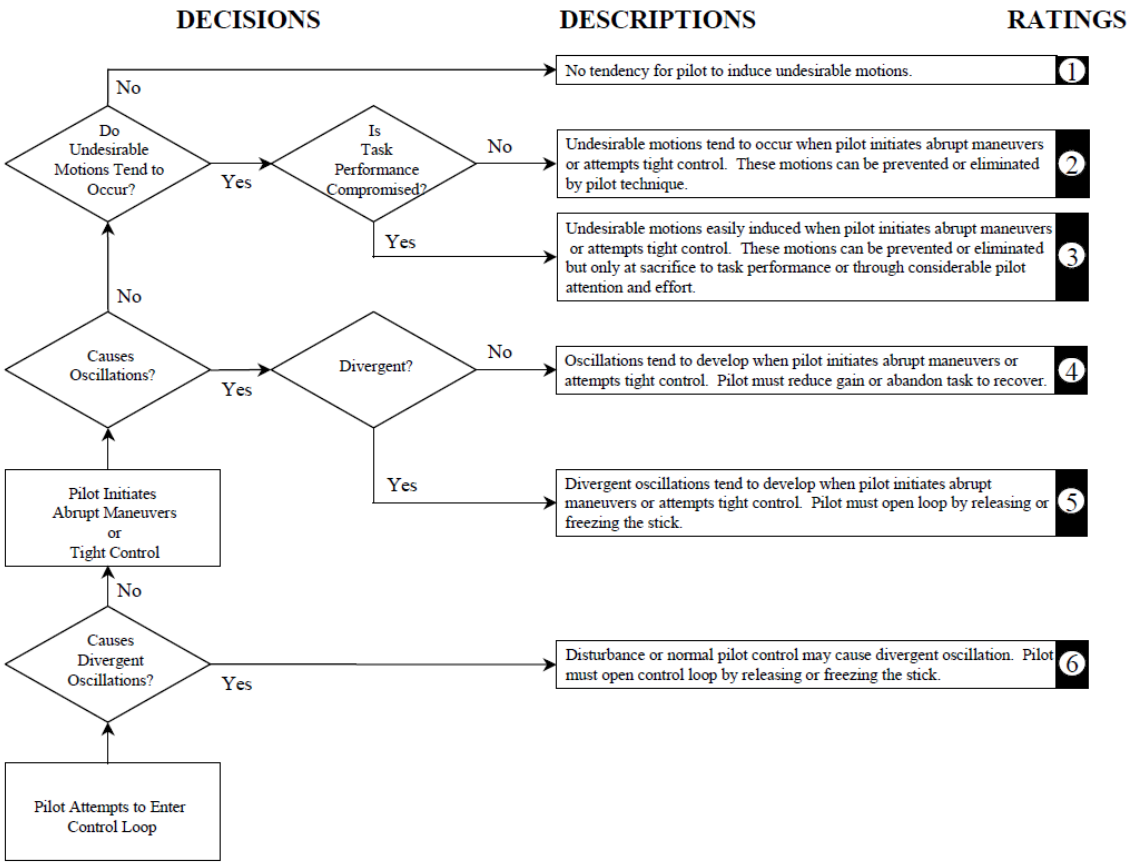

Figure 3: Pilot-in-the-loop Oscillation Rating Scale

Like the CH rating scale, the pilot performs a task, and then follows the PIO scale decision tree to arrive at a numerical rating.

When evaluating an aircraft's handling qualities, the CH and PIO rating scales, in conjunction with pilot comments and opinion serve to provide aircraft designers valuable information.

Augmented Flight Control

"Today, both military and civilian aircraft rely heavily on automatic control systems to provide artificial stabilization [Nelson, 1998]." Such is the case with the F-16 Fighting Falcon from which the flight control system not only stabilizes the bare airframe

dynamics, but additionally provides control that attempts to optimize maneuver performance. The following sub-sections discuss aircraft stability and how feedback control works to augment or stabilize aircraft in order to produce desired flying qualities and performance.

Aircraft Stability

Aircraft stability can be defined as the tendency to return to equilibrium following a disturbance [Nelson, 1998]. Equilibrium, also known in flight as the 'trim' condition, is achieved when the forces and moments on the aircraft equate to zero. The initial response of the aircraft following a disturbance, whether from the atmosphere or pilot control input, is referred to as 'static' stability and pictorially described in the figure below.

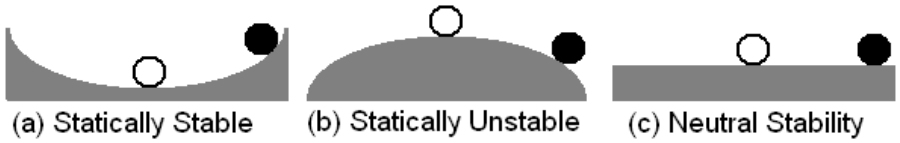

Figure 4: Static Stability

An aircraft's initial tendency following a disturbance can be either 'statically stable,' 'statically unstable,' or 'neutrally stable.' Static stability occurs when the forces and moments work to return the aircraft towards the trim condition as is the case with a ball in a bowl that has been disturbed from the center position (a). Static instability occurs when the forces and moments work to accelerate the aircraft motion away from the equilibrium point as is the case with a ball that has been disturbed from a balanced point on top of a curved surface (b). Neutral stability occurs when no forces or moments exist

to either return the disturbed aircraft to trim or accelerate it away from trim. Such is the case with the ball on a flat surface that has been disturbed from an equilibrium point (c).

Dynamic stability is "concerned with the time history of the motion of the vehicle after it is disturbed from its equilibrium point [Nelson, 1998]." The long term motion can be either oscillatory or non-oscillatory and can converge towards an equilibrium (damped), oscillate indefinitely (un-damped), or diverge with or without oscillations (divergent). Of note, an aircraft can be statically stable, yet dynamically unstable, however, a dynamically stable aircraft must be statically stable.

An aircraft's stability is governed by many factors including size, shape, weight distribution, aircraft length, wing and tail size and shape, flight condition, etc. In addition, high performance aircraft's stability characteristics can change drastically over the wide fight envelope as flight conditions change.

Flight Control and Stability Augmentation

Most modern aircraft require a form of stability augmentation and in some cases, control would be impossible without an automatic control system [Steven and Lewis, 2003]. While stability augmentation systems (SAS) are used to stabilize or damp unwanted aircraft motions, a control augmentation system (CAS) is used to enhance the handling qualities and performance of an aircraft. Stability and control augmentation is accomplished through the use of feedback. "Feedback is defined as returning to the input of a system a signal obtained from its output [Stevens and Lewis, 2003]. Both SAS and CAS use an aircraft's sensed states and feeds back a converted version of the signal(s) to the flight control input signal. While a SAS is used to provide suitable damping and frequencies to aircraft, a CAS is used to provide a particular type of response to a pilot's

control input [Stevens and Lewis, 2003]. The following figure presents a simplified version of a typical single loop feedback control architecture.

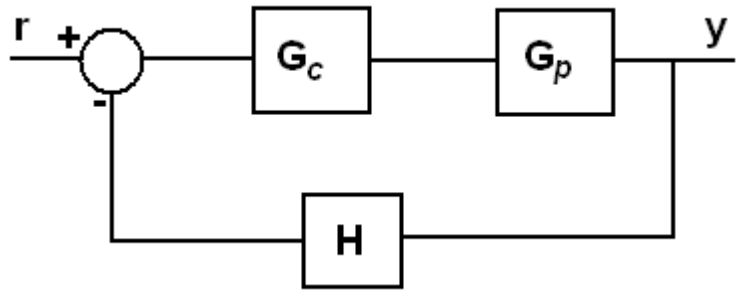

Figure 5: Typical Feedback Control Diagram

The blocks, H, G_c, and G_p represent the feedback compensation, feedforward compensation, and the system plant respectively. The input, r, to output, y, transfer function is represented by the equation:

$$\frac{y}{r} = \frac{G_c G_p}{1 + H G_c G_p} \tag{11}$$

The feedback signal(s) require compensation or gains due to control input command requirements that vary drastically as dynamic pressure on the aircraft changes. Design requires knowledge of the aircrafts stability derivatives for a given flight condition. If the stability derivatives of the aircraft are known, a variety of techniques can be used to design a SAS or CAS that provide the desired response.

Disturbance Observer

As stated earlier, the goal of automatic flight control systems and augmentation is to provide good handling qualities throughout a large flight envelope. Whether to

stabilize or dampen oscillations and disturbances with a SAS or to generate desired responses to inputs with a CAS, the goal is the same. One of the difficulties in designing flight control systems that produce good handling qualities is that aircraft dynamics change significantly over the entire flight envelope [Blue et al, 2002]. The disturbance observer (DO) is a controller that serves as both a SAS and a CAS by generating a desired response to a control input while damping out disturbances and attenuating noise. The DO uses a simple feedback architecture (Figure 6) and produces control inputs without the requirement to gain schedule.

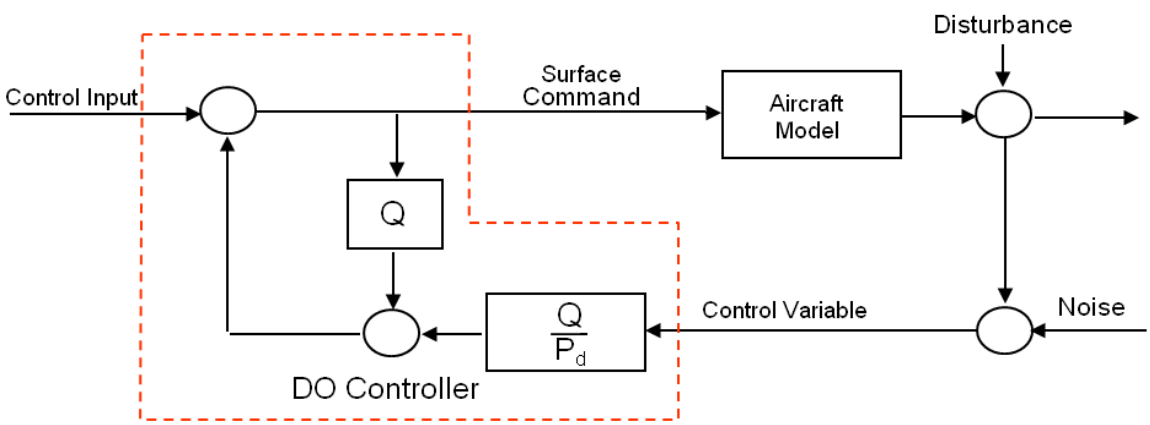

Figure 6: Disturbance Observer Architecture

The design filter (Q) is combined with the 'desired dynamics' filter (P_d) to generate the appropriate control input signal to force the aircraft to produce the desired response.

Analyzing the input-output transfer functions associated with the disturbance observer architecture gives us some insight into the form of Q [Blue et al, 2002]. The controller, when implemented, should provide good tracking and disturbance rejection at low frequencies, and noise rejection at high frequencies. The loop gain for the closed loop aircraft represented by Figure 6 is:

$$L(h,M) = \frac{Q}{1-Q}\frac{G(h,M)\cdot G_a}{P_d} \tag{12}$$

The model tracking transfer function H, disturbance rejection transfer function S, sensor noise rejection transfer function T, and performance error transfer function E are given by the following [Blue et al, 2002]:

$$H(h,M) \equiv \frac{q}{\delta_c} = \frac{P_d \cdot Model}{P_d \cdot (1-Q) + Model \cdot Q} \tag{13}$$

$$S(h,M) \equiv \frac{q}{d} = \frac{P_d \cdot (1-Q)}{P_d \cdot (1-Q) + Model \cdot Q} \tag{14}$$

$$T(h,M) \equiv \frac{-q}{n} = \frac{Model \cdot Q}{P_d \cdot (1-Q) + Model \cdot Q} \tag{15}$$

$$E(h,M) \equiv P_d - H(h,M) \tag{16}$$

where δ_c is the stick command, d is a disturbance, and n is noise. A study of these transfer functions shows that to meet the design objective we need to define Q as a low-pass, unity gain filter. By doing so, we are left with our desired dynamics, P_d, at low frequencies where $q/d_c \rightarrow P_d$ and $q/d \rightarrow 0$. High frequency noise is attenuated with $q/n \rightarrow 0$. The error transfer function E goes to zero at low frequencies providing the desired dynamics.

When referring to the DO control architecture, we see that for Q/P_d to be achievable, Q must be of the same form and order as P_d [Ackermann, 2002]. Therefore, the design filter will be of the form:

$$Q = \frac{\omega_Q^2}{s^2 + 2\zeta_Q \omega_Q s + \omega_Q^2} \tag{17}$$

leaving us with the design parameters, ζ_Q and ω_Q.

Now that the architecture and form of the design filter is known, we can proceed with the design of the disturbance observer controller parameters. Generating the controller involves setting a design objective (desired dynamics P_d), modeling the system, and then determining the controller variables in Q that allow you to meet the design objective.

Design Objective

The design objective is to generate good handling qualities throughout a large flight envelope. The DO architecture allows the designer to pick the filter, P_d, to represent the 'desired dynamics.' In picking P_d, the MIL-STD-1797B is referred to for flying qualities specifications that predict level 1 handling qualities. For a pitch-rate, q, feedback design, Table 1 in conjunction with Figure 7 list specifications for determining P_d.

Table 1: Pitch Rate Time Response Characteristics to a Step Input

Level	Effective Time Delay	Transient Peak Ratio	Effective Rise Time*	
			Flight Phase Categories A and B	Flight Phase Category C
1	$t_1 \leq .12$ sec	TPR $\leq .3$	$9/V_T \leq \Delta t \leq 500/V_T$	$9/V_T \leq \Delta t \leq 200/V_T$
2	$t_1 \leq .17$ sec	TPR $\leq .6$	$3.2/V_T \leq \Delta t \leq 1600/V_T$	$3.2/V_T \leq \Delta t \leq 645/V_T$
3	$t_1 \leq .21$ sec	TPR $\leq .85$		

*V_T is true airspeed in ft/sec

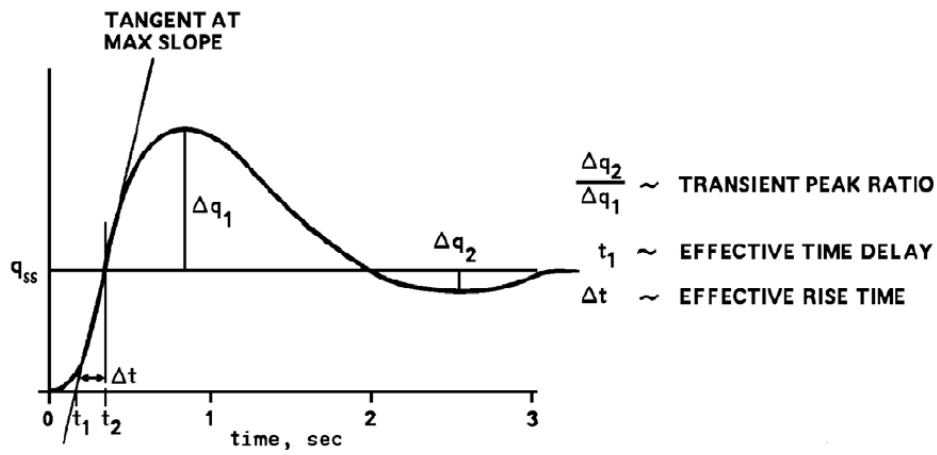

Figure 7: Pitch Rate Response to a Step Input

The standard form of the second-order differential equation allows the designer to pick ζ and ω_n that will, when a step input is applied, generates values that meet the level 1 specifications in Table 1. The desired dynamics for the system are now in the form of a second order differential equation and will be defined as:

$$P_d = \frac{\omega_{Pd}^2}{s^2 + 2\zeta_{p_d}\omega_{p_d}s + \omega_{Pd}^2} \tag{18}$$

Aircraft Model

Aircraft dynamics change significantly over a large flight envelope due to differences in flight condition. To model the pitch rate control dynamics, the short period approximation of the equations of motion at a specific flight condition are represented by:

$$\frac{d}{dt}\begin{bmatrix}\alpha \\ q\end{bmatrix} = \begin{bmatrix} Z_\alpha & 1 \\ M_\alpha & M_q \end{bmatrix}\begin{bmatrix}\alpha \\ q\end{bmatrix} + \begin{bmatrix} Z_{de} \\ M_{de}\end{bmatrix}\delta_{ed} \tag{19}$$

where α (deg) is the angle of attack, q (deg/sec) is the pitch rate, and δ_{ed} (deg) is the elevator deflection[Blue et al]. The dimensional coefficients for a given trimmed flight condition are represented by Z_α, M_α, M_q, Z_{de}, and M_{de} and can be expressed as functions of altitude, h, and Mach number, M. The short period approximation expressed as a function of h and M is:

$$G(h,M) = \frac{d}{dt}\begin{bmatrix}\alpha \\ q\end{bmatrix} = \begin{bmatrix} Z_\alpha(h,M) & 1 \\ M_\alpha(h,M) & M_q(h,M) \end{bmatrix}\begin{bmatrix}\alpha \\ q\end{bmatrix} + \begin{bmatrix} Z_{de}(h,M) \\ M_{de}(h,M)\end{bmatrix}\delta_{ed} \tag{20}$$

The aircraft's elevator actuator can be modeled by the first order approximation for actuator dynamics, G_a:

$$\delta_{ed} = G_a \delta_{ec} \tag{21}$$

$$G_a = \frac{-20.2}{s+20.2} \tag{22}$$

where δ_{ec} is the elevator command and δ_{ed} is the elevator deflection in degrees. [Blue et al, 2002].

The actuator model combined with the short period approximation as a function of altitude and Mach can be represented as:

$$Model = G(h, M) \cdot G_a \tag{23}$$

Modeling errors can be accounted for by applying an uncertainty factor to the model that represents the difference between the actual aircraft and the model. The uncertainty is frequency dependent. That is, modeling is more accurate at low frequencies and uncertainty goes up as frequencies increase [Ackermann, 2002]. The frequency dependant magnitude of the uncertainty factor is represented by W_u, also called the uncertainty weight. When applied to our aircraft model we have

$$Model_{Weighted} = G(h, M) \cdot G_a \cdot (1 + W_u \cdot \Delta) \tag{24}$$

where $||\Delta||_\infty \leq 1$.

In addition to a model uncertainty weight, a performance weight, W_p, and command weight, W_c, are applied based on guidance from the MIL-STD-1797B. The command and performance weights are applied to the model to account for the typical frequency ranges of pilot's commands and model matching respectively [Blue et al, 2002]. Adding the weighted uncertainties to the baseline model provides us with the following architecture that describes the entire model to be used when picking the controller variables in the design filter, Q.

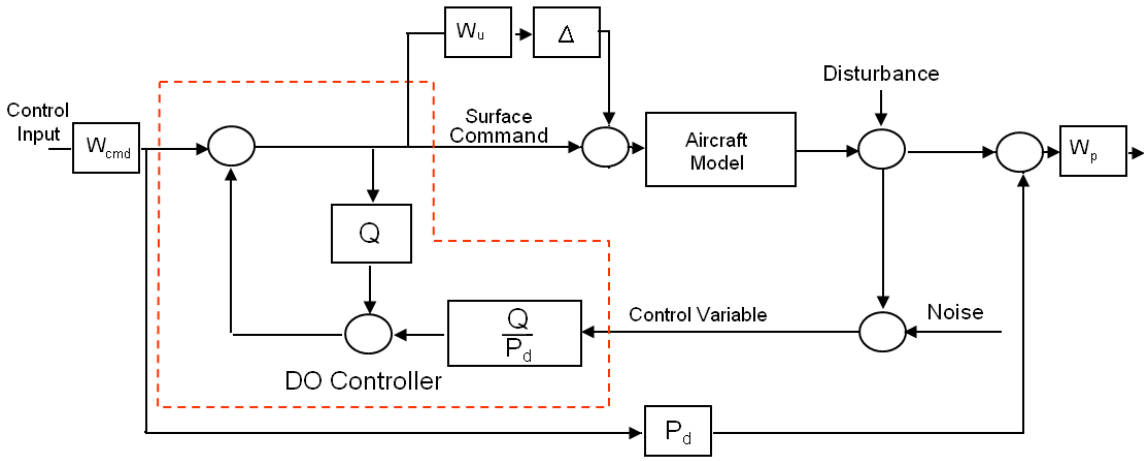

Figure 8: Weighted Disturbance Observer Model

Design Filter Q

The design objective is to produce desired handling throughout a large flight envelope. The desired dynamics represented by P_d are applied to the control architecture and combine with the design filter Q to produce the desired aircraft response. The aircraft dynamics have been modeled with uncertainties accounted for. All that is left is to choose the design filter, Q. Blue et al used H_∞ parameter space control design methods to pick Q that will provide robust stability and nominal performance throughout the design envelope. Using the weighted design model (Figure 8), the design parameters are mapped into a plane of feasibility that is bounded by conditions of performance and feasibility [Blue et al, 2002]. The closed loop characteristic equation of our weighted model is represented by:

$$p_{ce}(h, M, \omega_Q, \zeta_Q) \tag{25}$$

We ensure stability by only allowing values of ζ_Q and ω_Q where the roots of P_{ce} are in the left half of the complex plane, or:

$$roots\{p_{ce}(h, M, \omega_Q, \zeta_Q)\} \subset C^- \qquad \text{(Nominal Stability)} \qquad (26)$$

It is not enough to only ensure stability, however. We need to further bound the solution space by ensuring robust stability and performance. This is done by imposing the following conditions to our weighted model:

$$\left\| W_u \cdot T(h, W, \omega_Q, \zeta_Q) \right\|_\infty \leq 1 \qquad \text{(Robust Stability)} \qquad (27)$$

$$\left\| W_p \cdot E(h, W, \omega_Q, \zeta_Q) \cdot W_c \right\|_\infty \leq 1 \qquad \text{(Nominal Performance)} \qquad (28)$$

where robust stability includes the multiplicative affect of modeling uncertainties and nominal performance bounds the solution space by the frequency range specified in the command and performance weightings [Blue et al, 2002]. Values for ζ_Q and ω_Q that meet the three conditions of equations 26, 27, and 28 define the acceptable feasibility region for the design filter Q.

Summary

This chapter presented the concepts and theory behind disturbance observer design and the necessary tools in understanding how to generate and assess good flying and handling qualities. Chapter 3 continues with the specific design of the disturbance observer and how it was applied to the lateral and directional axes.

III. Methodology

Chapter Overview

This chapter presents the specific methods and preliminary analysis used in designing the three axis disturbance observer (DO). As stated earlier, the pitch axis DO was originally developed by Blue et al. Research was continued and the lateral and directional axes were added with marginal success [Coldsnow, 2009]. The methods of Blue and Coldsnow are presented and changes to the lateral and directional axes are discussed. In this chapter, the DO design method described in Chapter 2 was applied to a model of the Variable stability In-flight Simulator and Test Aircraft (VISTA) within the flight envelope encompassing 5,000 to 25,000 feet and 0.4 to 0.8 Mach.

Pitch Axis Design

The method described in chapter 2 was used by Blue et al to develop the pitch axis DO with a pitch rate feedback control variable. Recall that the form of the desired dynamics was represented by the second order transfer function:

$$P_d = \frac{\omega_{Pd}^2}{s^2 + 2\zeta_{p_d}\omega_{p_d}s + \omega_{Pd}^2}$$

with parameters ζ_{Pd} and ω_{Pd}. Using the MIL-STD-1797B specifications for pitch rate response to a step input, the parameters $\zeta_{Pd} = 0.5$ and $\omega_{Pd} = 4$ (rad/sec) were chosen to meet level 1 flying qualities. The resulting response to a step input is shown in Figure 9 below.

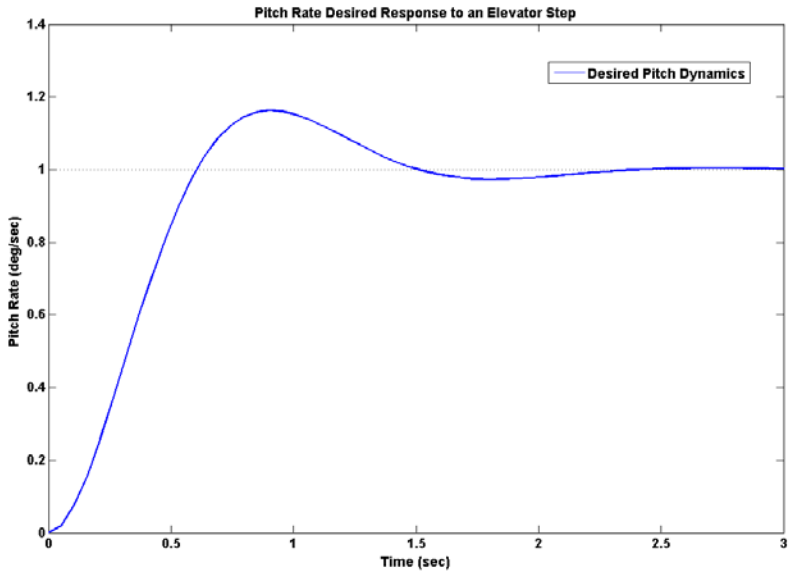

Figure 9: Desired Pitch Dynamics

Moving on to the design of the filter Q, it was necessary to choose appropriate values representing the modeling uncertainty weighting W_u, command weighting W_c, and performance weighting W_p. An uncertainty weighting of

$$W_u = 2 \cdot \frac{s + 0.2 \cdot 1256}{s + 2 \cdot 1256} \tag{29}$$

was chosen to represent 20% modeling error at low frequencies and 200% error at high frequencies. Again, the command and performance weightings were motivated by the MIL-STD-1797B and represent the typical frequency range of a pilot's commands and frequency range of desired model matching. The chosen values are as follows:

$$W_c = \frac{10}{s + 10} \tag{30}$$

$$W_p = 18 \cdot \frac{s}{(s+1)^2} \tag{31}$$

The H_∞ parameter space design techniques were used to map the feasibility range for values of ζ_Q and ω_Q that make the design filter Q. The values chosen by Blue et al that met the robust stability and nominal performance criteria are $\zeta_Q = 0.5$ and $\omega_Q = 26.5$ (rad/sec) [Blue et al, 2002].

With the pitch axis DO design complete, a non-linear simulation of a commanded step input was conducted on the Steven and Lewis F-16 model at the four corners of the design flight envelope [Stevens and Lewis, 1998]. First, the open loop response to the step reveals the effect of changes in dynamic pressure across the flight envelope and is shown in Figure 10.

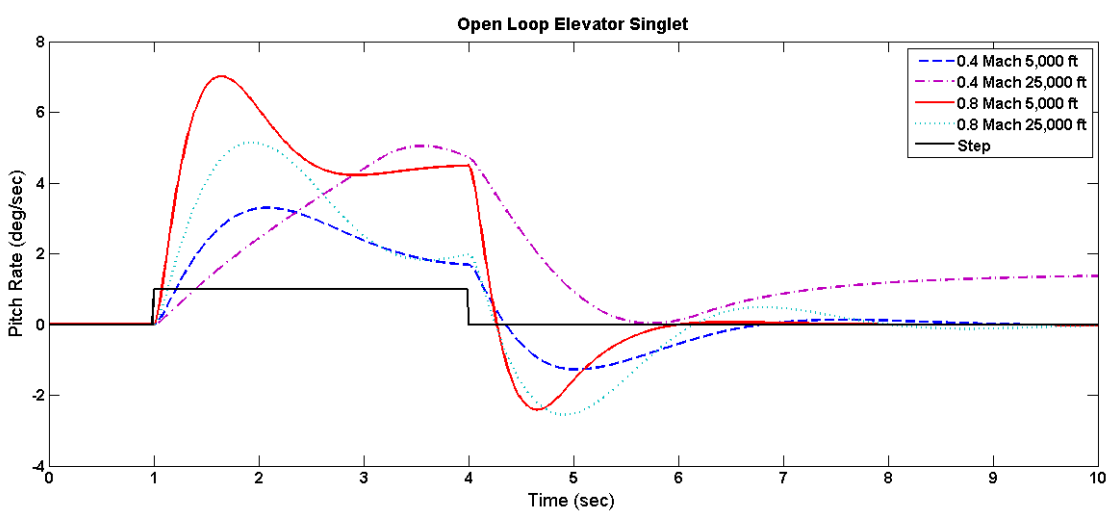

Figure 10: Open Loop Pitch Step Response

Next, the DO was applied to the model and the step response shows desired performance being achieved throughout the flight envelope with only minor differences at the extremely low dynamic pressure point of 0.4 Mach and 25,000 feet (Figure 11).

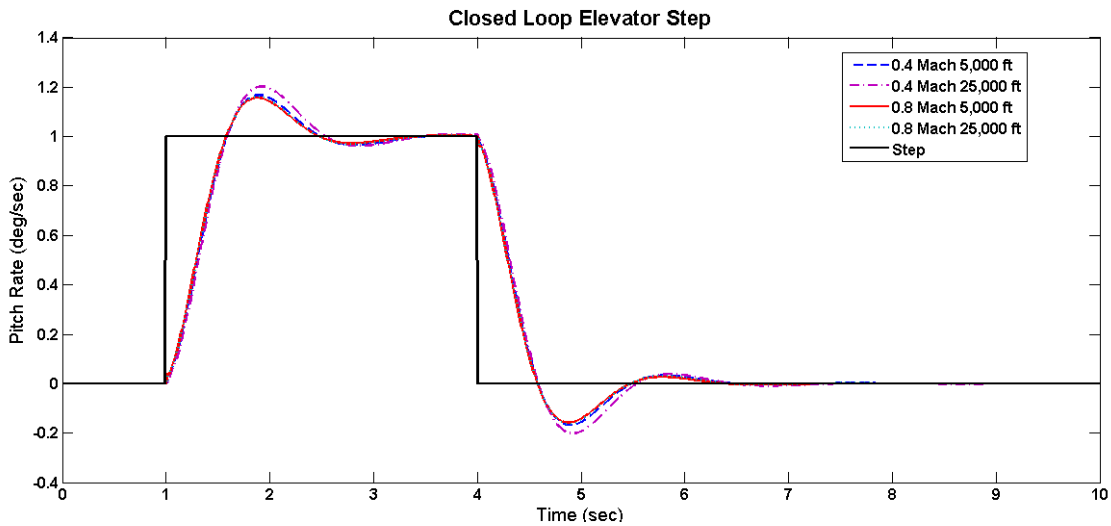

Figure 11: Closed Loop Pitch Step Response

The pitch axis DO, as design by Blue et al, was determined to be adequate for simulation and flight test, and no changes to the design were necessary in order to proceed.

Roll Axis Design

Research conducted by Coldsnow in conjunction with an investigation in alternate methods of gain scheduling led to the development of the lateral and directional axes DOs [Coldsnow, 2009]. To design the roll axis, Coldsnow first chose the command variable, p_s, which represents a roll about the aircraft's stability axis and is defined by:

$$p_s = p \cdot \cos(\alpha) + r \cdot \sin(\alpha) \tag{32}$$

where p is the body axis roll rate, r is the yaw rate, and α is the angle of attack. A roll about the stability axis is commonly used on high performance (fighter) aircraft, as rolling about the body axis at high alpha would generate excessive amounts of sideslip.

The roll rate to aileron command transfer function can be approximated as first order, desired roll dynamics can be expressed as:

$$p_{d\_roll} = k_{roll} \cdot \frac{1/T_{roll}}{s + 1/T_{roll}} \tag{33}$$

where k_{roll} is the gain associated with the roll desired dynamics, and T_{roll} is the roll mode time constant. The MIL-STD-1797B was used to choose a value of $T_{roll} = 0.8$ to produce the desired response for fighter-type aircraft. Next, the design filter Q_{roll} was chosen as a first order, low pass filter of the following form [Coldsnow, 2009]:

$$Q_{roll} = \frac{k_Q}{s + k_Q} \tag{34}$$

where k_Q was given the value $k_Q = 1$. The design was applied to the Stevens and Lewis F-16 model and full aileron deflection roll steps were conducted to choose a value for k_{roll} that provided predicted level 1 flying qualities. A value of $k_{roll} = 10$ was chosen based on meeting the specifications listed in Table 2, which was extracted from the MIL-STD-1797B [Coldsnow, 2009].

Table 2: MIL-STD-1797 Roll Performance Specifications

Level	Speed Range*	Time to Achieve the Stated Bank Angle Change (seconds)				
		Category A			Category B	Category C
		$\phi_t = 30°$	$\phi_t = 50°$	$\phi_t = 90°$	$\phi_t = 90°$	$\phi_t = 30°$
1	$V_{o_{min}} \leq V < V_{o_{min}} + 20$ kts	1.1			2.0	1.1
	$V_{o_{min}} + 20$ kts $\leq V <$ $1.4V_{o_{min}}$	1.1			1.7	1.1
	$1.4V_{o_{min}} \leq V < 0.7V_{o_{max}}$			1.3	1.7	1.1
	$0.7V_{o_{max}} \leq V \leq V_{o_{max}}$		1.1		1.7	1.1

Open and closed loop simulation was conducted in a similar manner to the pitch axis, resulting in the following two plots (Figure 12).

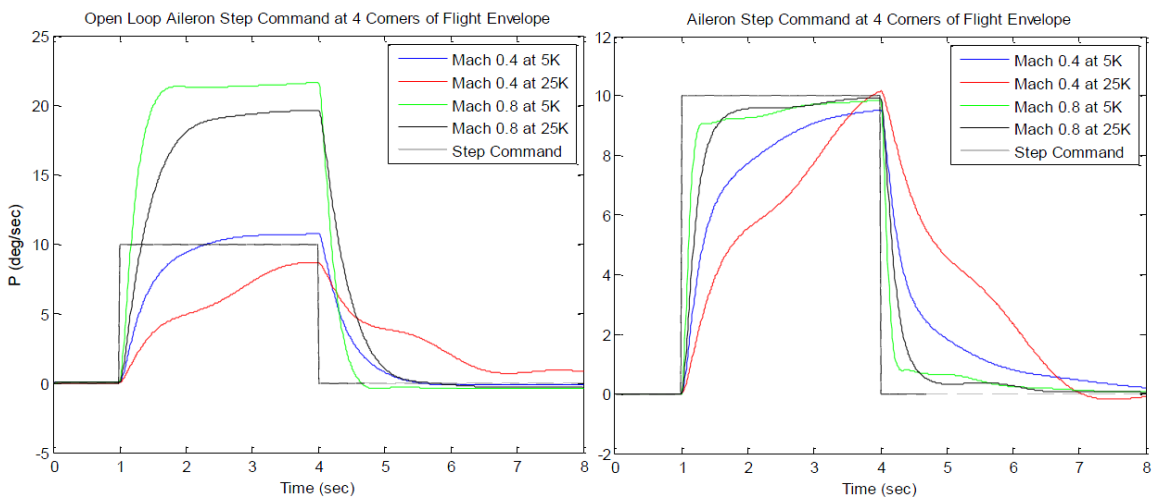

Figure 12: Open and Closed Loop Roll Step Response

The DO controlled results show an improvement over the open loop, however, the desired roll dynamics were not tracked consistently throughout the flight envelope and oscillations are evident which is not indicative of having good handling qualities.

The first step in improving the roll axis DO was to identify the limitations of the current design. It was noted that modeling the roll axis as having a first order response led to the one degree-of-freedom design. In addition, though a roll about the stability

axis is desired in fighter aircraft, it requires feedback of the sensed parameter, α. In keeping true to the goal of controlling flight throughout a large flight envelope without the use of 'air data,' the roll control variable was changed from p_s to p with the acknowledgment that a body axis roll is not ideal for fighter aircraft at high angles of attack.

To deal with the limited option design of the first order roll mode, it was determined that a second-order representation of the desired roll dynamics could be used, and an additional design variable would be available. To make a second order differential equation behave like the first order roll mode we choose a value for the damping ratio ζ that is greater than or equal to 1. The resultant response to a step input provides the following response that resembles the first order desired roll dynamics we were looking for.

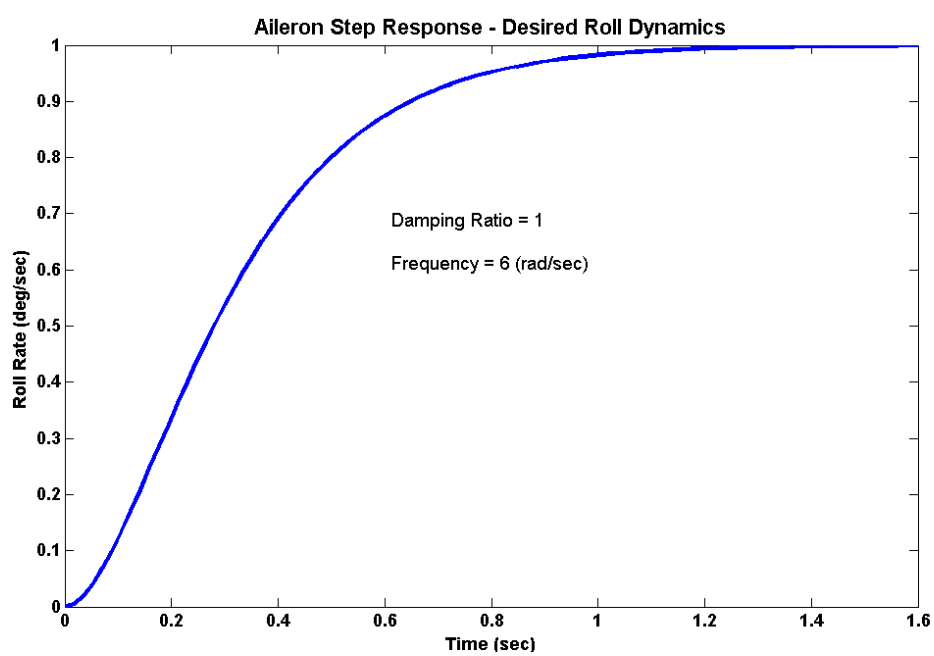

Figure 13: Second Order Desired Roll Dynamics

The values chosen to represent the new desired roll dynamics were $\zeta_{roll} = 1.0$ and $\omega_{roll} =$ 6 (rad/sec) and equated to a roll time constant of $T_{roll} = 0.3$.

Changing the desired roll dynamics from first to second order required a similar change to the roll design filter. An initial choice was made to use the pitch design filter values for the roll design filter. Closed loop simulation produced the following results (Figure 14).

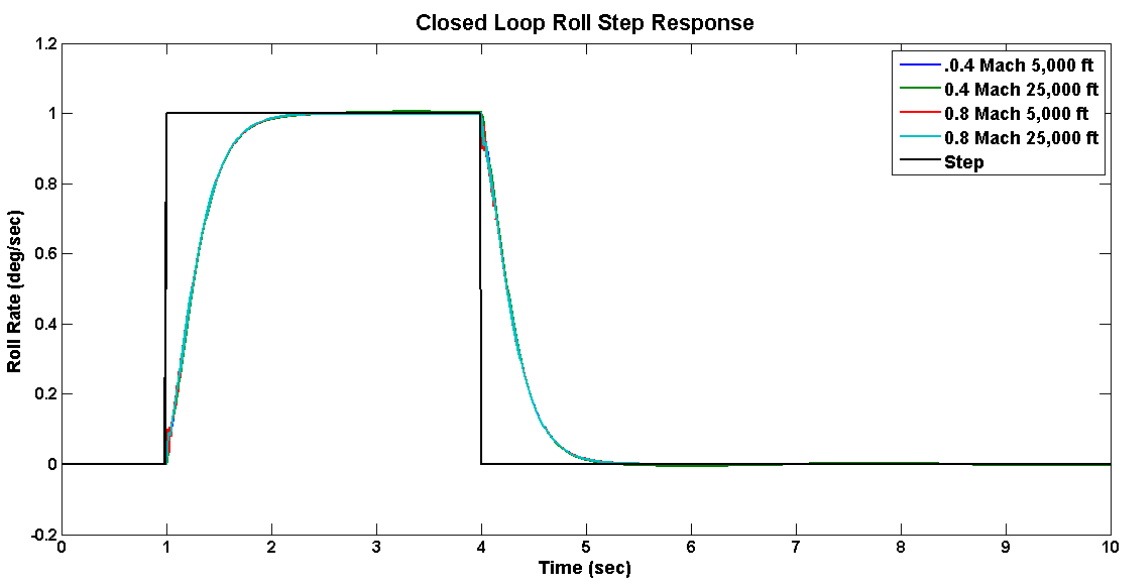

Figure 14: Closed Loop Roll Step Response

The closed loop results clearly show improved tracking throughout the flight envelope.

A brief investigation in further adjusting the parameters of the roll design filter led to no improvement in performance, therefore the final design for the roll axis was settled on with:

$$P_{d\_roll} = \frac{6^2}{s^2 + 2 \cdot 1 \cdot 6 \cdot s + 6^2} \tag{35}$$

$$Q_{roll} = \frac{26.5^2}{s^2 + 2 \cdot 0.5 \cdot 26.5 \cdot s + 26.5^2} \tag{36}$$

Yaw Axis Design

Coldsnow applied the methods described in Chapter 2 to design a disturbance observer for the yaw (directional) axis of the Stevens and Lewis F-16 [Coldsnow, 2009]. Design limitations were noted and marginal performance was met. This discussion briefly describes the specifics of the yaw DO design and presents minor improvements that were made to generate desired yaw dynamics throughout the design flight envelope.

First, sideslip angle, β, was used as the command variable for the yaw DO as it provides good roll induced sideslip damping [Coldsnow, 2009]. The limitation to this command variable, however, is that it assumes the β signal is available during air data failure. In addition, the signal can be noisy and sensitive to airflow disturbances [Blakelock, 1991]. Despite the limitations, the design proceeded since it was the most logical choice for the purposes of the project [Coldsnow, 2009].

The directional motion associated with a rudder input can be approximated by a second order equation, as with the pitch axis, and is known as the dutch roll approximation. A second order transfer function results and the form of the desired yaw dynamics is:

$$P_{d\_yaw} = \frac{\omega_{yaw}^2}{s^2 + 2\zeta_{yaw}\omega_{yaw}s + \omega_{yaw}^2} \tag{37}$$

Referring, again, to the MIL-STD-1797B for specifications leading to level 1 flying qualities, the parameters chosen were $\omega_{yaw} = 3$ (rad/sec), and $\zeta_{yaw} = 0.7$ [Coldsnow, 2009]. Modeling of the entire system, with desired yaw dynamics applied to the yaw axis, led to generation of the feasibility plane for values of ζ_{Q_yaw} and ω_{Q_yaw} that make up the design filter Q_{yaw}. The resulting yaw DO is represented by P_{d_yaw} and Q_{yaw} below.

$$P_{d\_yaw} = \frac{3^2}{s^2 + 2 \cdot 0.7 \cdot 3 \cdot s + 3^2} \tag{38}$$

$$Q_{yaw} = \frac{150^2}{s^2 + 2 \cdot 0.9 \cdot 150 \cdot s + 150^2} \tag{39}$$

Open and closed loop simulation of a rudder step applied to the Stevens and Lewis F-16 produced the following results (Figure 15)

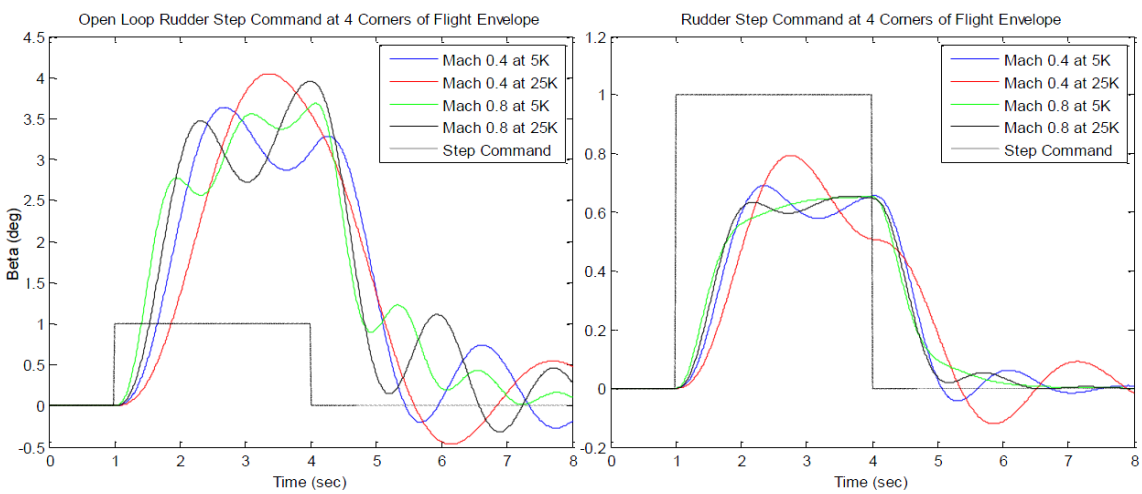

Figure 15: Open and Closed Loop Rudder Step Response

Like the original roll axis results, the DO produced improved tracking over the open loop response, however, the performance wasn't consistent throughout the flight envelope and oscillations existed that predict poor handling qualities ratings.

In an attempt to improve the tracking results of the yaw axis DO, the first change was to adjust the desired dynamics to increase the damping while maintaining predicted level 1 flying qualities. The justification for increasing the damping lies in the fact that the focus of the yaw axis controller is to damp sideslip that is induced by roll inputs. In

essence, the yaw DO was treated as a yaw damper rather than a yaw controller. The values selected were $\zeta_{yaw} = 1.0$ and $\omega_{yaw} = 2.4$. The change in the desired yaw dynamics is graphically displayed below in Figure 16.

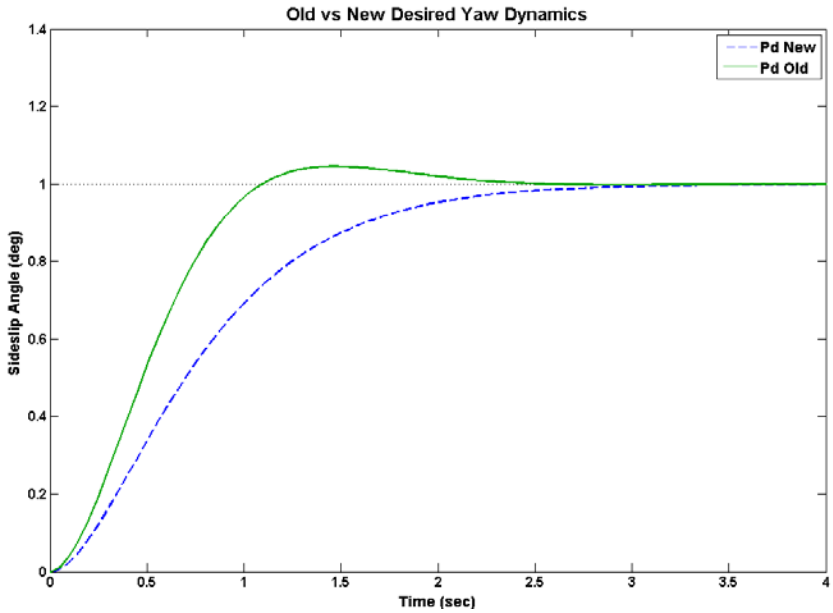

Figure 16: Desired Yaw Dynamics

After changing the desired dynamics, the design filter parameters were adjusted to maintain performance. The values chosen were $\omega_{Q\_yaw} = 50$ (rad/sec) and $\zeta_{Q\_yaw} = 0.9$. Changing the desired yaw dynamics resulted in the following closed loop response to a rudder step (Figure 17).

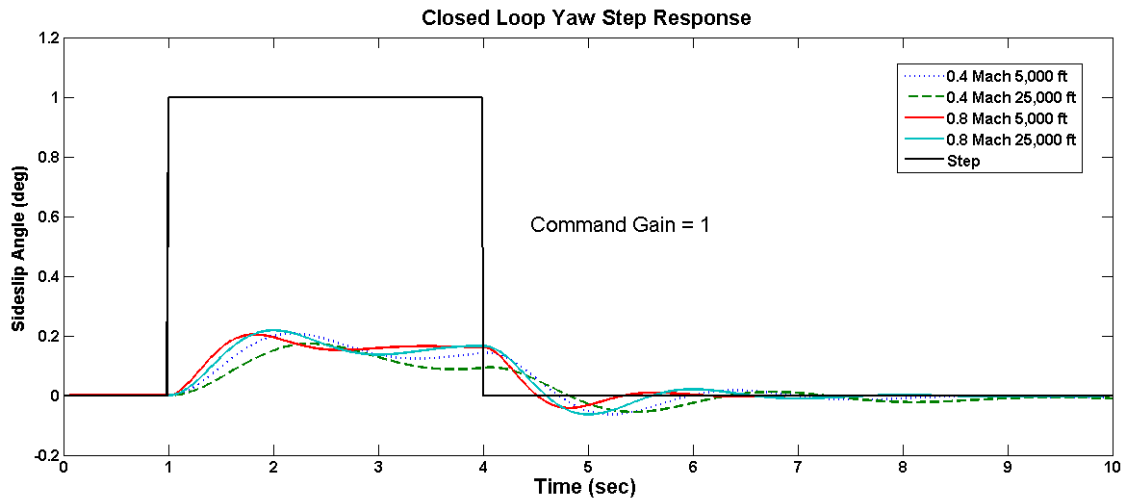

Figure 17: Closed Loop Response to a Rudder Step

The resultant performance had not improved much from the previous design. Experimentation during simulation led to improved tracking performance when a command gain (Figure 18) was implemented on the surface command signal.

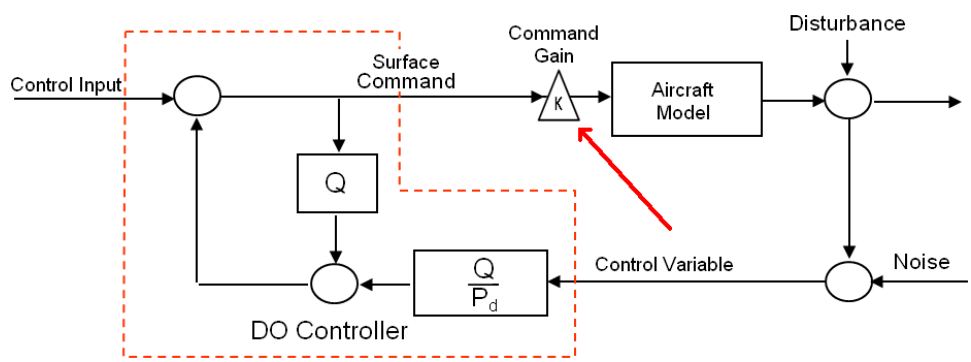

Figure 18: DO with Command Gain Applied

The resultant gain of $k_{cmd} = 10$ generated the improved performance seen in Figure 19.

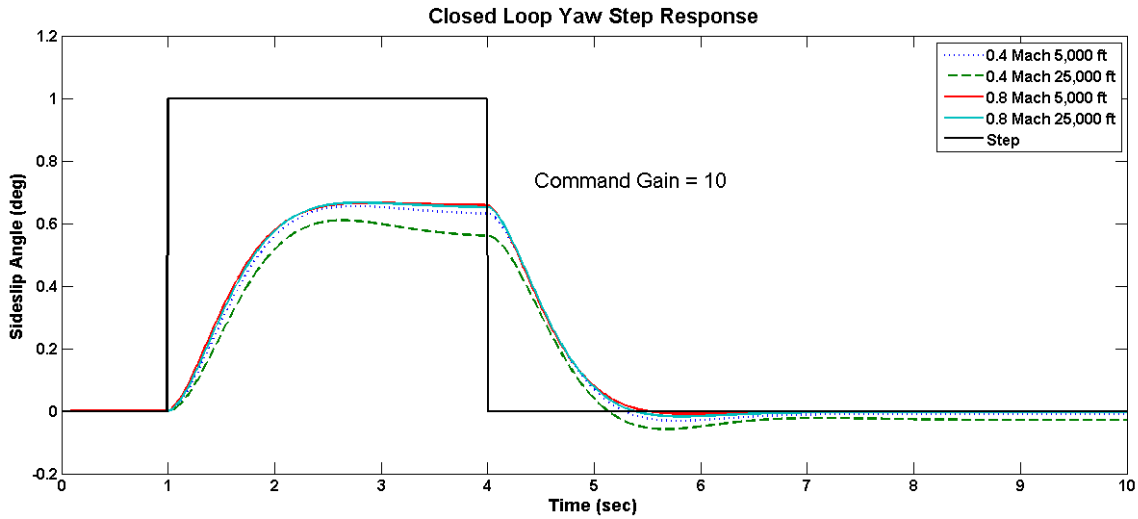

Figure 19: Closed Loop Yaw Step Response

Though the addition of the command gain was accomplished by means of experimentation, the results were considered sound, as multiple full deflection rudder step inputs were conducted throughout the entire flight envelope with no noted discrepancies.

The minor improvements to the yaw axis DO generated improved damping and consistency throughout the flight envelope and were considered adequate for piloted simulation testing.

Summary

This chapter presented preliminary development of the three axis DO. The pitch axis DO was developed by Blue et al and considered adequate for simulation and flight test. The lateral and directional axes DOs were developed by Coldsnow and improvements were made to provide consistent tracking throughout the flight envelope. The following chapters discuss the piloted simulation and flight test methods and results.

IV. Simulation Results and Analysis

Chapter Overview

The previous chapter presented the design and analysis of the three-axis disturbance observer. This chapter discusses the results of handling qualities testing that was conducted in the Octonian flight simulator at the Air Force Research Laboratory's Air Vehicles Directorate, Simulation Branch.

Methodology

The overall objective of the simulator testing was to validate the claim that the disturbance observer can generate desired handling qualities throughout the design flight envelope. To meet the objective, tracking tasks were designed for both the pitch and roll axes, and were flown by 18 volunteer pilots. The tasks generated performance measurements and pilot comments regarding the controller likability and PIO susceptibility. Three different controllers per axis were evaluated at two corners of the flight envelope accounting for a total of twelve tracking tasks per pilot. The flight conditions tested were 0.8 Mach at 5,000 ft and 0.4 Mach at 25,000 ft and designated 'low' and 'high' respectively. The reason for the two points chosen was that they represented the two extremes of the design flight envelope with respect to dynamic pressure. Testing more flight conditions would have added a considerable amount of test points and the project was limited by the amount of simulator time per pilot.

A design of experiments test matrix was created by the Simulation Branch at AFRL to determine controller and flight condition task order. The goal was to mitigate

the potential of task learning and performance improvements by the pilots affecting the results.

Test Platforms

As previously discussed, the initial simulations were run using a non-linear aeromodel of an F-16 generated from data presented in the Stevens and Lewis text [Stevens and Lewis, 2003]. The aeromodel was implemented in Simulink® which allowed for flexibility in adjusting parameters and settings.

The Octonian flight simulator located at AFRLs Simulation Branch of the Air Vehicles Directorate was a high fidelity, pilot-in-the-loop simulator that contained 300º wrap around visibility. A heads up display was projected on the screen in from of the pilot and could be configured to provide a variety of display options depending on the needs of the user. A throttle and sidestick configuration that modeled the F-22 cockpit was incorporated in the simulator.

Controllers

The three-axis DO controller described in the previous chapter was integrated with the Octonian flight simulator and given the designation 'Level 1 DO' for the purposes of the test. A nominal Block 40 F-16 controller (actual F-16 simulation model) was used during the testing as the 'experimental control' test article. It was given the designation 'Block 40.' A third controller, designated 'Level 2/3 DO' was used primarily to demonstrate the flexibility in designing the disturbance observer. Values were chosen for the pitch and roll axes DOs that were predicted to produce 'less than level 1' handling qualities and performance results. A summary of the parameters used for all DO controllers is listed in Table 3 below.

Table 3: Disturbance Observer Controller Summary

Controller	Desired Dynamics (P_d)		Design Filter (Q)	
	ζ_{pd}	ω_{pd}	ζ_Q	ω_Q
Level 1 Pitch	0.5	4	0.5	26.5
Level 2/3 Pitch	0.6	3	0.15	25
Level 1 Roll	1	6	0.5	26.5
Level 2/3 Roll	1	4	0.4	13
Yaw	1	2.4	0.9	50

Note that the yaw axis was not individually evaluated; therefore, the desired yaw dynamics chosen previously were used on both the level 1 and level 2/3 controllers. In addition, during tasks with a level 2/3 controller, the axis not being evaluated was configured with the respective level 1 controller. A graphical representation of the different desired dynamics is shown in Figure 20 below.

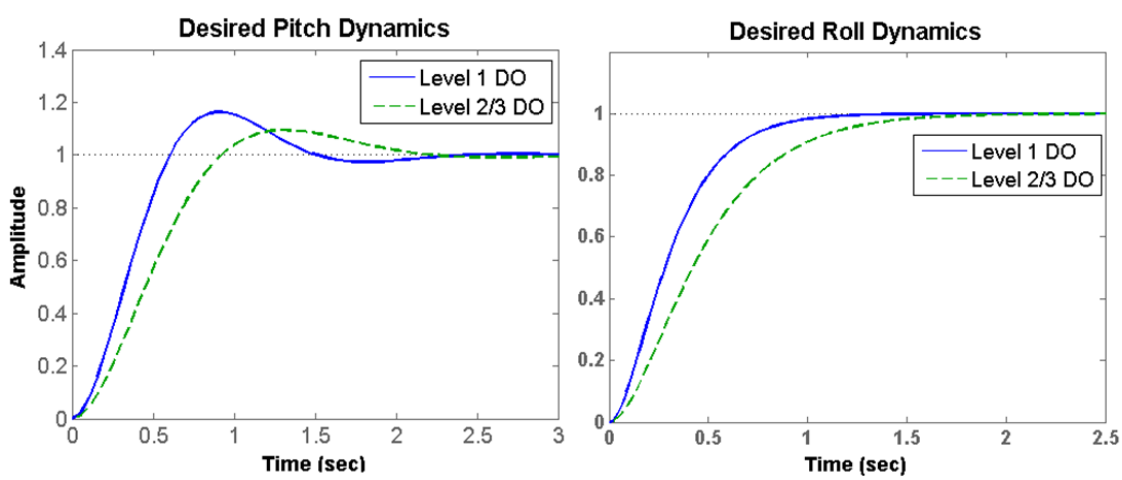

Figure 20: Desired Pitch and Roll Dynamics (Level 1 & Level2/3)

Pitch Task

To evaluate the pitch axis handling qualities, a heads-up-display (HUD) tracking task was developed that required the pilots to keep the HUD gun cross within projected horizontal solid lines that formed the boundaries of the task (Figure 21).

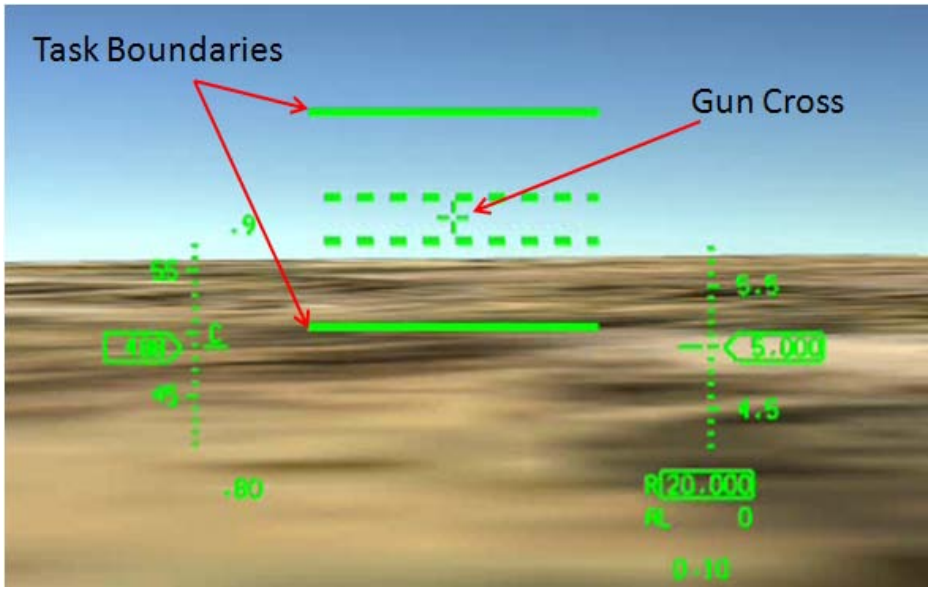

Figure 21: Pitch Tracking Task HUD Display

When the task was initiated, the pilot was given a 10 second grace period to get a feel for the current control configuration. After the 10 second grace period, the horizontal boundary lines would begin to move up and down in the HUD, requiring the pilot to pitch the aircraft to keep the gun cross within the boundaries. At the end of the 20 second task, if the pilot succeeded in avoiding boundary excursions, the task was run again with an incrementally smaller margin between boundaries. The series of tasks was terminated when the pilot was unable to complete a given task without crossing one of the boundaries. The task would then reset with a new controller and wide boundaries.

To avoid the potential for learning tasks, four different tasks were generated using a desktop simulator that accounted for the physiologically uncomfortable effect of excessive pitch down motions. This was a lesson learned during the BAT DART test management project (TMP), where a similar HUD tracking task was used with a sum of three sine wave function generating a random pitching motion. The effect was that the task generated physically uncomfortable negative-g pushovers that made the task too difficult [Dotter, 2007].

Roll Task

The roll tracking task was similar to the pitch task in that the pilot's goal was to avoid tracking outside a set of imposed boundaries (Figure 22).

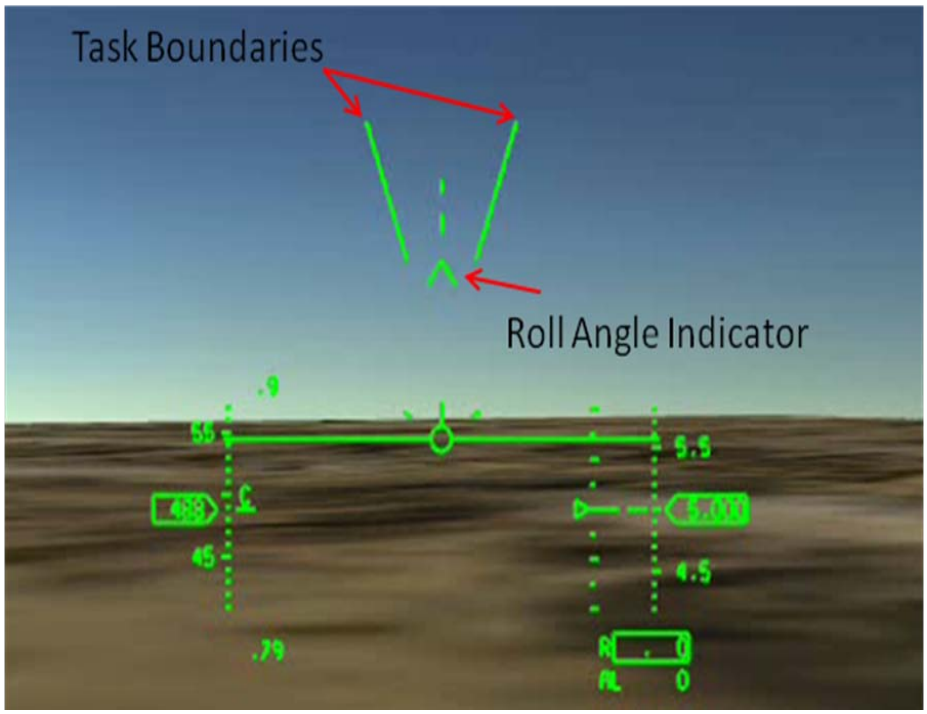

Figure 22: Roll Tracking Task HUD Display

The task was developed for use during the AT BAT TMP at the USAF Test Pilot School and incorporated a sum of sins function that generated the 'random' rolling motion that was to be tracked by the pilot [Blake, 2008]. Unlike the pitch task, the roll task was continuously run with the boundaries incrementally shrinking every 30 seconds. The Task was terminated when the pilot exceeded a boundary.

Pilot Performance Criteria

Pilot performance was measured based on minimum boundary successfully completed for the pitch tasks, and total time before boundary excursion for the roll task. In addition, the pilots were asked to rate the controllers based on 'likability'. The Cooper-Harper rating scale was not used to generate ratings because none of the volunteers had experience in using the CH rating scale with most having never heard of it. In addition, since the objective was to assess the handling qualities of the DO at different points in the flight envelope and compare them to the nominal Block 40 F-16, it was determined that adequate comparisons could be made in a given test session. The pilots were asked to rate the controller from 1 to 5 with 1 representing a perfect, very likable controller and 5 representing a terrible controller.

In addition to a 'likability' rating, the pilots were asked to rate each controller following completion of a task for its susceptibility to PIO. Again, the PIO rating scale was not used for similar reasons as above. The pilots were told that a rating of 1 should be assigned to a controller with no PIO susceptibility, and a 5 should be assigned to a controller that tends to PIO as soon as the pilot enters the control loop.

Pitch Axis Results

Each pilot flew the pitch tracking tasks with each of the three controllers at the two flight conditions previously discussed. Task performance was based on the last completed boundary width successfully flown. The average performance and pilot rating per controller type and condition were normalized to scale from 0 to 1. This allowed the results to be displayed on a single chart. Pilot ratings were normalized using the following function:

$$Rating_{norm} = \frac{Rating - 5}{5} \tag{40}$$

The performance results were normalized by dividing the average number of completed tasks by the total number of possible tasks. The results are displayed in Figure 23 below.

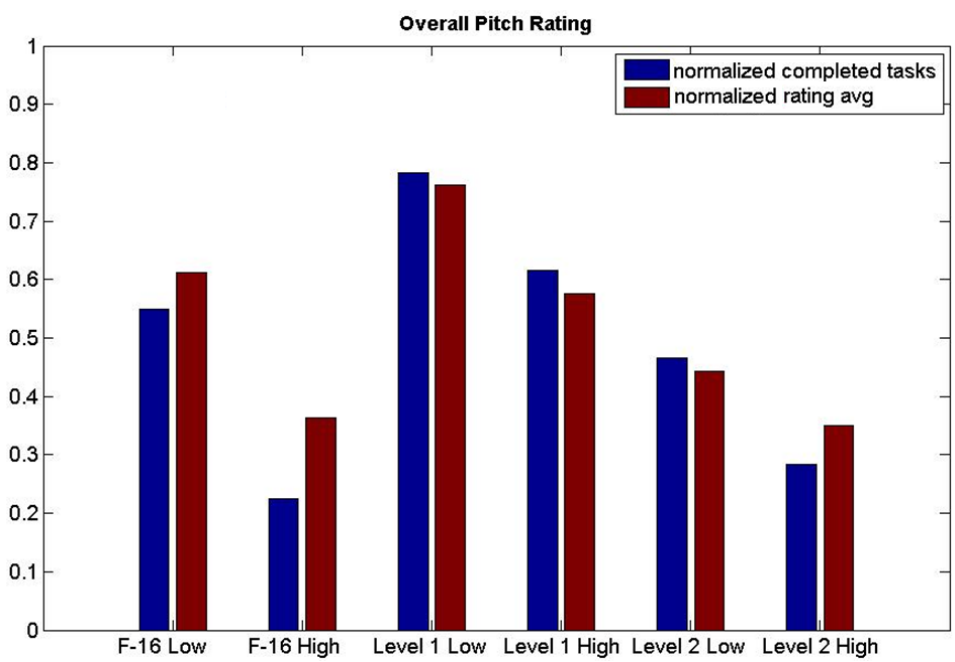

Figure 23: Pitch Task Performance and Pilot Ratings

It is clear that the controller ratings fell in line with task performance, which is a result that can be expected due to the fact that the pilots normally associate performance with quality of handling. Next, it is clear that the low altitude, high speed condition performed and rated better than the high altitude, slow speed condition for all controllers. Finally, the level 1 DO controller rated and performed the best with the level 2/3 DO rating and performing the worst.

The normalized PIO ratings for the pitch tasks are shown in Figure 24.

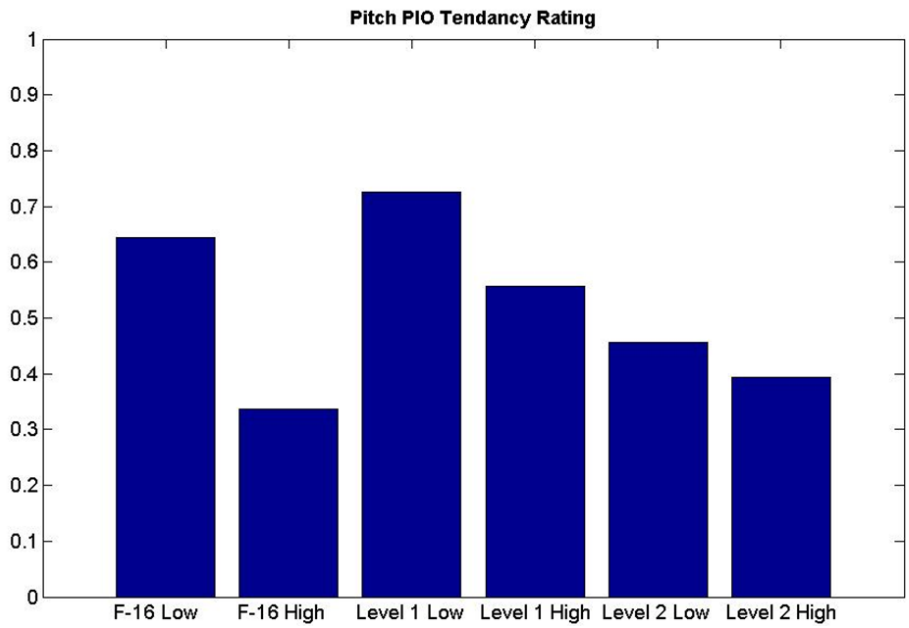

Figure 24: Pitch Task PIO Ratings

The PIO ratings follow similar trends to the performance and 'likability' ratings above with the level 1 DO rating the best and the level 2/3 rating the worst.

One more result worth noting is that the DO controller ratings and performance differences were smaller between the high and low tasks, then the Block 40 F-16. That is to say the DOs behaved more consistently across conditions, than the F-16.

Roll Axis Results

The Roll axis performance and pilot rating were normalized on a scale from 0 to 1 and are displayed in Figure 25.

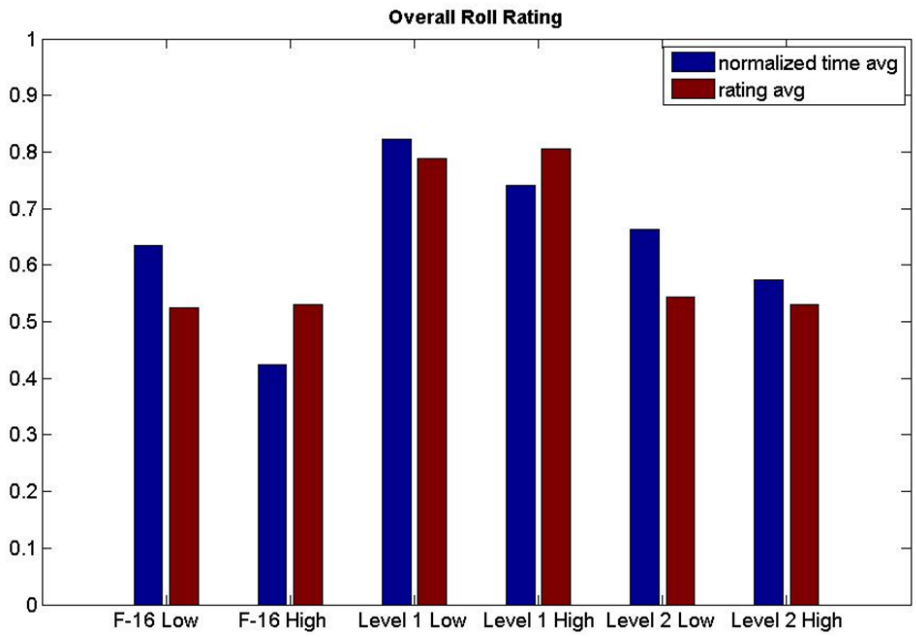

Figure 25: Roll Task Performance and Pilot Ratings

The results trend similar to the pitch task results, however, the pilots tended to rate and perform more consistently between the flight conditions.

The normalized PIO ratings for the roll tasks are shown in Figure 26.

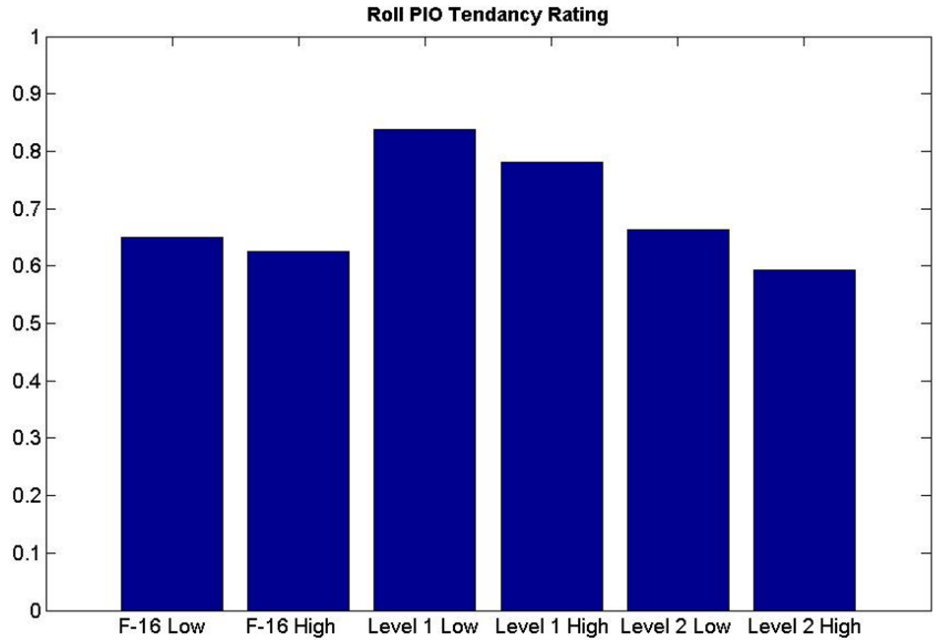

Figure 26: Roll Task PIO Ratings

The PIO ratings follow the same trends as the performance and handling ratings.

Simulation Limitations

Several limitations were present during simulation testing that need to be mentioned. First, the DO controllers were originally intended to be applied to the Block 40 F-16 aeromodel for the test. This proved to be a difficult and time prohibitive task as the F-16 contains a highly complex flight control system that blends control surface movements. The DO controllers were therefore flown using the Stevens and Lewis aeromodel that was used during desktop analysis. The limitation that needs to be considered is that the ratings and performance comparison between the Block 40 F-16 and the disturbance observer is not a pure 'apples to apples' comparison. Compounding the comparison issue is that the Block 40 F-16 in a clean configuration is a 'g-command' system. That is, the flight control system tracks the pilot's request for a load factor, or g,

rather than pitch rate, as is the case with the DO. This difference is expected to produce varying handling qualities opinions for a given task.

The final limitation worth noting is the lack of time available to perform tasks at other points in the design flight envelope. The expected result is that the DO would have produced more closely aligned performance and handling ratings at the middle altitudes and airspeeds. The 'high' point used for simulation testing was chosen because it represented the extreme corner of the design envelope and if the controller performed and handled well at that point, it could be inferred that it would handle well in the rest of the envelope. As it was, the performance and handling qualities were slightly worse than at the 'low' point.

Summary

This chapter presented the methodology and results of the piloted simulator study conducted in the Octonian simulator at AFRL. The disturbance observer produced good handling qualities ratings and performance at the two extreme corners of the design flight envelope. The 'level 2/3' disturbance observer produced the lowest ratings and performance, which was in line with predictions. Simulation testing limitations were noted and full evaluation and verification of DO theory requires the flight testing discussed in the next chapter.

V. Flight Test Results and Analysis

Chapter Overview

The disturbance observer was evaluated during flight test conducted as part of the author's joint AFIT-TPS test management project, Have MURDOC, and described in detail in the Have MURDOC Technical Information Memorandum [Rein et al, 2009]. The author served as the program manager for the project that conducted 12 test sorties on the VISTA totaling 16.4 flight hours. To narrow the scope of the project, the pitch DO was the only axis evaluated. The primary objective of the project was to demonstrate longitudinal flight control with the DO controlling the pitch axis of the VISTA. The secondary objective was to conduct an approach and runway touchdown with the DO controlled VISTA. This chapter presents the test methodology and flight test results of the project.

Methodology

The pitch axis DO developed by Blue et al and discussed in Chapter 3 was implemented on the USAF TPS handling qualities simulator and Calspan VISTA 'hotbench' for ground validation, and the VISTA for flight test. Implementation and test preparation occurred between March and September 2009.

Test Platforms

The USAF TPS handling qualities simulator is used in the TPS curriculum to provide flying and handling qualities instruction. It is also used for various research side projects of TPS staff and students. The simulator contains multiple aeromodels including

a high fidelity model of the VISTA. A center and sidestick are available for use and three, 24 inch, flat panel, color displays are used for visibility. The simulator incorporates a Simulink® interface to provide flexibility when experimenting with new control designs or gains.

Calspan Corporation uses the 'hotbench' as a hardware-in-the-loop simulator for use when implementing new control laws or models on the VISTA. It contains a complete VISTA model to include all configurations, safety trips and limits.

The VISTA (Figure 27) is a highly modified Peace Marble II Block 30 F-16D with Block 40 avionics. It is capable of in-flight high fidelity simulation of "model" aircraft characteristics in the real flight environment. Airframe modifications included a large dorsal, heavy duty landing gear, programmable heads-up-display (HUD), variable feel system for center stick, and high performance control surface actuators. The VISTA Simulation System (VSS) uses five control surfaces and the engine to mimic the feel and response of the simulated aircraft. The VSS can be modified with different control architectures for the purpose of evaluating new control systems such as the DO. The VSS also contains a complete aircraft model that enables the aircraft to be 'flown' on the ground. During testing, the system evaluation pilot (EP) occupies the front cockpit and the safety pilot (SP) occupies the rear cockpit. In the VSS mode, Programmable Test Inputs can be initiated by either cockpit to evaluate the dynamic response of the aircraft and/or controller performance.

Figure 27: Variable stability In-flight Simulator and Test Aircraft (VISTA)

The Digital Flight Control Computer (DFLCC) continually monitors pilot inputs for safety. If the VSS commands to the control surface actuators approach basic aircraft limits, the DFLCC disengages the VSS and reverts to the basic F-16 control mode. The VSS also includes dual sensors for all required signals and sensor failure causes an automatic safety trip. Either pilot can initiate a manual safety trip as well. Following a safety trip, aircraft control instantly returns to the Safety Pilot occupying the rear cockpit.

Implementation

The DO was integrated on the pitch axis of the VISTA and the lateral-directional axes were controlled by a nominal flight control configuration often used on the VISTA to represent an 'F-16 like' control scheme. Integration was first conducted on the TPS handling qualities simulator that contains a complete VISTA model. The DO as depicted in Figure 28 was provided via Simulink® block diagram form. The DO output signal provided the horizontal tail surface command and the feedback signal consisted of the VISTA pitch rate sensor output.

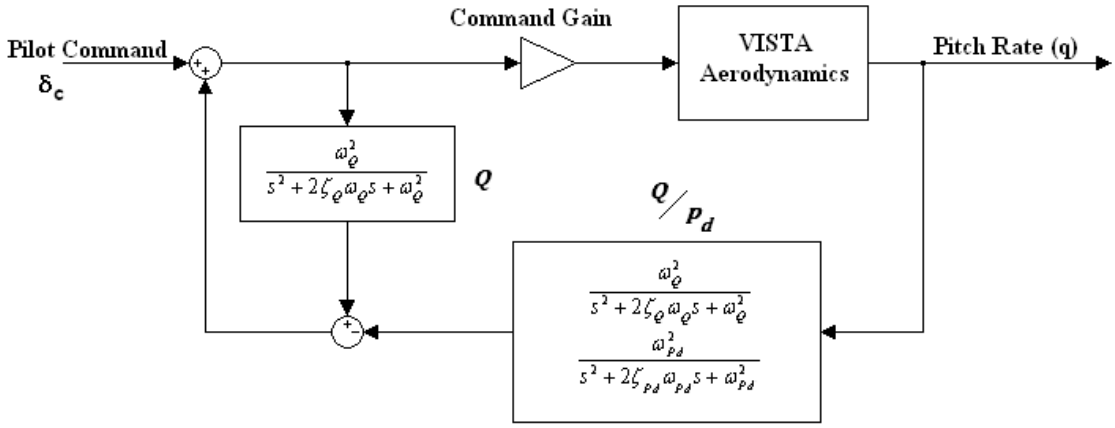

Figure 28: Pitch DO Integration

Following simulator integration, the controller was integrated on the VISTA 'hot bench' at the Calspan Corporation in Niagara, NY. The hot bench provided hardware-in-the-loop capabilities that allowed the test team to validate the controller integration and usability with the VISTA.

Calspan engineers configured the VISTA to be able to allow the pilots to initiate PTIs and adjust the PTI parameters from within the cockpit. Both pitch step and doublet PTIs were programmed with the ability to adjust the magnitude and duration of each. Initial parameters were determined during simulation conducted in the TPS handling qualities simulator.

Flight Test Matrix

To meet the primary objective, the test team planned to conduct a series of PTI steps and doublets at each combination of speed and altitude (0.4, 0.6, 0.8 Mach and 10, 15, 20K ft). The PTIs were used to measure the aircraft's frequency and damping at each condition and compare them to predictions. In addition to the PTIs, a sampling of aerobatic maneuvers was planned to qualitatively assess the DO as the aircraft

transitioned across the entire design envelope speed and altitude range. Simulated turbulence was also initiated at each of the flight conditions to qualitatively assess the DO controller in turbulence. The simulated turbulence was a feature of the VISTA that fed a turbulence model directly to the control surfaces and was not a part of the DO control loop.

Once the primary objective test matrix was complete, the buildup to landing phase of the test was initiated. Step and doublet PTIs were conducted in the approach configuration (gear down) first at 220KIAS then at the nominal approach speed equating to 11˚ α. Following completion of the approach configuration PTIs, the controller handling qualities were assessed during three sorties conducted in formation with a target T-38 aircraft. Handling qualities of the VISTA and DO controller were evaluated through a series of formation tracking tasks. At speeds ranging from 220 KCAS to 11 ± 2˚ α, the evaluation pilot performed tracking tasks and assigned PIO ratings using the PIO rating scale. A Cooper-Harper task was performed and a CH rating was recorded along with pilot comments. Tracking tasks included both low gain formation station keeping and high gain tracking. Two techniques were used during the high gain tracking to evaluate whether the aircraft exhibited any instabilities or tendencies to PIO. The 'workload buildup' technique involves performing a tracking task while avoiding defined boundaries [Gray, 2007]. Boundaries were treated as critical and every attempt was made to remain within them or the task was terminated. As boundaries were incrementally reduced in size, pilot gains naturally increased and potential handling qualities deficiencies were discovered. The second technique was to accomplish point tracking while attempting to maintain zero error. This technique was used, like the

workload buildup technique, to discover potential handling qualities deficiencies as pilot gain increases. To accomplish the tasks, the evaluation pilot flew the VISTA in the route position shown in Figure 29.

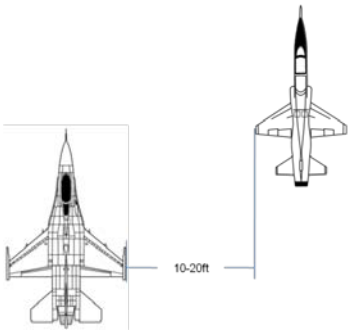

Figure 29: Tracking Task Lateral Offset

The pilot started the task with a vertical offset then attempt to capture the projected T-38 wingtip within one of the circles that the star emblem creates on the side of the T-38 as shown in Figure 30.

Figure 30: Tracking Task Visual Reference

The simulated landing Cooper-Harper task was initiated from a stack-high route position shown in Figure 31. The pilot simulated a landing flare by descending to capture the T-38 wingtip projected on the star as in the previous workload buildup task.

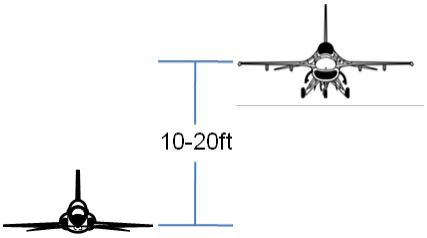

Figure 31: CH Task Vertical Offset

The CH 'desired criteria' was to arrest the sink rate within the blue circle (Figure 30) with one or less pitch overshoots. 'Adequate criteria' was attained if the flare was arrested within the outer circle with one or less pitch overshoot.

The second CH task was to fly in the stack-level route formation while the target aircraft performed a series of shallow climbs and descents (±5 degrees pitch attitude). Desired performance was met by keeping the projected wingtip within the blue circle (Figure 30) for 75% of a 20 second task. Adequate performance was met by keeping the wingtip within the outer circle for 75% of a 20 second task.

Following the handling qualities evaluation, the DO was qualitatively evaluated by each project pilot during four sorties of approaches and runway touch-and-goes. Each pilot was able to assess the DO during 2-3 nominal (2.5˚ approach path angle) approaches and one each shallow 2˚ and steep 3˚ approach.

Results and Analysis

Ultimately, the DO met all flight test objectives set by the TMP team, however, there were a few issues experienced that were not predicted during simulation analysis and testing.

Implementation Results

When the DO was integrated on the handling qualities simulator at TPS, initial simulations resulted in the controller commanding an unstable response. It was determined that the VISTA model in the handling qualities simulator contained a time delay that the Stevens and Lewis (AFIT F-16) model used during previous research did not have. The time delay was discovered by running the two models (VISTA, AFIT F-16) in parallel with an identical input and analyzing the response. The simulation was run in Simulink® and the result is shown below in Figure 32.

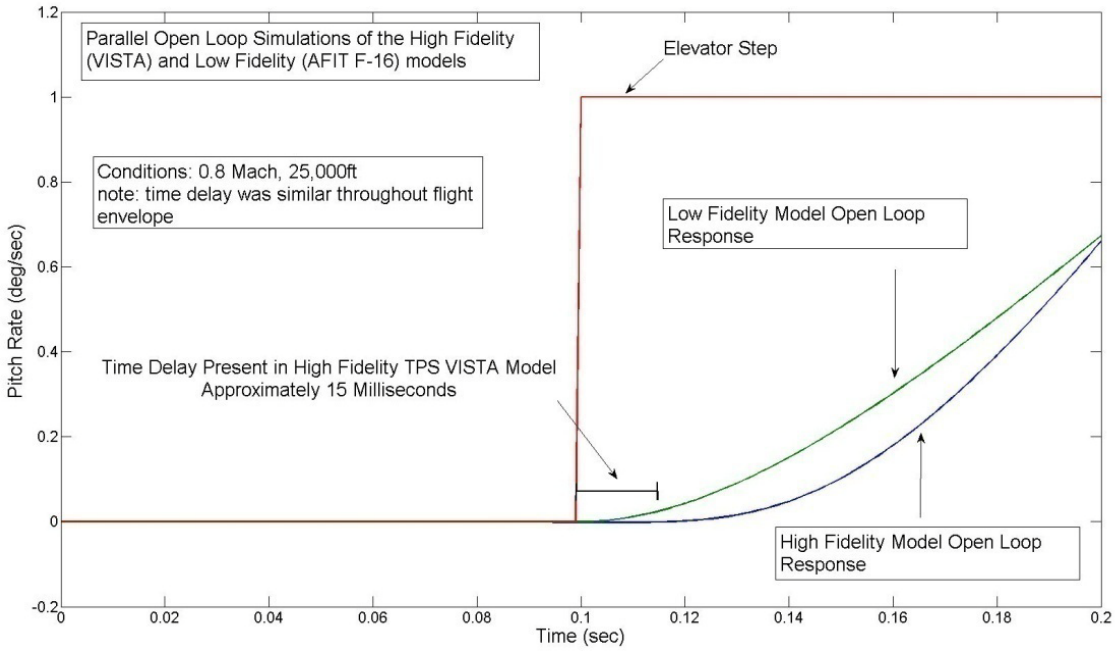

Figure 32: Time Delay Investigation

The effect of the time delay was to destabilize the DO as originally designed. The delay was a result of the way the VISTA operates. Calspan engineers explained that the actuator command signal solution is not passed to the actuator until one simulation time step after the solution is calculated. This led to a time delay that was equal to the simulation rate of 64Hz or 0.0156 seconds. Unfortunately, this result was discovered following completion of flight test, otherwise, the simulation rate could have been increased to minimize the time delay within the system.

To continue to flight test with the delay, it was discovered that if a reduced command gain (k_{cmd}) was applied to the surface command signal, that a stable and desired response could be achieved. Unfortunately, however, the optimal gain for producing desired performance changed with flight condition. Based on the relatively short timeline of the TMP process, an ad hoc gain schedule was developed to allow the project to continue to flight test. The gain schedule was developed using a Matlab® minimizing function in conjunction with simulations to determine an optimum gain for points throughout the flight envelope. The minimizing function searched for values of k_{cmd} that would generate the smallest difference between the derivative of the pitch rate response and the derivative of the desired response squared (see Appendix A for code). The gain schedule developed is displayed in Figure 33 and was a function of the VISTA sensed dynamic pressure $(\overline{q})$.

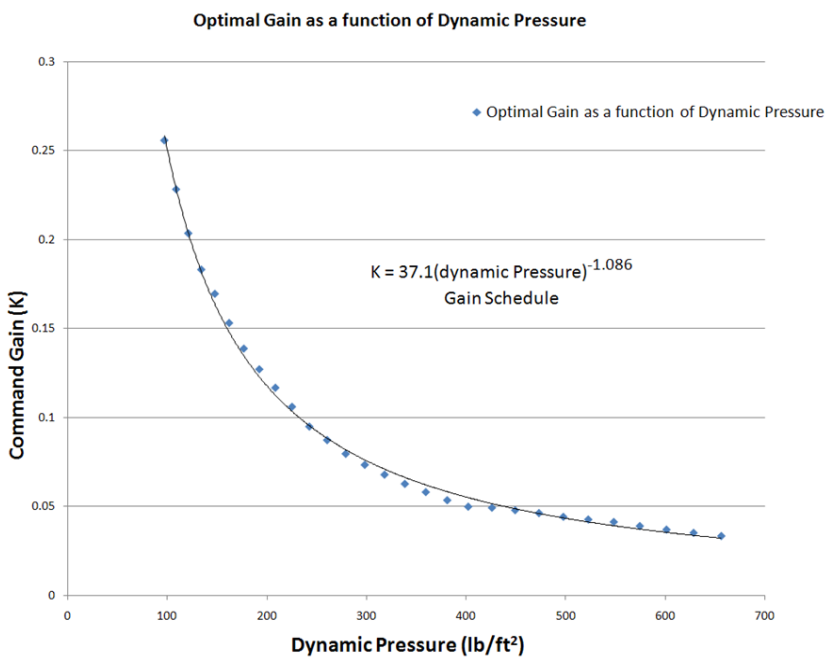

Figure 33: Surface Command Gain Schedule

Simulation conducted at the four corners of the test envelope with the gain schedule applied resulted in the following plot (Figure 34).

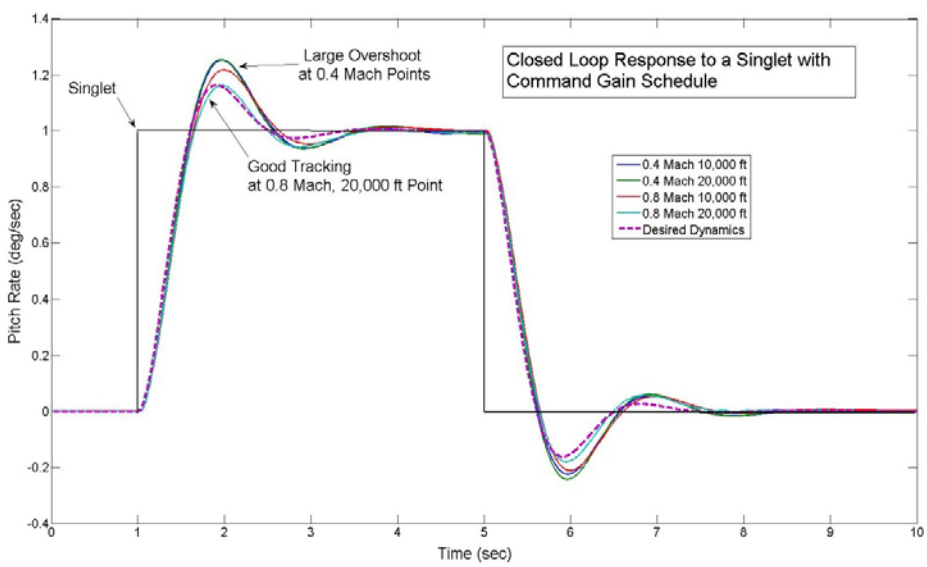

Figure 34: Closed Loop Step Response with Command Gain Schedule

The DOs performance had been adversely affected by the time delay and flight test was now predicted to result in reduced handling qualities due to the increased magnitude of the short period response overshoots.

The DO was originally designed for the cruise condition flight envelope $h \in$ [5,000; 25,000 ft], Mach $\in$ [0.4; 0.8]. Simulations were run in the approach configuration and at approach speeds to generate predictions and verify that the controller would work at those conditions. The following is a plot of a PTI step response at 170KCAS and 10,000 ft with the landing gear down and gain schedule applied (Figure 35).

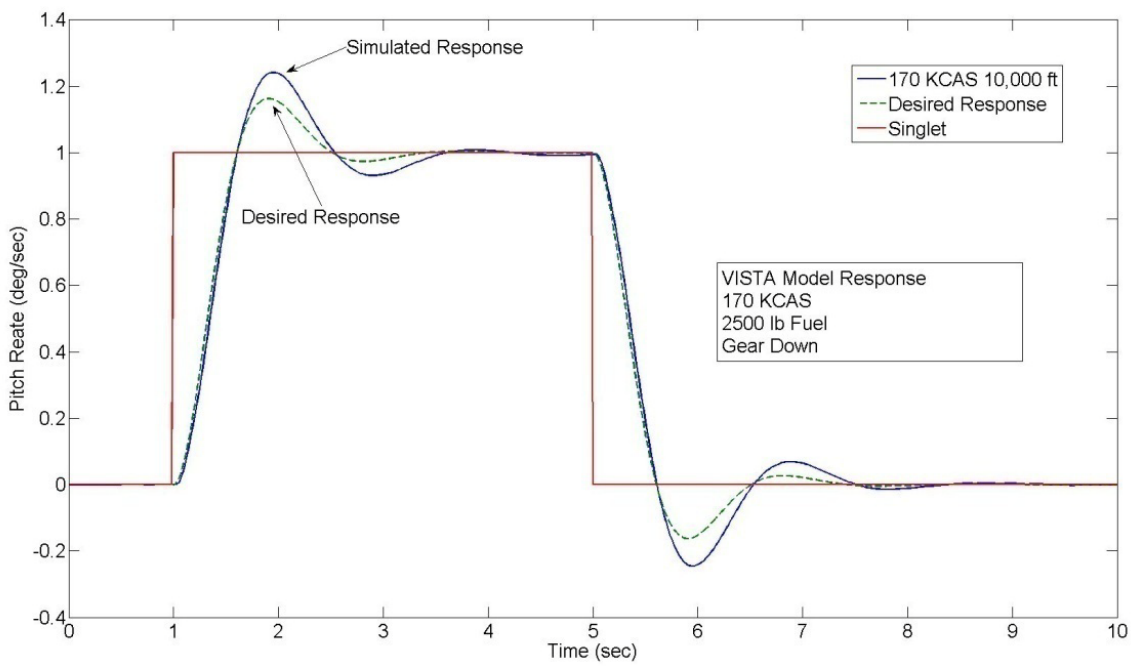

Figure 35: Approach Configuration Step Response

The response clearly shows lower damping than desired. Again, the prediction for flight test was reduced handling qualities.

Initial Flight Test Findings

With the VSS engaged, the horizontal tail surfaces tended to 'buzz' (oscillate) at a high frequency. The horizontal tail buzz was determined to be due to high frequency sensor noise that was amplified rather than attenuated by the DO. Figure 36 shows the horizontal tail command signal before and after VSS engagement.

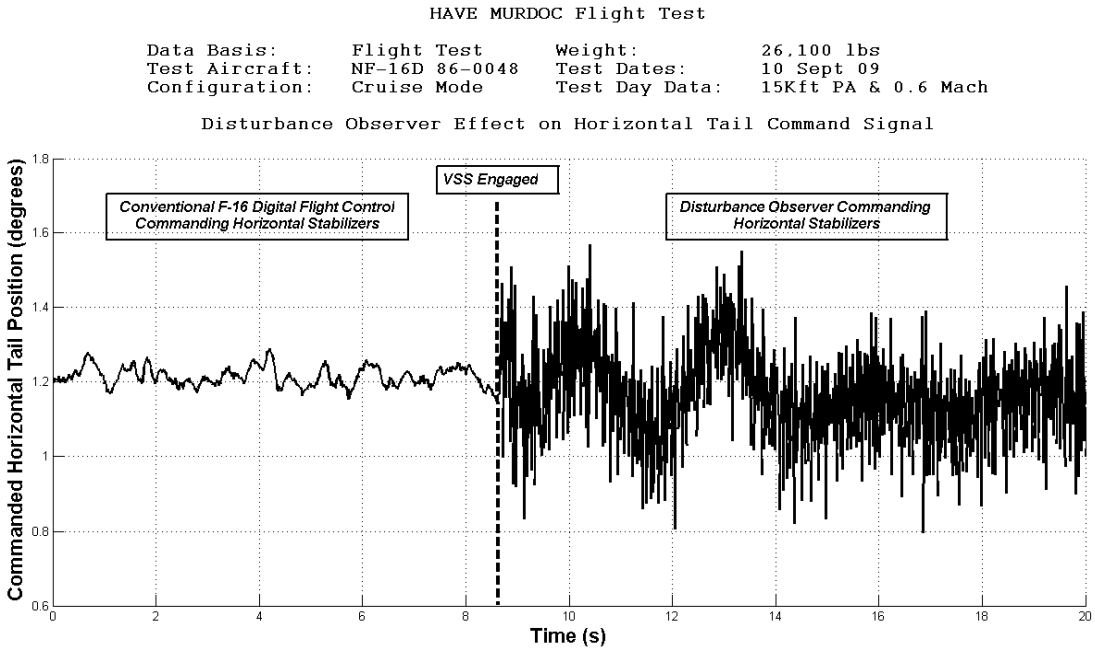

Figure 36: Horizontal Tail Command Signal

It was clear that the DO was acting to amplify pitch rate sensor noise. The noise rejection transfer function discussed in Chapter 2 predicted noise attenuation at frequencies above $\omega_Q = 26.5$ (rad/sec). However, the noisy feedback signal was amplified by an amount proportional to the ratio:

$$\frac{(Design\ filter\ frequency)^2}{(Desired\ dynamics\ frequency)^2} = \frac{(26.5)^2}{(4)^2}$$

Figure 37 shows a representative flight test result of the pitch rate signal noise amplification after passing through the DO filter, Q/P_d.

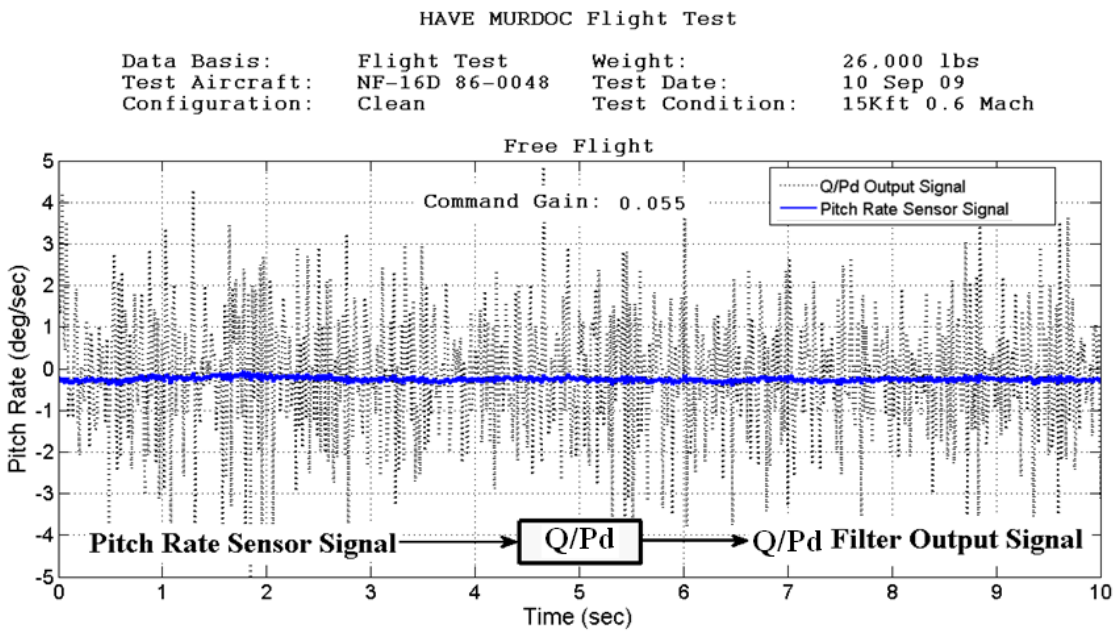

Figure 37: Pitch Rate Sensor Noise Amplification

The filter output signal contained noise that was roughly twenty times the magnitude of the pitch rate sensor noise. The large amplitude, high frequency error signal was then directed to the horizontal tail actuator and created the buzz witnessed by the evaluation pilot. The horizontal tail buzzing was not detrimental to the collection of data and testing continued.

The VISTA simulator had the capability of adding sensor noise to the feedback signal. This capability was implemented and the flight test 'noise amplification' results were replicated in the simulator. A preliminary investigation into eliminating or reducing the noisy signal led to a change in the Q parameters. Changing the design filter frequency from 26.5 to 8 (rad/sec) and using the same pitch rate sensor signal as in Figure 37 led to the following result shown below (Figure 38).

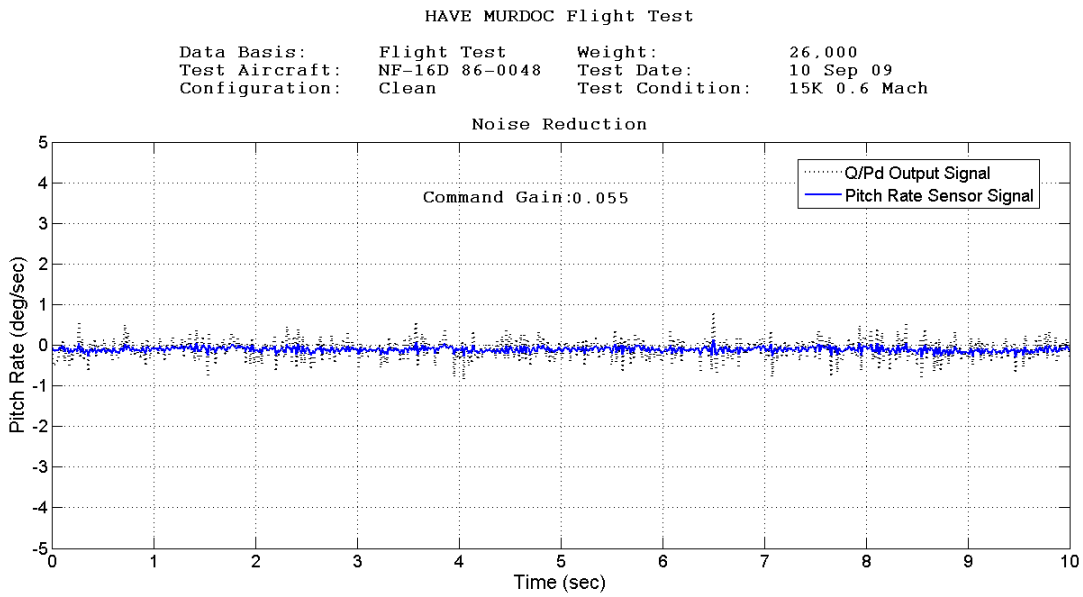

Figure 38: Reduced Noise with New Q Parameters

The new parameters for Q are well within the feasibility region discussed in Chapter 3 and result in much less sensor noise passing through to the control surface. Though the change significantly reduced the noise that was passed to the control surface actuator, the sensor noise was not attenuated as theorized.

Flight Test Flying Qualities

The DO controlled VISTA response to PTI doublets and steps resulted in significantly reduced damping and a slight reduction in natural frequency. Frequency and damping were calculated using the 'logarithm decrement' method depicted in Figure 39 [Rivin, 1999].

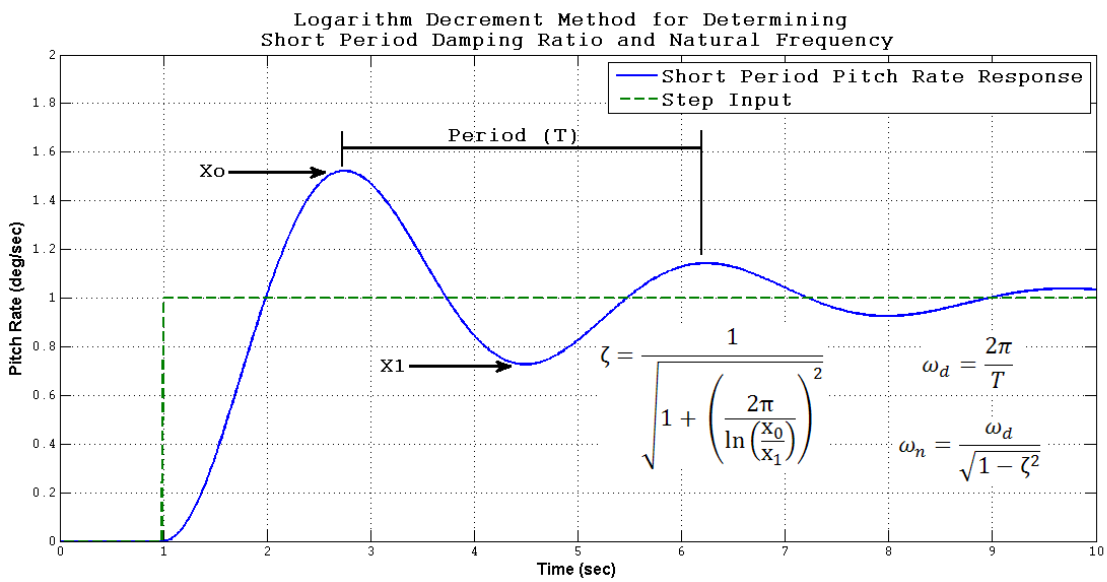

Figure 39: Logarithm Decrement Method for Calculating Frequency and Damping

The following is a representative PTI step response conducted at 20,000 ft and 0.6 Mach (Figure 40).

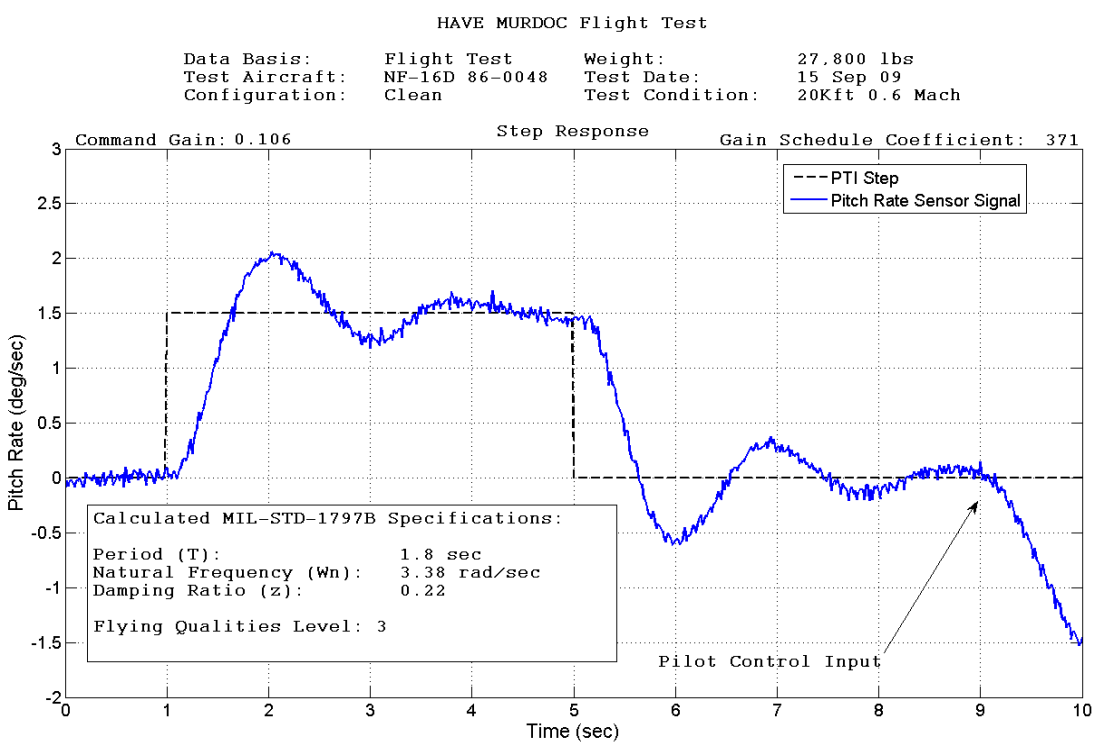

Figure 40: PTI Step Response (20K, 0.6 Mach)

Natural frequency and damping ratio were calculated to be 3.38 (rad/sec) and 0.22 respectively for the initial step. The values met the MIL-STD-1797B specifications for predicted level 3 flying qualities. In general, for each PTI, the calculated ω_n and ζ were slightly slower and significantly less damped than the 'desired' values of $\omega_n = 4$ (rad/sec) and $\zeta = 0.5$. This result was consistent with results found during simulation (see Figure 34). In no case was the natural frequency or damping ratio during flight test faster or more damped than the controller specified values.

A PTI doublet at 20,000 feet PA and 0.6 Mach produced similar results as the step at the same condition (Figure 41).

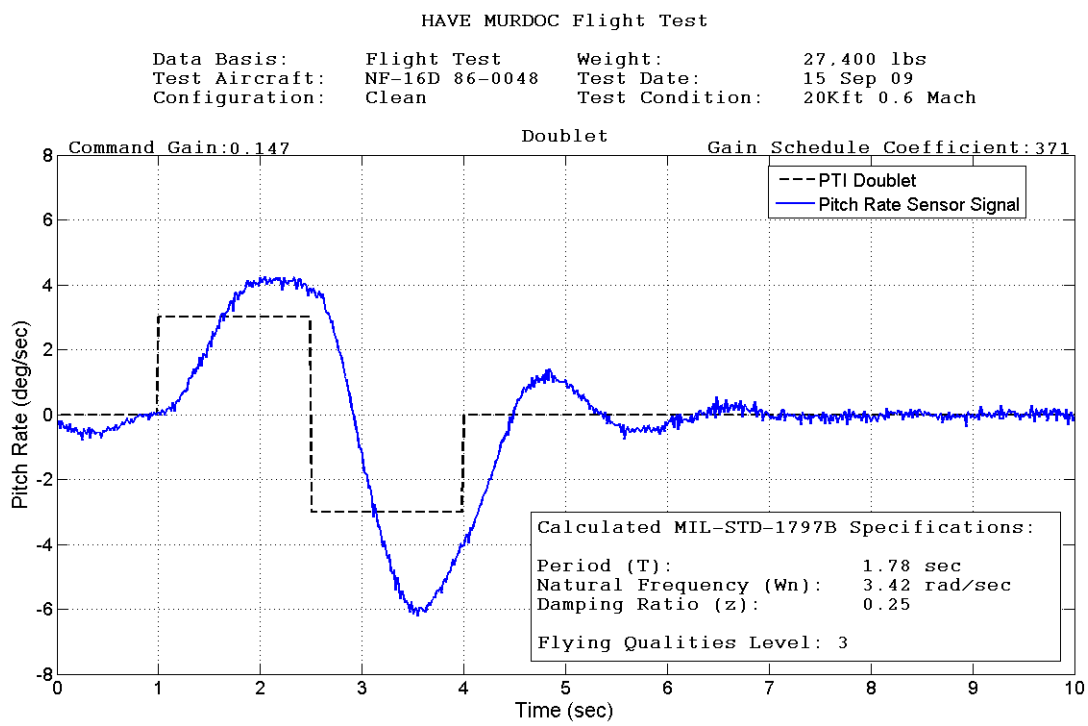

Figure 41: PTI Doublet Response (20K, 0.6 Mach)

The natural frequency and damping ratios were calculated to be 3.42 (rad/sec) and 0.25 respectfully. Again, the calculated values predict MIL-STD-1797B level 3 flying qualities due to the low damping ratio.

The PTI results were similar throughout the flight envelope. Appendix B contains all PTI plots as well as single plots containing all PTIs for a given flight condition. The following is a sample plot representing the PTI doublet response at three different flight conditions (Figure 42).

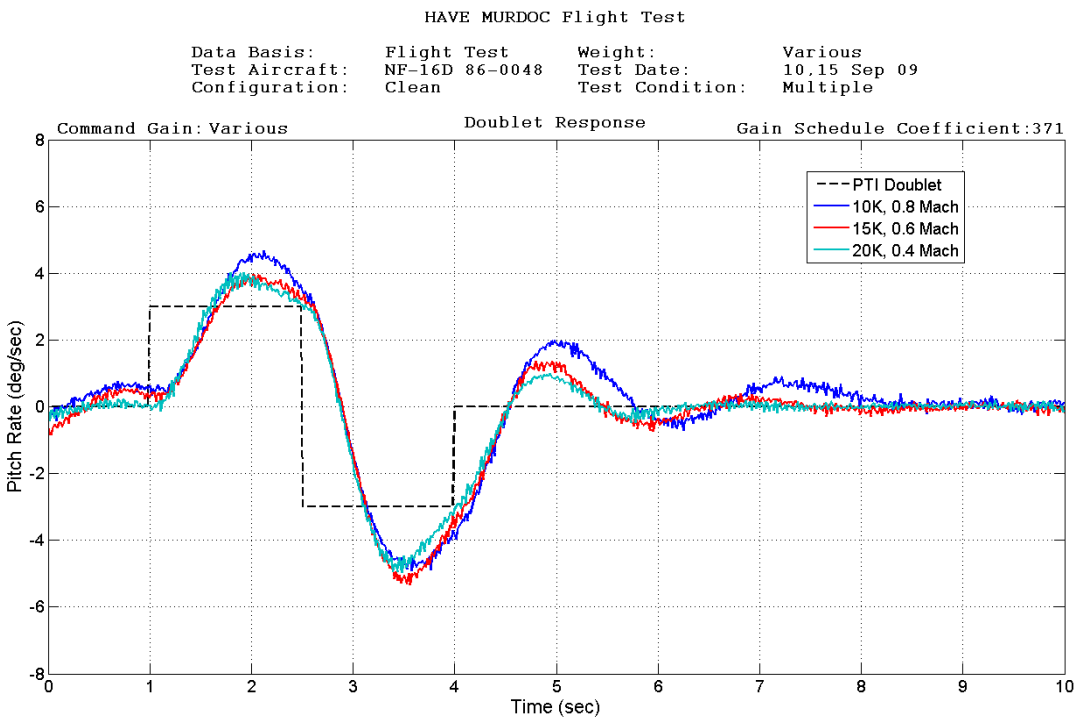

Figure 42: PTI Response at Three Flight Conditions

Of note is the less damped response at the 0.8 Mach, 10,000 ft condition. Simulation (Figure 34) predicted the best performance would occur at the 0.8 Mach condition.

The DO performance was evaluated in the powered approach configuration by conducting PTI steps and doublets at 220KCAS, 11 deg α and 10,000 feet. PTIs were

executed in a similar manner to those conducted during cruise configured flight. Initial attempts at generating the PTIs resulted in multiple 'surface-rate-limit' trips of the VSS. The rate limit trips were caused by the horizontal tail surface command signal exceeding VISTA safety trip limits. Simulation did not predict this result because pitch-rate sensor noise was not simulated prior to flight test. The large control deflections required at low dynamic pressures in conjunction with sensor noise caused the surface command signal to exceed the VSS actuator rate limits. The command signal gain (k_{cmd})[1] was reduced from 371 to 170 and subsequent PTIs were completed without rate limit trips. Figure 43 shows the effect of reducing the command gain at 10,000 feet PA and 220 KIAS. The aircraft response was much less damped resulting in multiple overshoots.

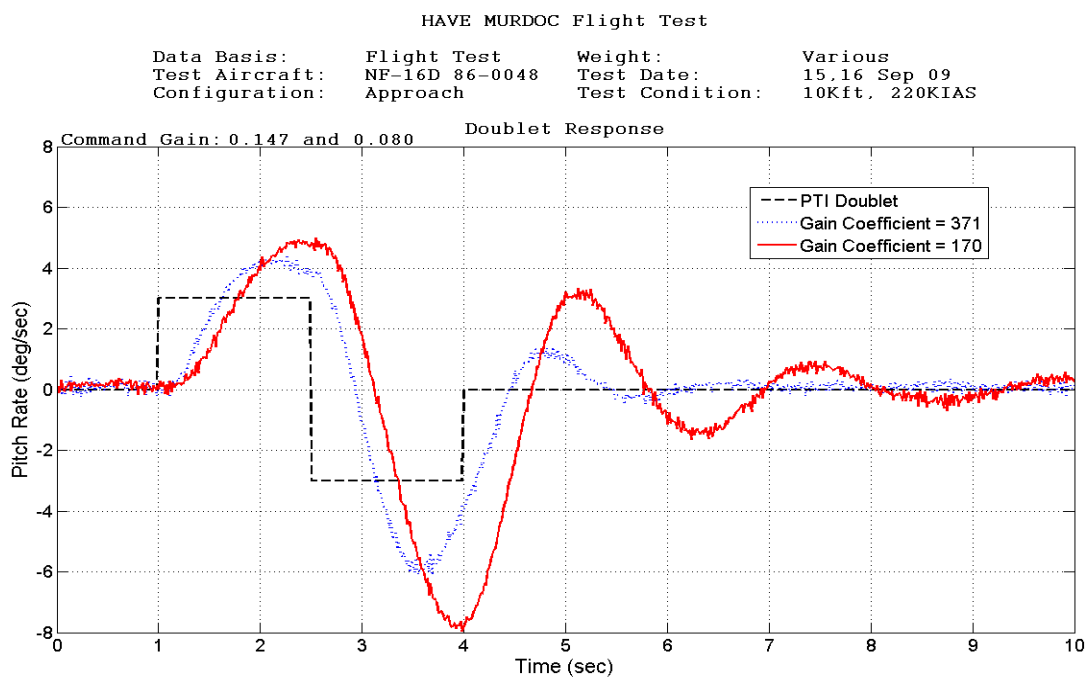

Figure 43: PTI Doublet Comparison between k_{cmd} = 37.1 and 17.0

[1] The actual command gain coefficients were 37.1 and 17.0 per the gain schedule, however, the VISTA interface convention required removing the decimal.

The change in command gain schedule coefficient was necessary to continue with the test plan without risking multiple rate-limit trips interrupting data collection during the approach configuration test points. Figure 44 shows the short period response to a doublet with the command gain set to 170.

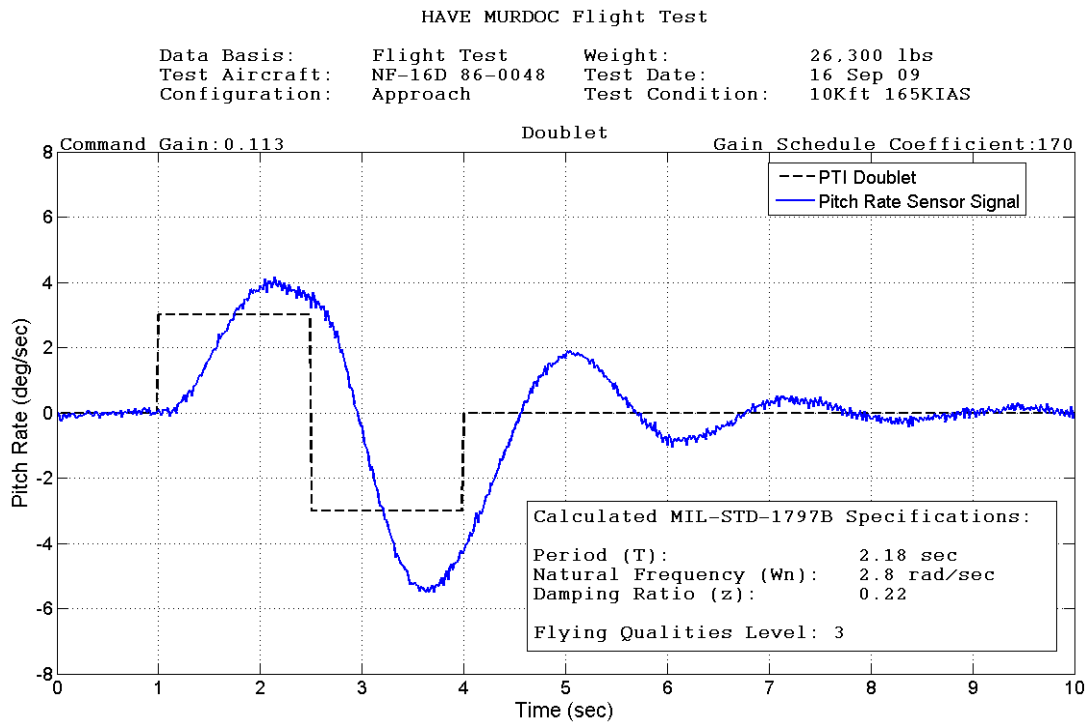

Figure 44: PTI Doublet Response (10K, 165KIAS, k_{cmd} = 17.0)

The calculated natural frequency and damping ratio at 10,000 feet PA and 165 KIAS were ω_n = 2.8 rad/sec and ζ = 0.22. Again, the short period was characterized by a slower and less damped response. Damping was better at 165 KIAS than 220 KIAS as was evident from the higher magnitude and increased number of overshoots at 220 KIAS (Figures 43, 44, and Appendix B).

Maneuvering Flight

Standard F-16 aerobatic maneuvers were flown to qualitatively assess the handling qualities during maneuvering flight with widely varying dynamic pressures. Loops, slicebacks, and slow down turns were flown within the previously cleared flight envelope of altitudes, airspeeds, and angles of attack, α, to assess the longitudinal control characteristics of the DO as airspeed, load factor, and α were varied. The loop was entered at military power with a 4 g pull at 430 KCAS. The pitch control was modulated to maintain 200 KCAS at the top of the loop with a maximum α of 13˚. The loop was completed with a 4 g pull to capture 400 KCAS. The sliceback was completed at 400 KCAS, military power and 120˚ bank. Load factor was varied to maintain 400 KCAS through the maneuver. The slow down turns were flown at 350 KCAS and 400 KCAS. The turns were executed with idle power and a 5 g level turn until 200 KCAS was reached. Throughout the tested envelope, the DO qualitatively performed predictably and satisfactorily for longitudinal control during maneuvering flight. This result was consistent with what was expected from simulation results with the gain schedule applied.

Simulated Turbulence

Simulated turbulence was used to qualitatively evaluate the response of the DO to turbulent air as a buildup to the approach and touchdown phases of the test. With the DO engaged, simulated turbulence was activated by the safety pilot and the evaluation pilot maintained pitch and bank within ±5 degrees while assessing ride quality. In general, the magnitude of the turbulence model was appropriate and assessed to represent light to moderate turbulence. The pilot commented that the turbulence felt like the lateral

component of turbulence was unrealistically large relative to the vertical component. Based on free-flight results, this was assessed to be due to the DOs attempt to generate a zero pitch rate and thus damp out the affect of the vertical component of turbulence. The lateral-directional components of turbulence, however, were not actively damped by the VISTA baseline flight control system. The DO response to turbulence was not objectionable for straight and level flight.

Handling Qualities

The T-38 Tracking tasks discussed in the methodology sub-section above were flown by all three project pilots on three separate sorties. The resultant PIO ratings are tabulated in Figure 45 and reflect the ratings associated with the type of task being performed.

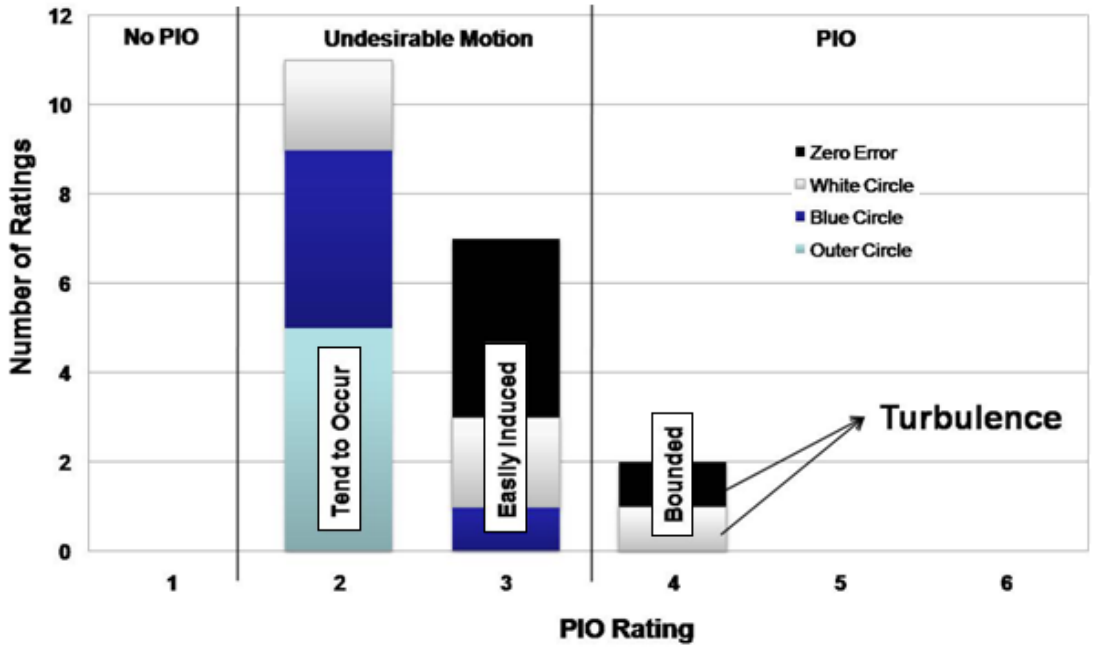

Figure 45: Tracking Task PIO Ratings

The pilots noticed a delay between the pitch rate and the change in the flight path during large magnitude inputs. This mismatch made the aircraft response less predictable during

tracking tasks. Pilots commented that the nose of the aircraft would move as desired, however the aircraft pivoted about the center of gravity with little change to the flight path. For a series of large inputs, the result was the pilot feeling slightly 'out of phase' with the aircraft. The PIO ratings of 2 and 3 reflected this characteristic with one pilot noting that his inputs were completely out of phase with the response of the aircraft and assigned a rating of 4. Of note, the tasks that produced the PIO 4 ratings were conducted with light to moderate turbulence and at 220 KIAS where PTIs resulted in the worst short period frequency and damping. The pilot commented that turbulence noticeably effected handling during high gain tracking. Figure 46 shows the PIO ratings assigned during the Cooper-Harper tracking tasks.

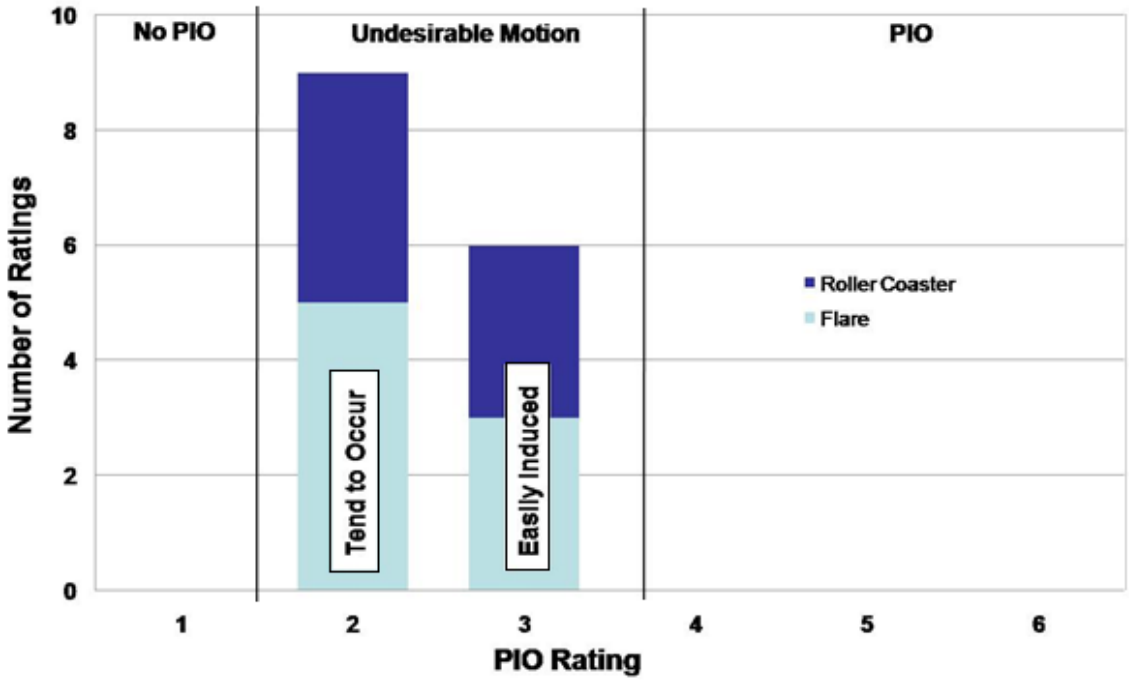

Figure 46: Cooper-Harper Task PIO Ratings

The PIO ratings from the CH tasks were similar to the workload buildup task ratings. No PIO occurred and all ratings were either a 2 or 3. The CH ratings for the tasks are presented in Figure 47.

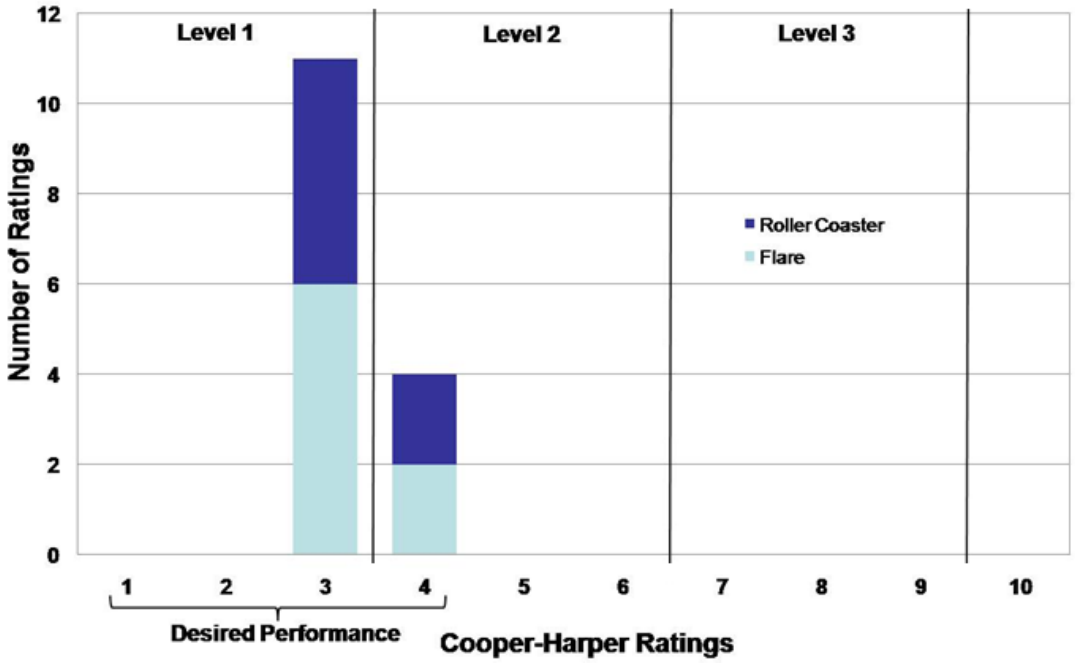

Figure 47: Cooper-Harper Ratings

Pilots noted that for slow, small magnitude corrections, the tracking task was tolerable, however larger corrections to formation position revealed the mismatch between the pitch rate and flight path change. The result was often adequate or desired criteria being obtained, but with a high degree of workload and compensation used to maintain the boundaries of the task. Pilots noted that the presence of light turbulence degraded the task performance more than expected. The handling qualities in the powered approach configuration and airspeeds were sufficient for low gain flight and showed a degradation of flight path control for high bandwidth corrections in the pitch axis. A bounded PIO only occurred during high gain tracking when in turbulent air at 220 KIAS. Therefore,

subsequent low approach and touchdown flight was only conducted when there was no turbulence greater than light. In addition, safety procedures were developed from which the pilots assessed their approach parameters at several distances and altitudes during the approach. If the pilot was outside any defined parameters, the approach was terminated and a go-around initiated.

Low Approach

Multiple low-approaches were flown by each test team pilot to demonstrate DO control when pilot input gains were increased due to the proximity to the runway. In addition, handling qualities were assessed as a buildup to completing the runway touchdown objective. All approaches were flown with the DO active for the final 4 to 5 miles. Each test team pilot flew their first low approach to a minimum 100 feet AGL go-around and subsequent approaches were flown to 50 feet AGL. Low approach conditions and pilot comments are listed in Table 4.

Table 4: Low Approach Pilot Comments

Sortie Number & Date	Pilot Background	Approach Type	Wind Conditions (Runway 22)	Pilot comments
6 16 Sep	F-15I F-16I 3500hrs	100ft	240/12	No problems other than trim
		50ft	250/15	Pitch angle capture generates small overshoots. Easily stopped by backing out of control loop.
		50ft	240/15	Smooth
7 18 Sep	F-16 2100hrs	100ft	270/8	Small amplitude pitch oscillations when fine tracking
		50ft	260/10	Smooth deliberate inputs work well.
		50ft	260/10	No issues preventing continue to touchdown
8 18 Sep	C-17 B-2 T-38 2800hrs	100ft	250/12	Similar to F-16 with slight lag and less damping
		50ft	250/10	Slight pitch bobble during fine tune tracking
		50ft	250/10	Lack of trim requires continuous forward stick compensation (same for all approaches)

The DO controlled VISTA handling was described as being similar to the F-16 with a less damped response to fine pitch changes (see Table 4 for pilot experience). This result was consistent with the handling qualities evaluations previously discussed. None of the approaches flown resulted in objectionable results preventing continued pursuit of the runway touchdown objective.

Landings

Several runway touch-and-goes were conducted with the DO controlling the longitudinal axis of the VISTA. The wind conditions were light and variable during first touchdown sortie and turbulence was negligible. Due to safety regulations, a Calspan evaluator pilot that flew the first touchdown sortie and made five runway touchdowns with the VSS engaged (Figure 48).

Figure 48: First Runway Landing with Disturbance Observer

The pilot determined the DO controller was not objectionable for approach and landing so the test team continued with the final three sorties. Each project pilot flew one of the final three test sorties. The primary objective of each sortie was to demonstrate a runway

touchdown. In addition, shallow (2˚) and steep (3˚) approaches were flown to qualitatively assess handling qualities during approach and touchdown. Pilot comments were the primary data collected during the touchdown sorties. All approaches were initiated just prior to east lakeshore (approximately 4 mile final) and continued to runway touchdown. At touchdown, the evaluation pilot planned to maintain landing attitude while the safety pilot disengaged the VSS with the rear cockpit paddle switch and initiated a go-around. The approach conditions and pilot comments are listed in Table 5.

Table 5: Pilot Comments for Landing

Sortie Number & Date	Pilot Background	Wind Conditions (Runway 22)	Approach Type	Pilot comments
10 21 Sep	F-15I F-16I	040/6	2.5˚	Safe touchdown, tiny burble, immediate trip
			2.5˚	Nose up pitch upon touchdown and VSS trip
			2.5˚	Safe touchdown
			3.0˚	Well timed flare and rate required
			2.0˚	No issues. Immediate safety trip at touchdown
11 23 Sep	F-16	270/8	2.5˚	No problems. Immediate trip at touchdown
			2.5˚	Increased aggressiveness causes small oscillations
			2.5˚	No issues
			3.0˚	Timing is key
			2.0˚	Lack of trim was only issue
12 23 Sep	C-17 B-2 T-38	260/12	2.5˚	Small oscillations with fine tuning control
			2.5˚	Similar to F-16, no issues
			2.5˚	Bobble when got behind on flare and made rapid input
			3.0˚	Easy with one smooth pull. When reversing control input, get oscillations
			2.0˚	Small oscillations due to small control reversals

All touchdowns resulted in an immediate VSS trip upon contact with the runway surface. The safety trips were due to elevator control surface rate limits. They were not unexpected due to the forces associated with runway touchdown acting on system

sensors. All runway touchdowns were completed safely, however, pitch oscillations were witnessed and consistent with what was expected due to the results of the previous handling qualities evaluation and simulation results.

Post Flight Test Simulation

The flight test plan did not allow for the fine tuning of the DO during execution of the test. Therefore, the test team was unable to change the desired dynamics to potentially improve the flying qualities that the original DO design produced. As discussed earlier and shown in Figure 35 above, the flying qualities were predicted to be slower and less damped than desired due to the affect of the time delay and resultant gain schedule. In an effort to improve the predicted flying qualities, the desired dynamics were changed to produce higher frequency and damping ($\zeta = 0.7$ and $\omega = 5$ (rad/sec)). The following is a plot of the simulated response to a doublet at three different flight conditions with the new DO parameters.

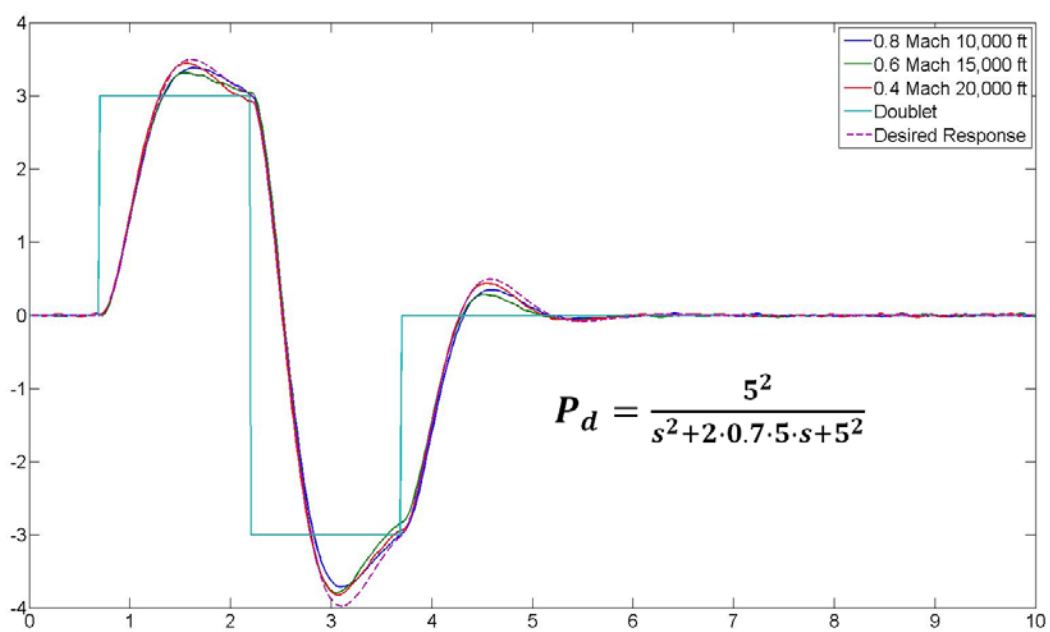

Figure 49: Doublet Response with New Desired Dynamics

The aircraft responses are plotted against the original desired response represented by $\zeta = 0.5$ and $\omega = 4$ (rad/sec). The plot clearly shows that changing the parameters in P_d can produce the flying qualities that one desires.

Summary

Flight test conducted in conjunction with project Have MURDOC at the USAF Test Pilot School demonstrated that the disturbance observer adequately controlled the pitch axis of the VISTA across a large flight envelope. Controller/VISTA integration led to the requirement to gain down the command signal to prevent instabilities. In addition, sensor noise was amplified rather than attenuated by the DO controller. Flying qualities were slightly worse than the DO defined 'desired dynamics' with reduced damping and natural frequency. Handling qualities were affected by light damping yet were adequate for low gain approaches and landings. Conclusions and suggestions for future research are discussed in the following chapter.

VI. Discussion

Chapter Overview

The overall objective of this effort was to validate disturbance observer theory through piloted simulation and flight test. Improvements were made to the lateral and directional axes designs with the pitch and roll axes tested in the Octonian simulator at AFRL. The pitch axis DO was evaluated during project Have MURDOC at the USAF Test Pilot School. This chapter presents the major conclusions of this effort and presents recommendations for future research.

Conclusions of Research

The first sub-objective of this research was to improve the design of the lateral and directional axes controllers. The roll axis controller performance was greatly improved by changing the desired dynamics and design filters from a first order to a second order transfer functions. Changing the number of variables allowed for greater design flexibility and improved performance. Though not fully investigated, this result suggests that potential exists to improve the overall DO design by fine tuning the form of P_d.

Handling qualities were evaluated in the Octonian flight simulator at AFRL. The 'level 1' DO generated the best performance and handling qualities ratings among the 20 pilots. The 'level 2/3' DO produced poor ratings and performance as predicted. The results solidify the claim that 'desired' handling qualities can be produced by the DO controller, whether good or bad, throughout the flight envelope.

The pitch DO showed a significant degradation in performance and ratings at the high and slow flight condition. Desktop simulation hinted at this result due to the slight overshoot of the desired dynamics when compared to the rest of the flight envelope. Though there was a degradation of performance and ratings between flight conditions, it was significantly less than those seen with the Block 40 F-16 results. This suggests that the DO is attempting to generate consistent flying qualities however it may be demanding more from the aircraft than is normally expected at such a low speed and high altitude.

DO integration on the VISTA simulator produced an unstable response that was due to a time delay inherent in the VISTA model that was not present in the AFIT F-16 model. When applying the same time delay to the AFIT F-16 the response was unstable. A command gain schedule was required to stabilize the DO as implemented on the VISTA. Flight test resulted in validation of the gain schedule and therefore the VISTA model contained within the handling qualities simulator at the USAF Test Pilot School. The time delay was a result of VISTA specific implementation and one can conclude that the DO would not require the command gain to be reduced as much with implementation on other aircraft. The performance would therefore improve with an increase in command gain.

Throughout all flight test, a high frequency 'buzz' was noticed by the pilots and determined to be due to pitch rate sensor noise. The DO feedback filter, Q/P_d, amplified the sensor noise by a factor proportional to the ratio of the design filter frequency over the desired dynamics frequency. The noise amplification was significantly reduced when the design filter frequency was changed to a value closer to the desired dynamics frequency.

Flight test flying qualities were less damped and slightly slower than simulation. This resulted in poor handling qualities during high gain tracking. Unfortunately, test plan limitations prevented the fine tuning of the desired dynamics' parameters. Post test simulation results show improved flying qualities when the parameters that define P_d are changed to command higher damping and frequency.

The DO ultimately demonstrated great potential for use on future aircraft. The simple flight control method proved that desired and consistent handling could be generated throughout a large flight envelope. The pitch axis controller successfully controlled the VISTA during 12 flight test sorties and culminated in multiple runway touchdowns.

Significance of Research

Most modern aircraft are highly augmented and use gain scheduling to ensure good handling throughout the flight envelope. The disturbance observer is a relatively simple, yet powerful controller that generates desired and consistent flying qualities throughout a large flight envelope. This research effort improved upon the lateral and directional axes designs and demonstrated that desired performance is achievable from all three axes throughout the simulation flight envelope.

Flight test resulted in determining some limitations that exist in the DO as currently designed. The existence of a time delay in the VISTA model, though not test halting, highlighted the need for proper modeling during design. Had the time delay been modeled into the original design, perhaps a DO filter combination would have been generated that didn't rely on a gain schedule for flight. Also, since the time delay was

specific to the way the VISTA operates in the simulation mode, the DO could potentially perform better when applied to other aircraft's flight control systems.

Sensor noise was not modeled during the original simulation, and thus the DO design that was flight tested allowed a high frequency 'buzz' to permeate the system. Both of these modeling error results speak to how important it is to conduct flight test. Years of research and multiple simulations were conducted with good results before the design limitations were discovered as a result of flight test conducted during this effort.

Despite the limitations of the current DO design, the controller was remarkably successful in controlling a highly maneuverable aircraft with F-16 performance capabilities. In less than nine short test flights, the DO went from theory, to controlling the VISTA to many successful runway touchdowns. The results of this effort helped pave the way for future DO research and flight test.

Recommendations for Future Research

The results of flight test conducted during this effort helped to validate the VISTA model in the TPS handling qualities simulator. Future research should include updating the system model to develop a design filter parameter feasibility region that accounts for varying amounts of time delay. In addition, if the DO is integrated on a variable stability aircraft with adjustable simulation rates, the simulation rate should be run as high as possible to minimize the built-in time delay.

The form of P_d should be examined further. Results seen when changing the roll axis from a first to second order model show that more flexibility exists when multiple parameters are available to tune. This may include adding zeros to the numerators of P_d and Q. In addition, the new DO design should focus on minimizing or eliminating the

sensor noise. The sensor noise amplification was the culprit in causing actuator rate limit trips while flying in the approach configuration. Future research should investigate the effects of adding noise filters to the sensor signal as well.

The roll axis DO should be implemented on the handling qualities simulator at TPS and fine tuned. The DO, as currently designed, is capable of providing educational value to TPS students. The controller allows the user to choose a desired response to an input, then see how the aircraft handles during flight in the simulator. Different desired dynamics can be programmed and flown in succession allowing the student to compare the flying qualities of aircraft with different frequencies and damping ratios.

Finally, the DO should be designed around and implemented on the Calspan variable stability Learjet. Doing so would provide more avenues for fine tuning the controller theory and allow the user to flight test the roll and yaw axes DOs.

Summary

The objective of this effort was to validate disturbance observer theory by conducting piloted simulation and flight test. The results clearly show that the DO has potential for use in future aircraft. The lateral and directional axes were re-designed and simulation resulted in desired and consistent performance. Flight test was successfully conducted on the VISTA during project Have MURDOC at the USAF Test Pilot School. The relatively simple design of the DO was effective in controlling the highly maneuverable and inherently unstable airframe of the VISTA. Limitations with the current design were discovered, however, potential exists to minimize or even eliminate them and develop a controller that can be used on future aircraft.

Bibliography

Ackermann, J., P. Blue, T. Bunte, L. Guvenc, D. Kaesbauer, M. Kordt, M. Muhler, D. Odenthal. *Robust Control: The Parameter Space Approach, Second Edition.* London: Springer, 2002.

Blake, Ryan D., *Boundary Avoidance Tracking: Consequences (and Uses) of Imposed Boundaries on Pilot –Aircraft Performance.* MS thesis, AFIT/GAE/ENY/09-M03. Air Force Institute of Technology, March 2009.

Blakelock, John H., Automatic Control of *Aircraft and Missiles, Second Edition.* New York: John Wiley & Sons, Incorporated, 1991.

Blue, P., D. Odenthal, M Muhler. *Designing Robust Large Envelope Flight Controllers for High-Performance Aircraft.* AIAA 2002-4450, Guidance, Navigation, and Control Conference and Exhibit, Monterey CA, August 2002.

Coldsnow, Matthew W., *Alternative Methods to Standby Gain Scheduling Following Air Data System Failure.* MS thesis, AFIT/GAE/ENY/09-S02. Air Force Institute of Technology, September 2009.

Cooper, G. E. and Harper, R.P, Jr. *The Use of Pilot Rating in the Evaluation of Aircraft Handling Qualitie.* NASA TN D-5153, 1989.

Department of Defense. *Flying Qualities of Piloted Aircraft*. MIL-STD-1797B. Wright-Patterson AFB, 15 February 2006.

Dotter, Jason. *An Analysis of Aircraft Handling Quality Data Obtained from Boundary Avoidance Tracking flight Test Techniques*. Air Force Institute of Technology, 2007.

Gray, William. A *Boundary Avoidance Tracking Flight Test Technique for Performance and Workload Assessment*. Society of Experimental Test Pilots, 2007.

Nelson, Robert C. *Flight Stability and Automatic Control, Second Edition*. Boston: McGraw-Hill, Incorporated, 1998.

Rein, Donevan A.; Kennedy, Jeff M.; Lachs, Shlomi; Dweyer, Derek R. *Multi-Use Rate Disturbance Observer Controller (Have MURDOC)*. AFFTC-TIM-09-08, 2009.

Rivin, Eugene I. *Stiffness and Damping in Mechanical Design*. New York: Marcel Dekker, Incorporated, 1999.

Stevens, Brian L. and Frank L. Lewis. Aircraft Control and Simulation, Second Edition. New Jersey: John Wiley & Sons, Incorporated, 2003.

Appendix A. Gain Schedule Determination

```
Optimization Function for finding the best Gain 'K' for the Host Sim
Model. ‘fminsearch’ varies the variables passed to it (design filter,
Qw Qz and command gain K1)in an attempt to minimize the function ‘f’
below.  The ‘minimize1’ simulation is called and run with the three
variables.  The output of the simulation ‘qdesdot’ and ‘qdot1’ are used
in the function ‘f’.  ‘fminsearch’ continues to run until the short
period response in the simulation is close to the desired response. The
design filter variables and command gain are output at the end of the
search.

close; clc; clear;
warning off
W = 4;
Z = .5;

Qw = 26.2;
Qz = .5;
k1 = .1;

x0=[.1 26.2 .5];
[x fval] = fminsearch(@(x) finder1(x(1), x(2), x(3)),x0);

function f = finder1(k1, Qw, Qz)

assignin('base', 'k1', k1);
assignin('base', 'Qw', Qw);
assignin('base', 'Qz', Qz);
sim minimize1
qdes=qdes.signals.values(10:500);
q1=q1.signals.values(10:500);
qdesdot=qdesdot.signals.values(10:500);
qdot1=qdot1.signals.values(10:500);
assignin('base', 'qdesdot', qdesdot);
assignin('base', 'qdot1', qdot1);
assignin('base', 'qdes', qdes);
assignin('base', 'q1', q1);

f =((qdesdot-qdot1).^2);
f = sum(f)
```

Simulink® model for design filter and command gain optimization:

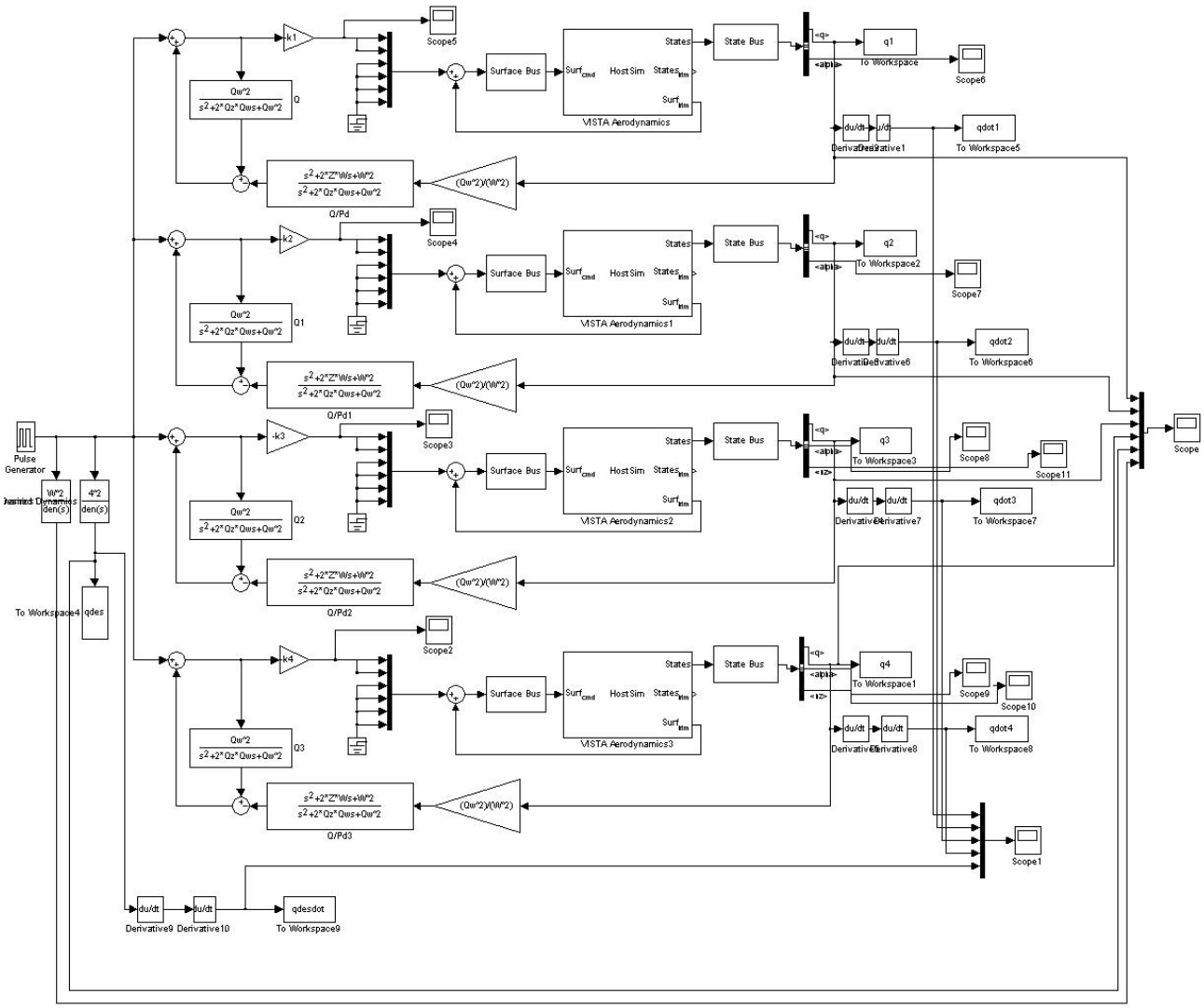

Appendix B. Half Page PTI Plots

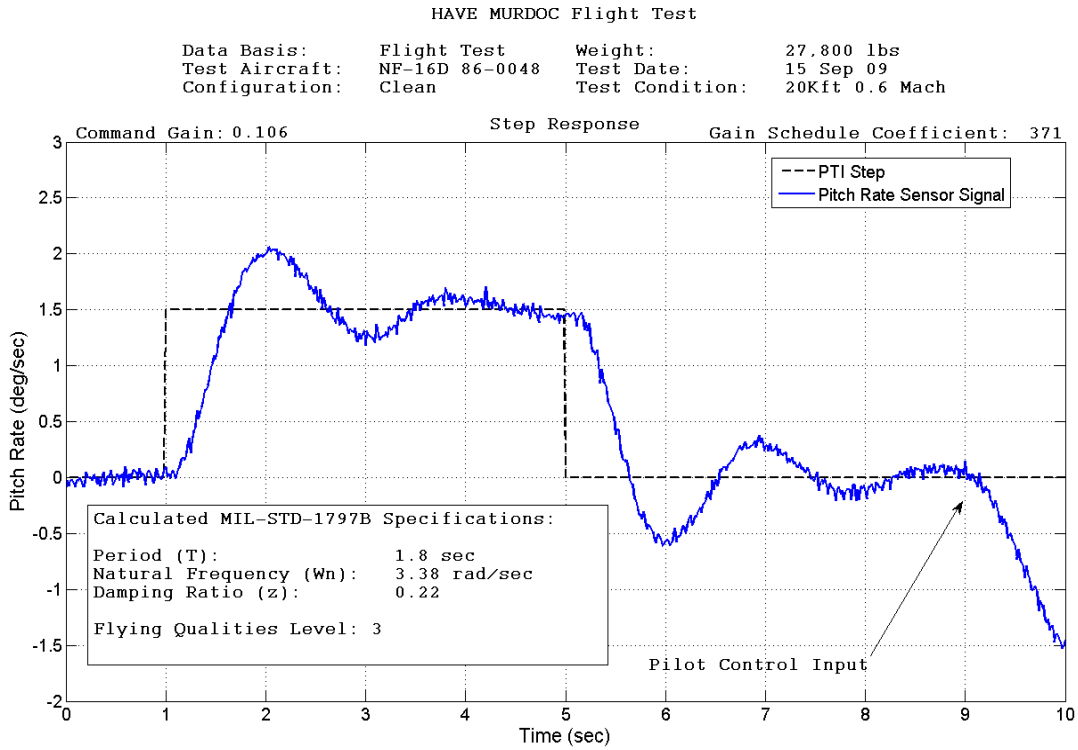

Figure 50: Step (20K, 0.6 Mach)

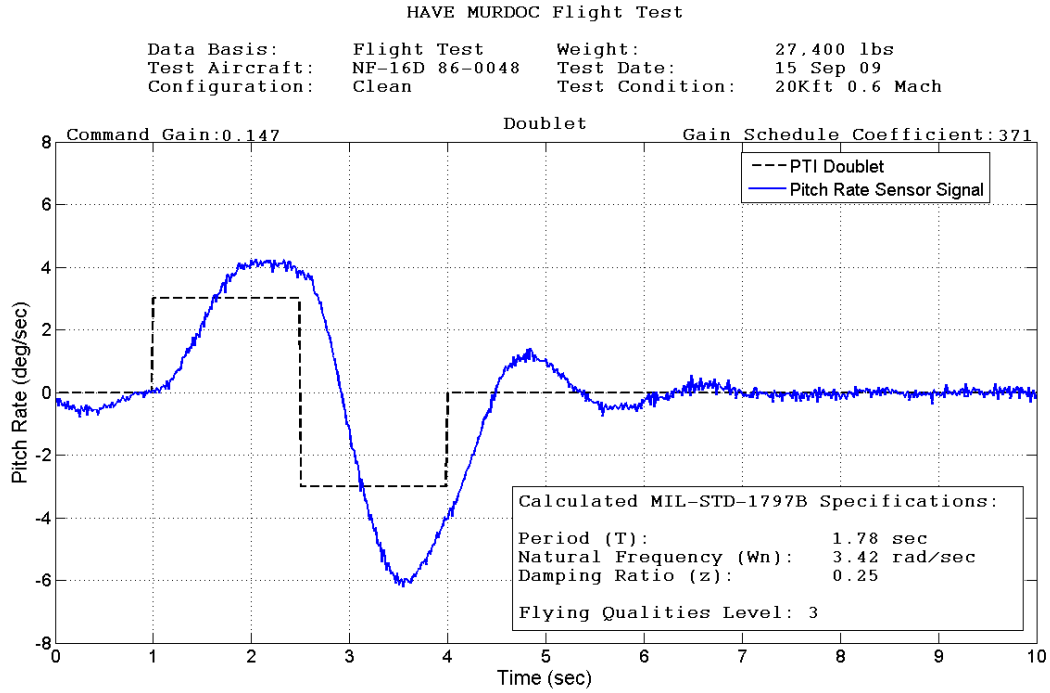

Figure 51: Doublet (20K, 0.6Mach)

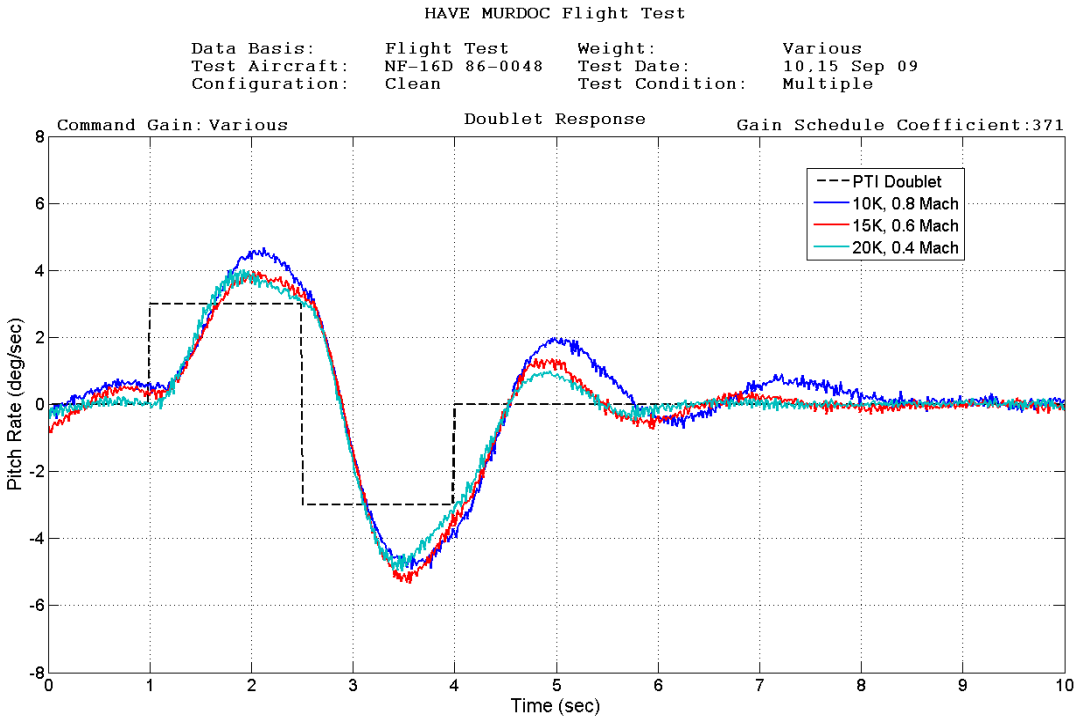

Figure 52: Doublet (Three Flight conditions)

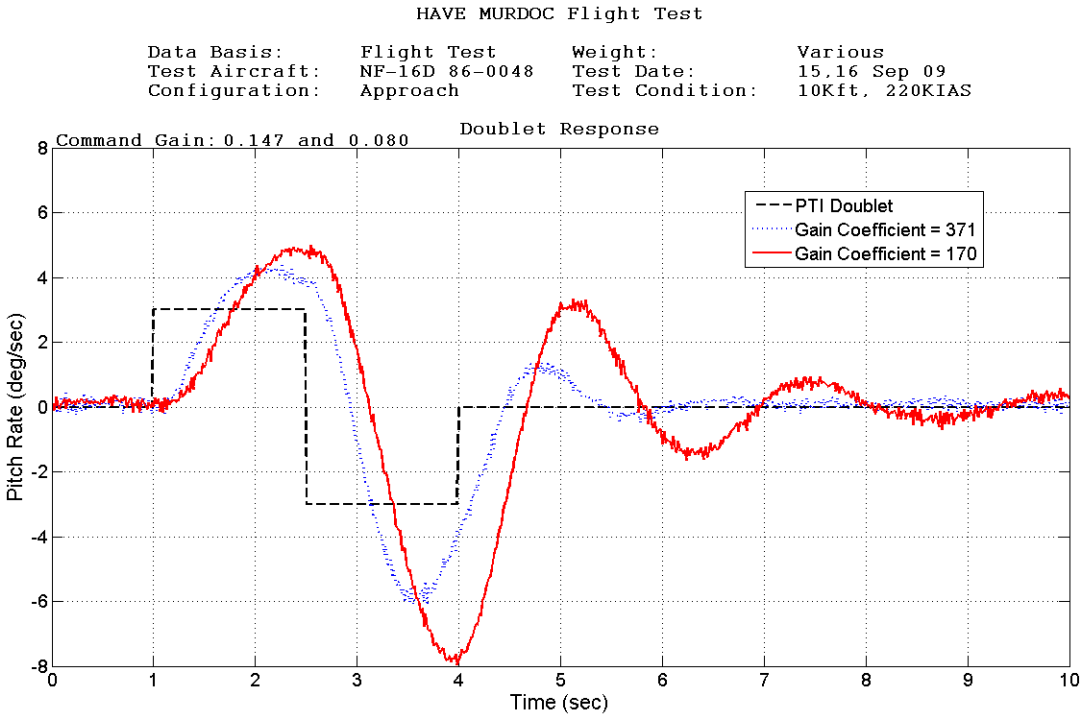

Figure 53: Doublet (10K, 220KIAS, k_{cmd} = 371 & 170)

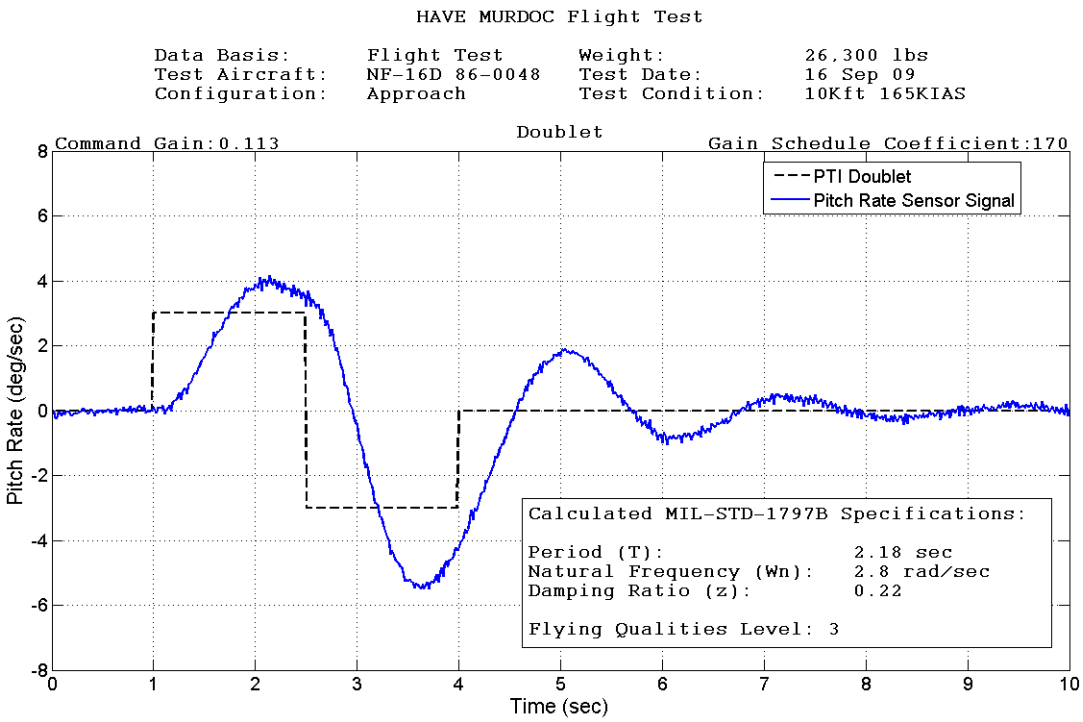

Figure 54: Doublet (10K, 165KIAS)

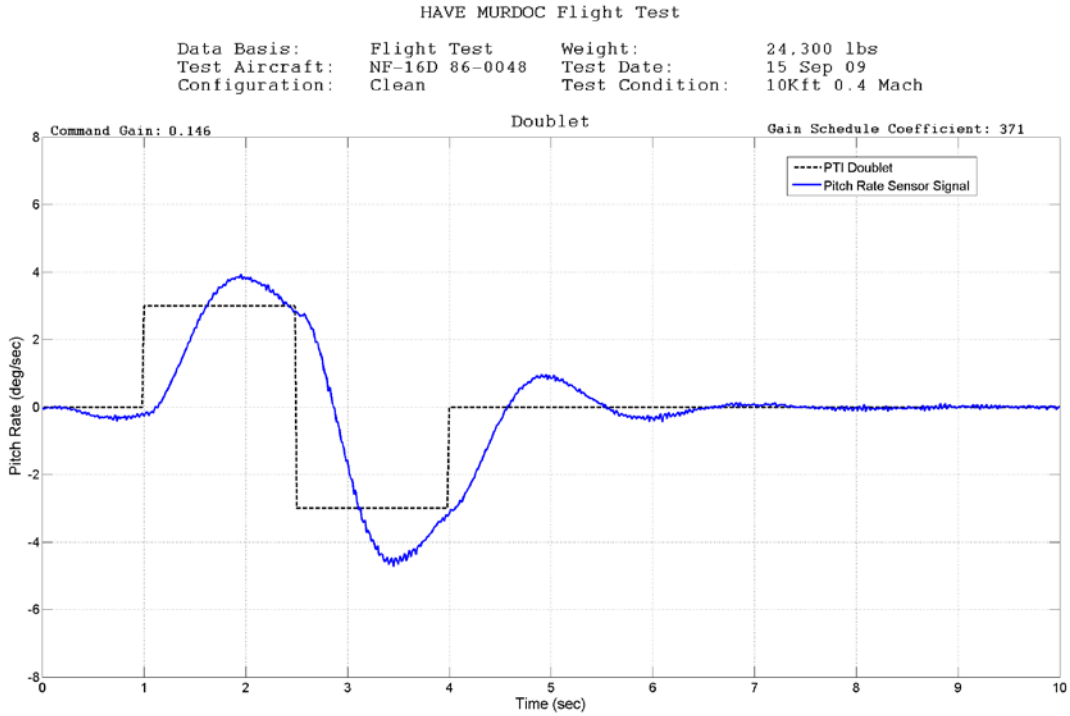

Figure 55: Doublet (10K, 0.4 Mach)

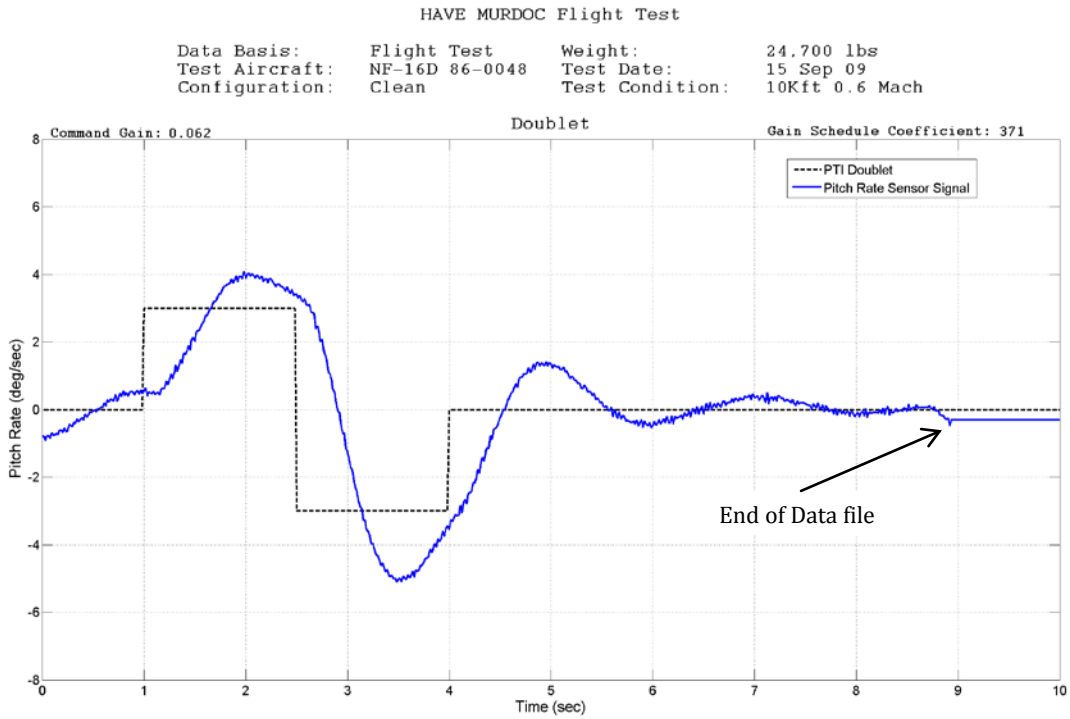

Figure 56: Doublet (10K, 0.6 Mach)

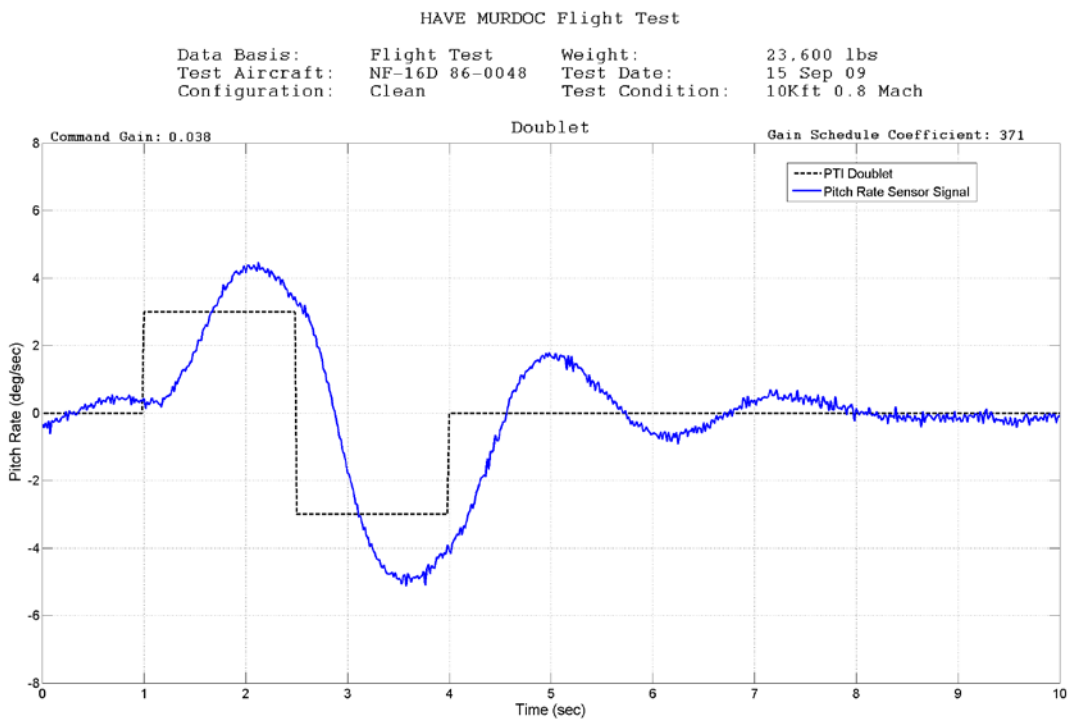

Figure 57: Doublet (10K, 0.8 Mach)

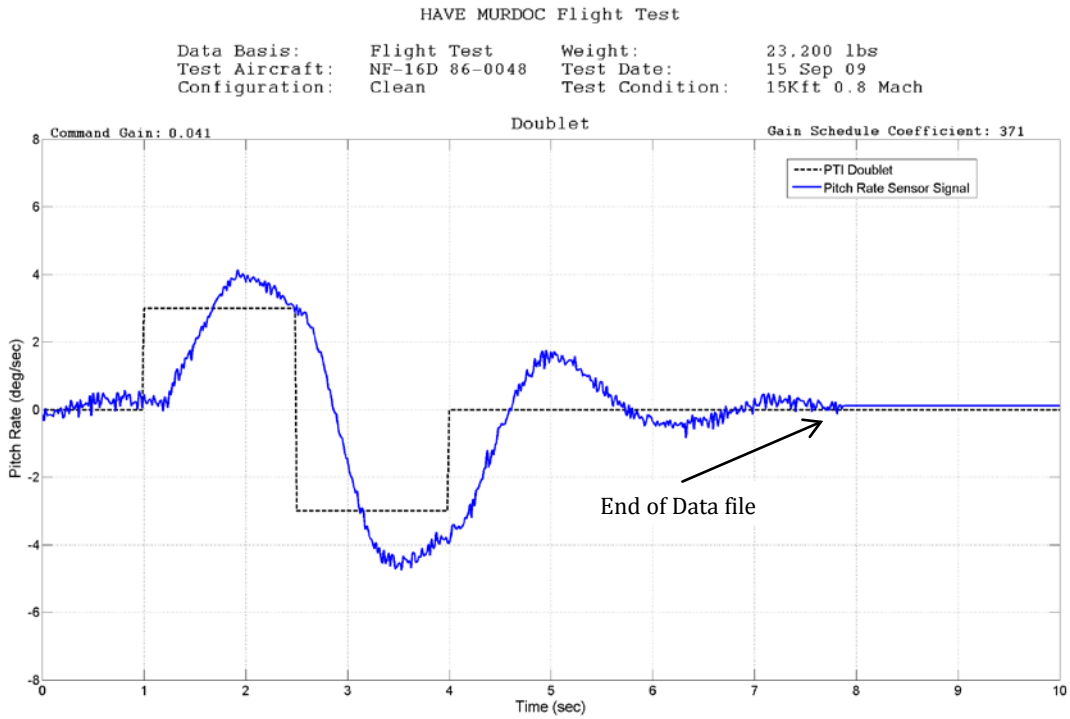

Figure 58: Doublet (15K, 0.8 Mach)

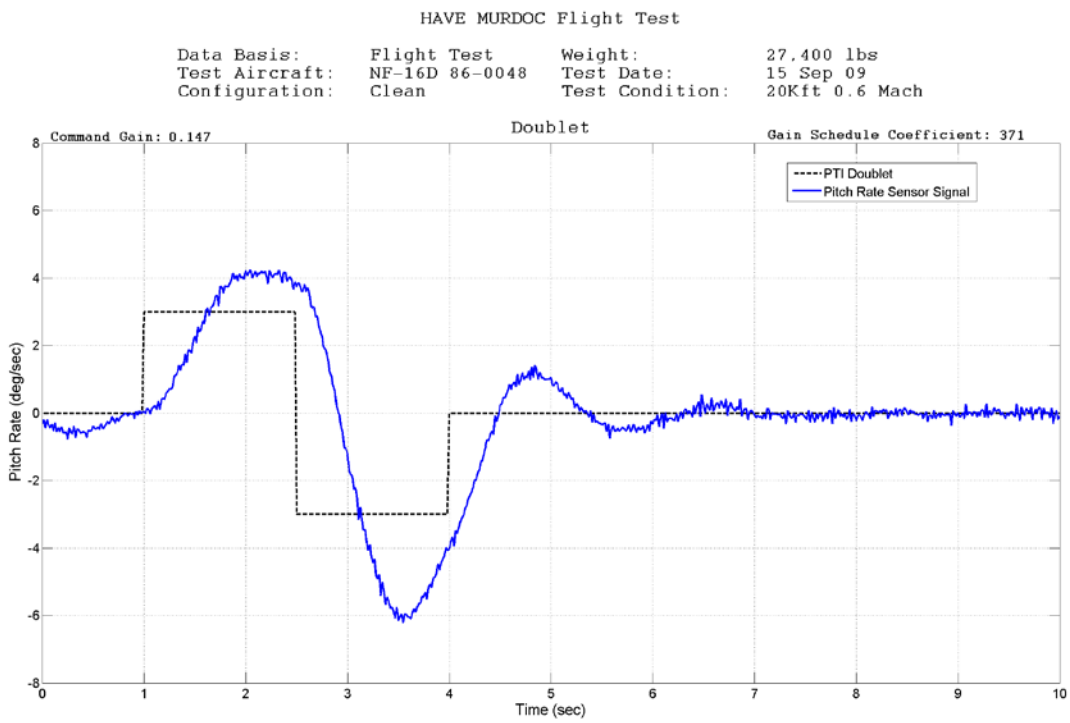

Figure 59: Doublet (20K, 0.6 Mach)

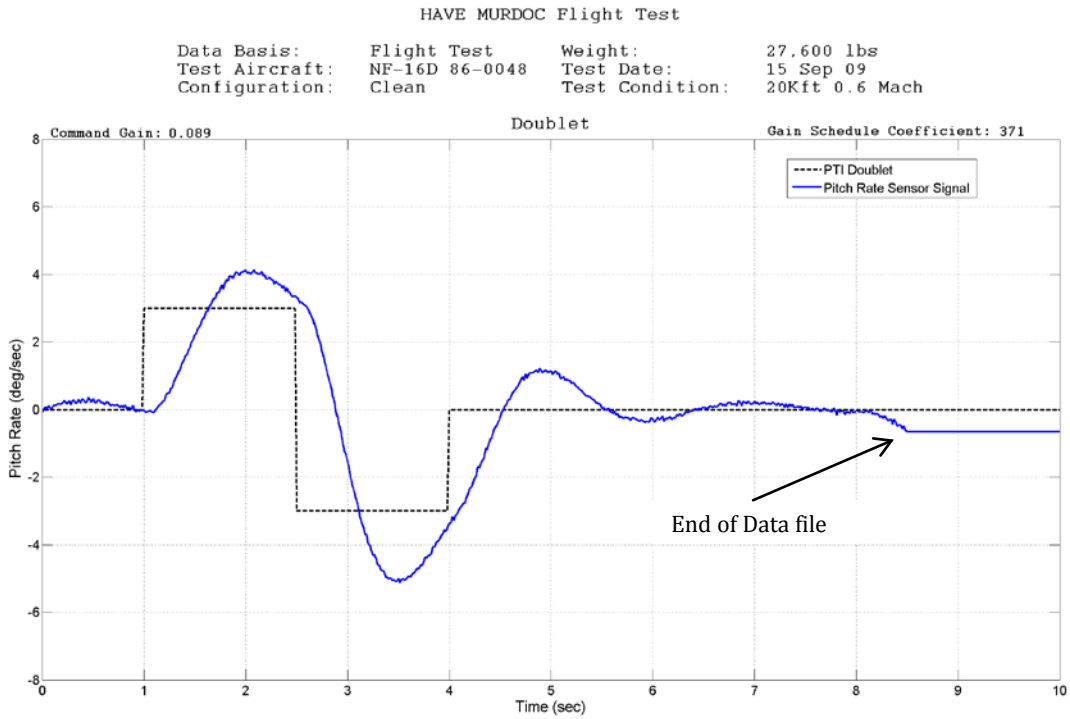

Figure 60: Doublet (20K, 0.6 Mach)

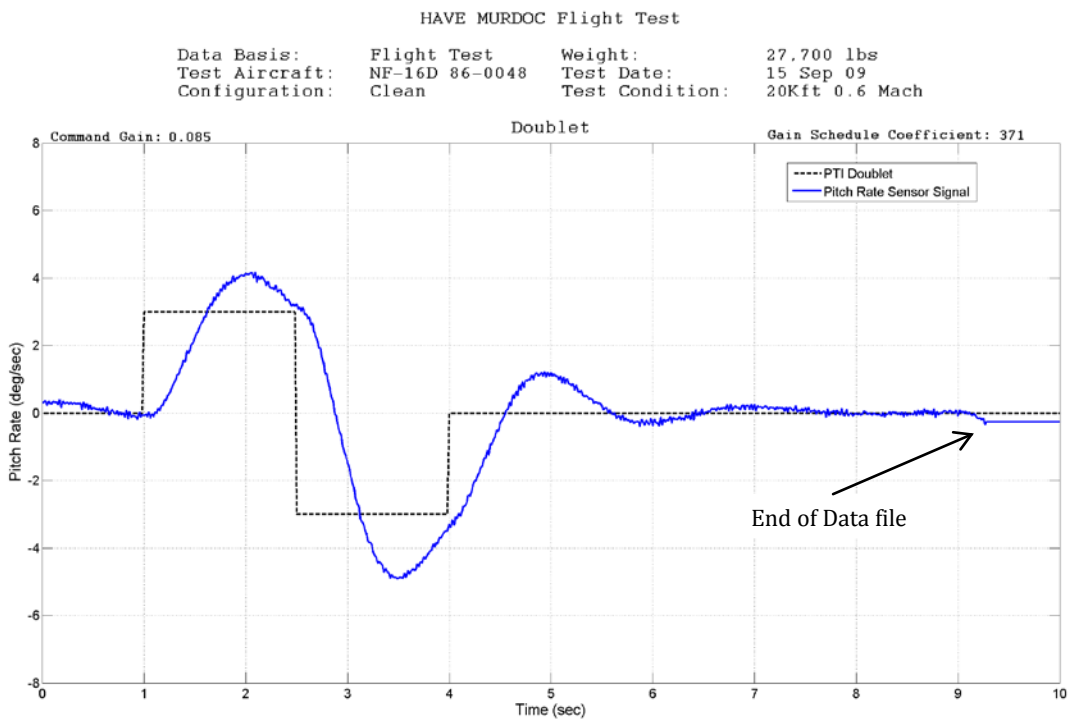

Figure 61: Doublet (20K, 0.6 Mach)

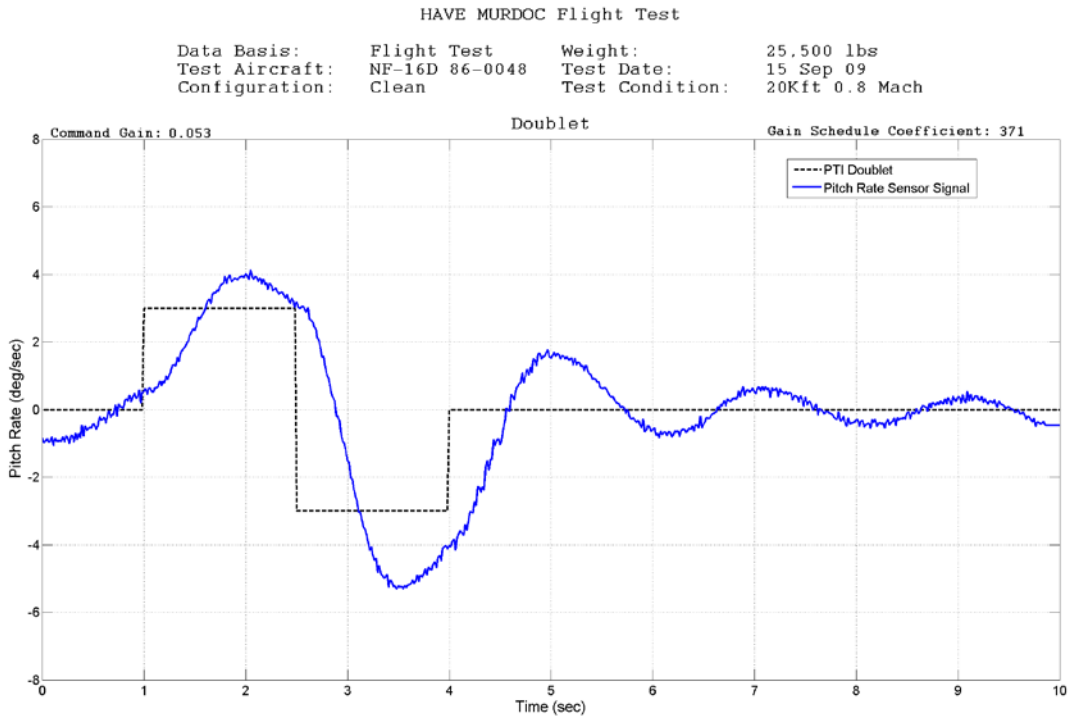

Figure 62: Doublet (20K, 0.8 Mach)

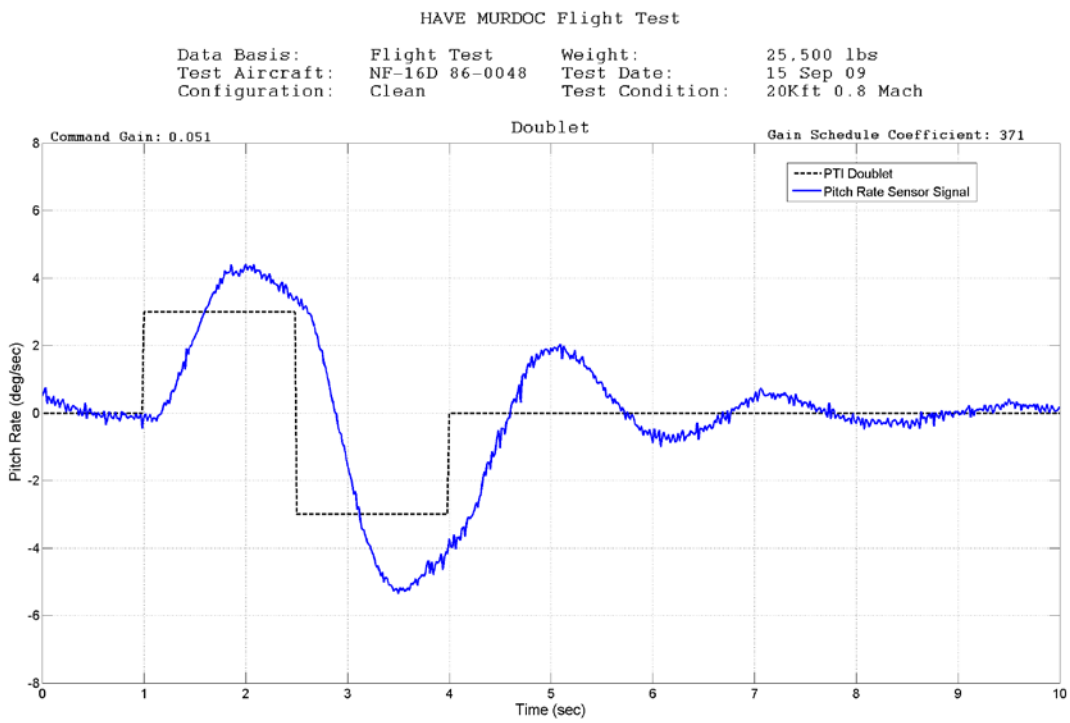

Figure 63: Doublet (20K, 0.8 Mach)

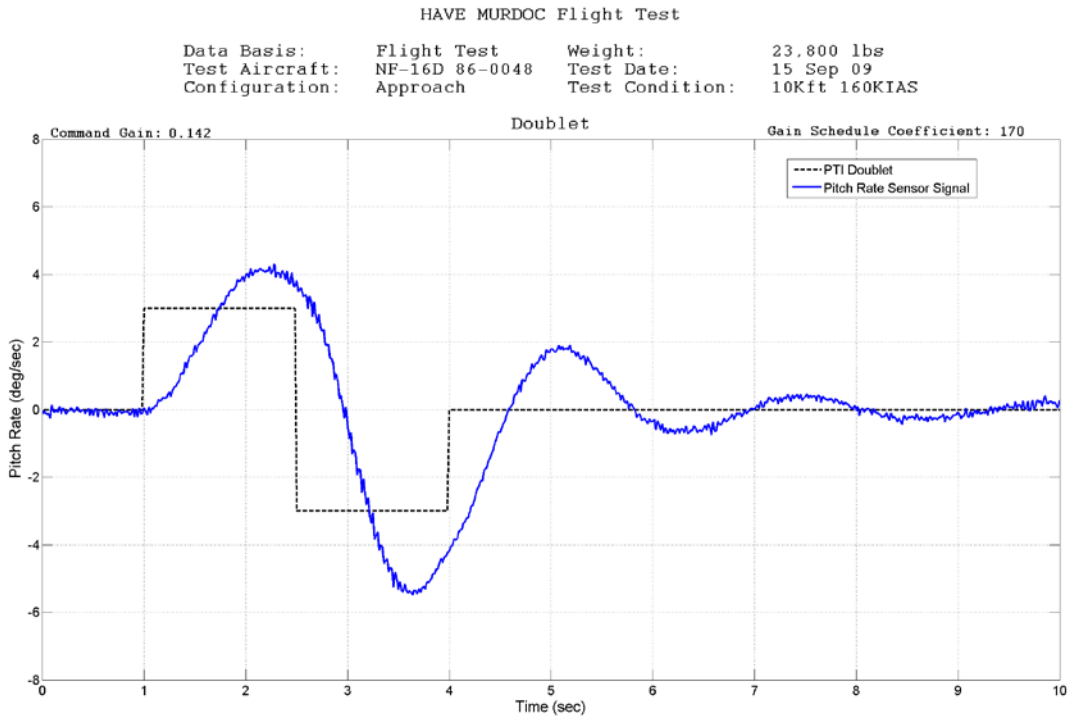

Figure 64: Doublet (10K, 160KIAS)

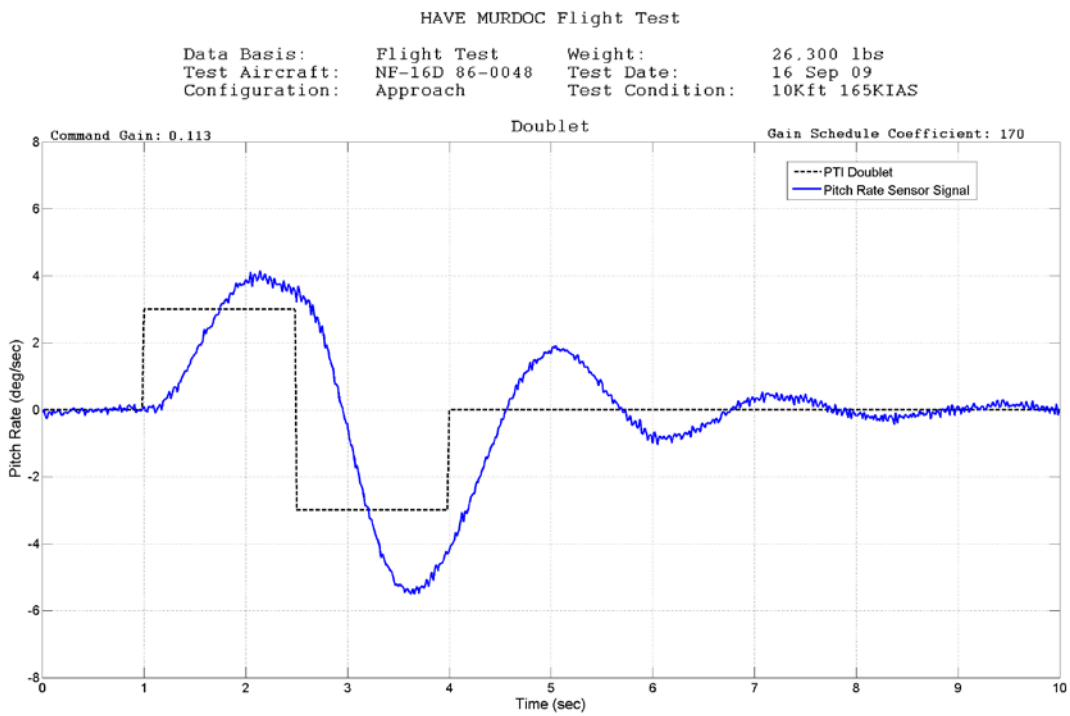

Figure 65: Doublet (10K, 165KIAS)

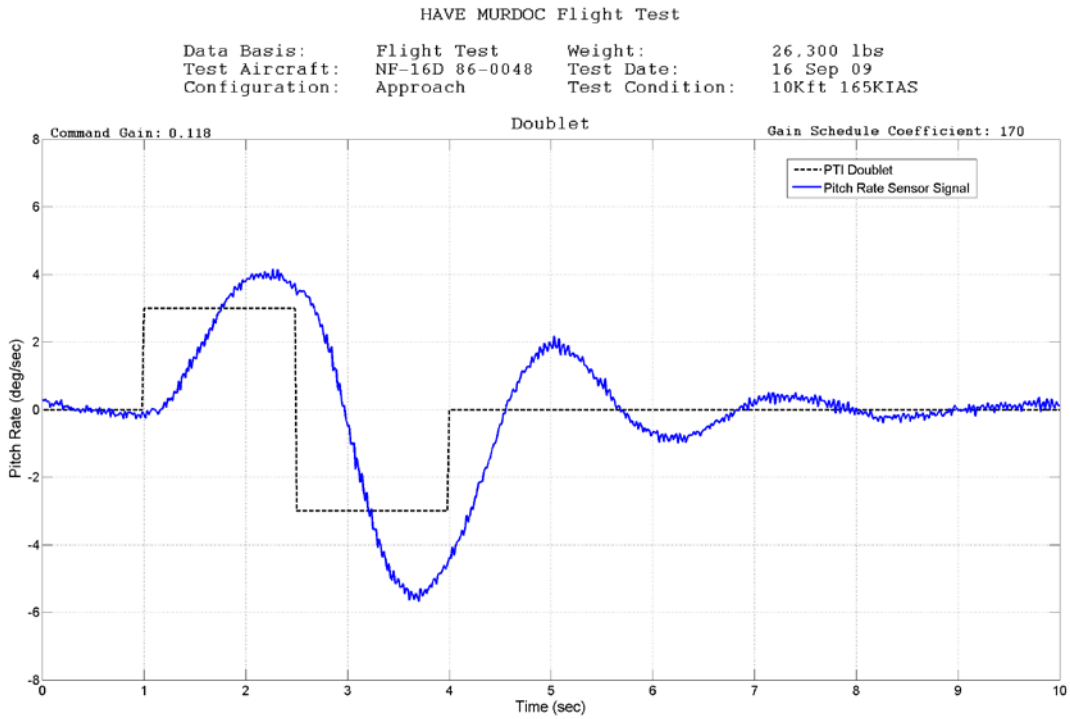

Figure 66: Doublet (10K, 165KIAS)

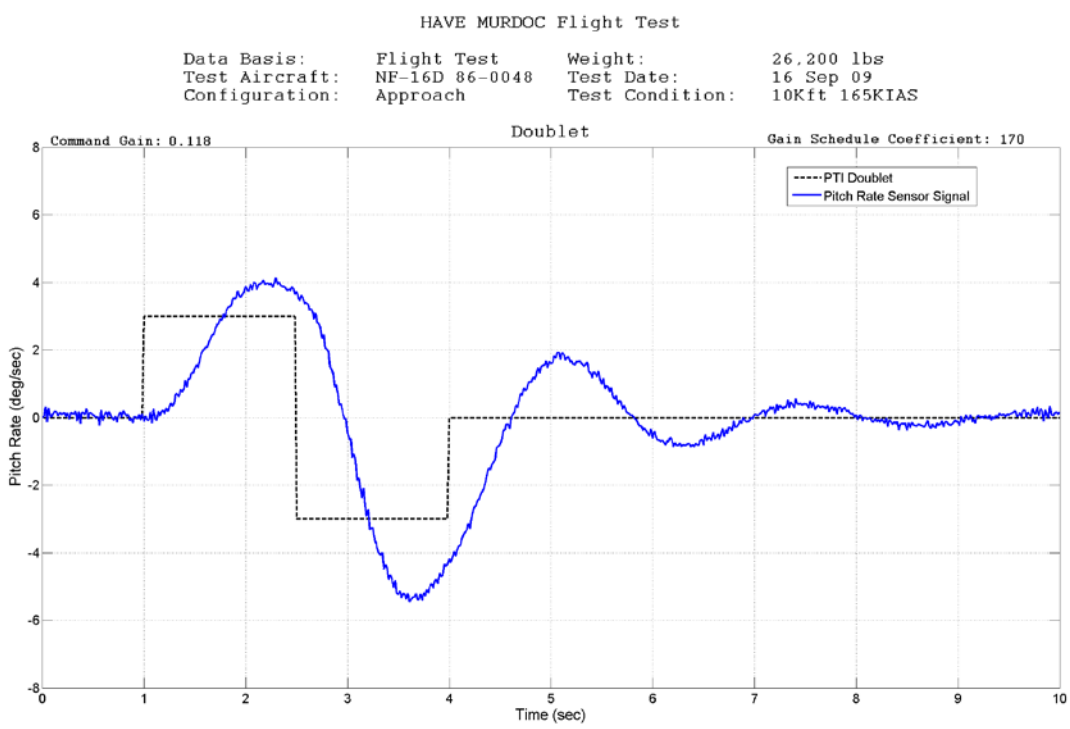

Figure 67: Doublet (10K, 165KIAS)

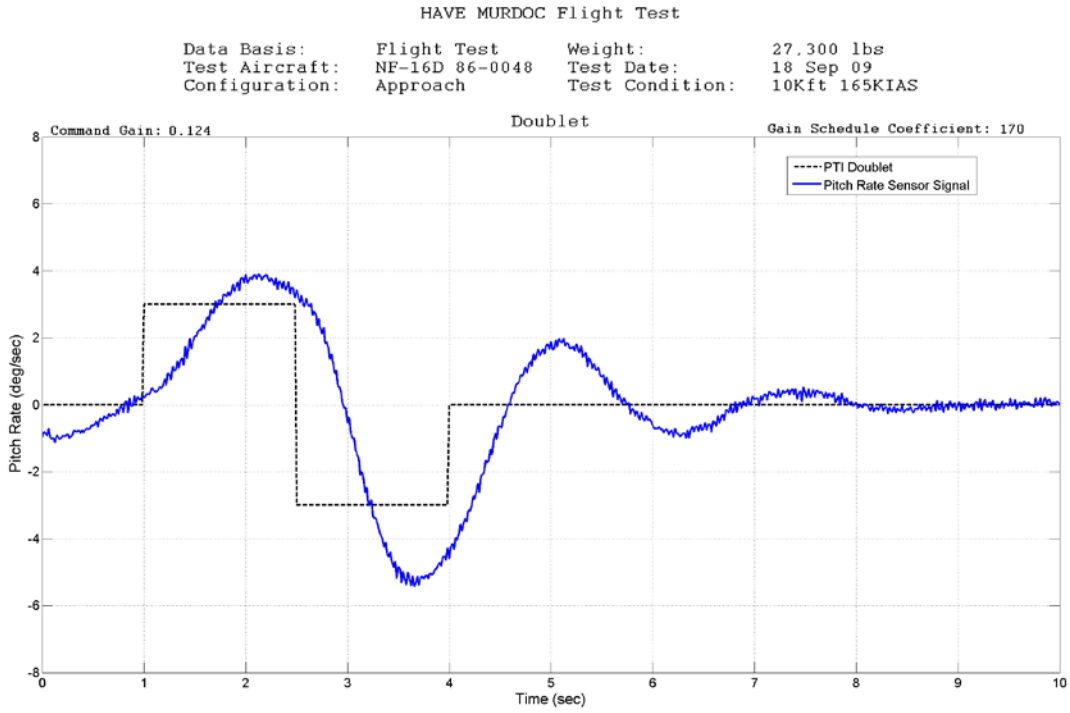

Figure 68: Doublet (10K, 165KIAS)

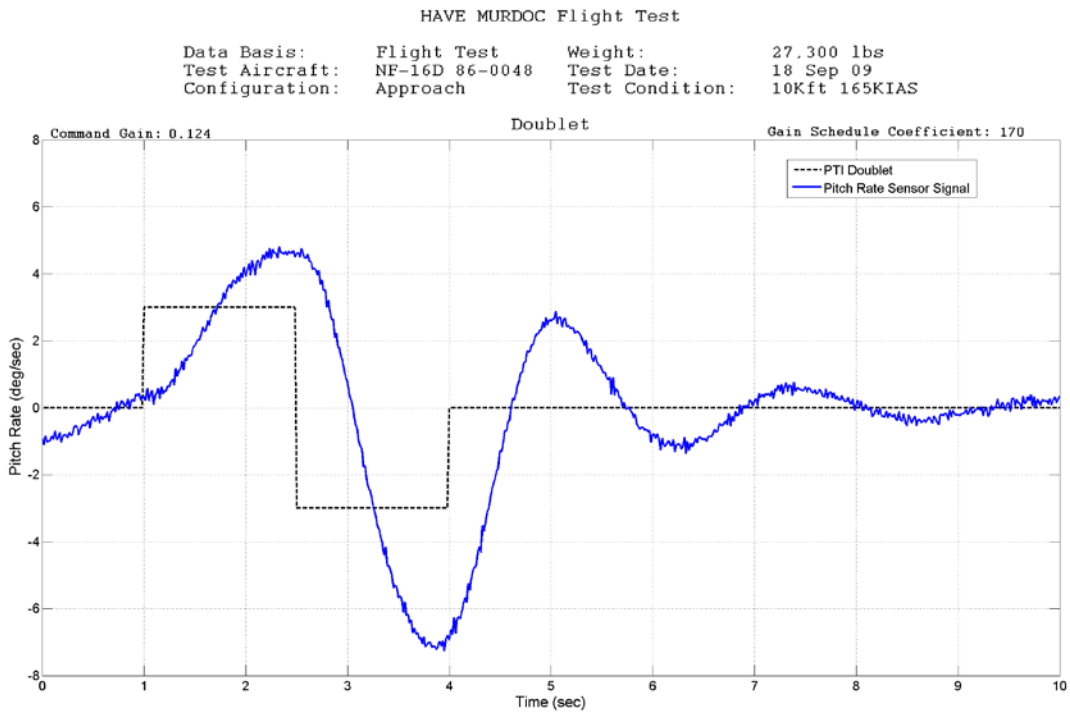

Figure 69: Doublet (10K, 165KIAS)

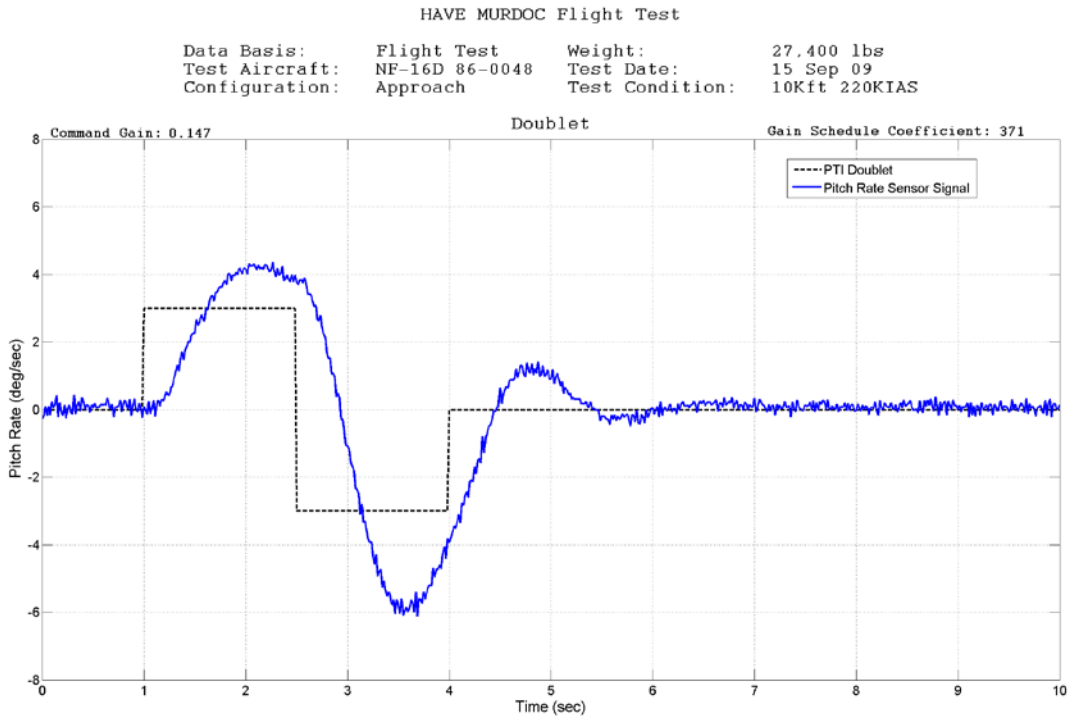

Figure 70: Doublet (10K, 220KIAS)

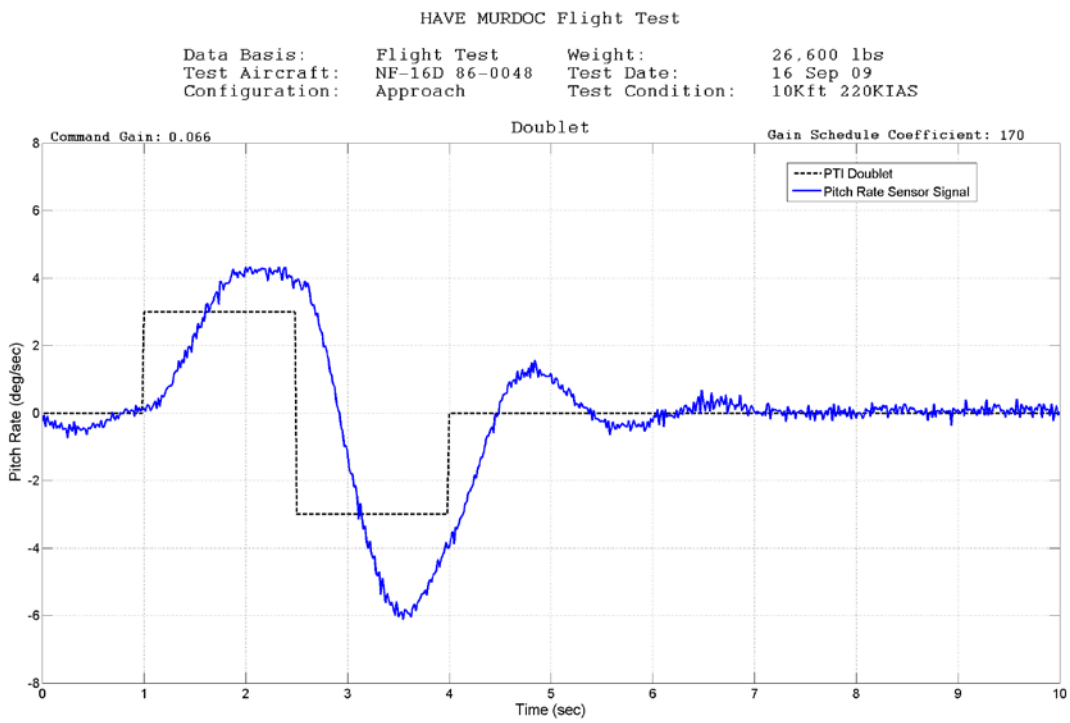

Figure 71: Doublet (10K, 220KIAS)

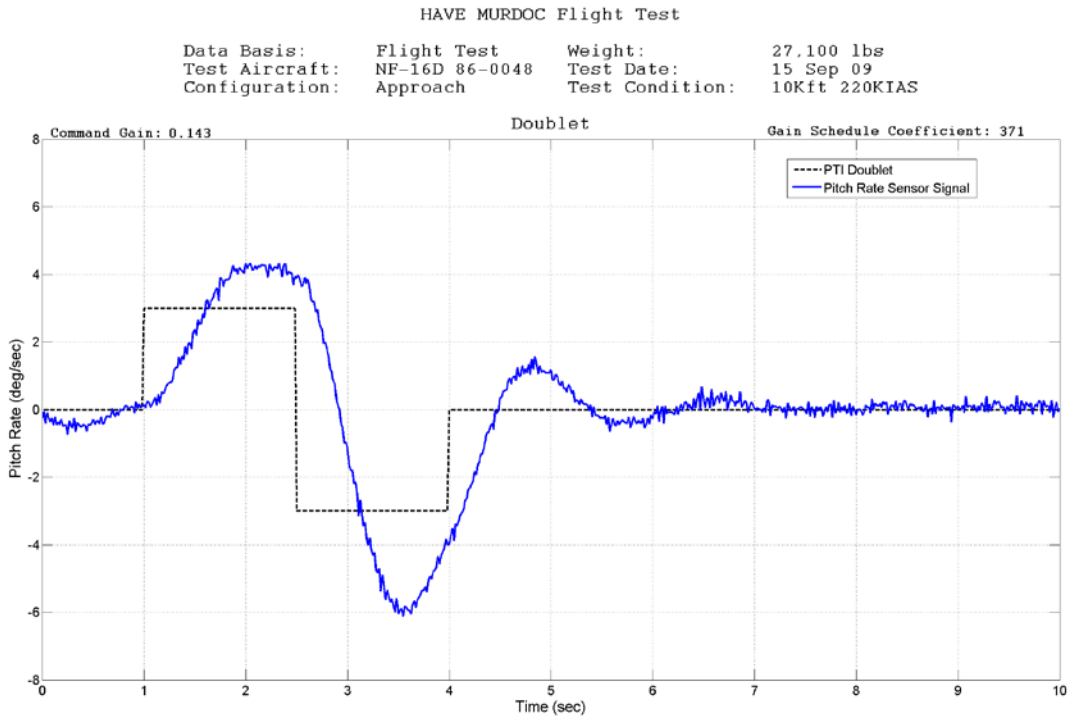

Figure 72: Doublet (10K, 220KIAS)

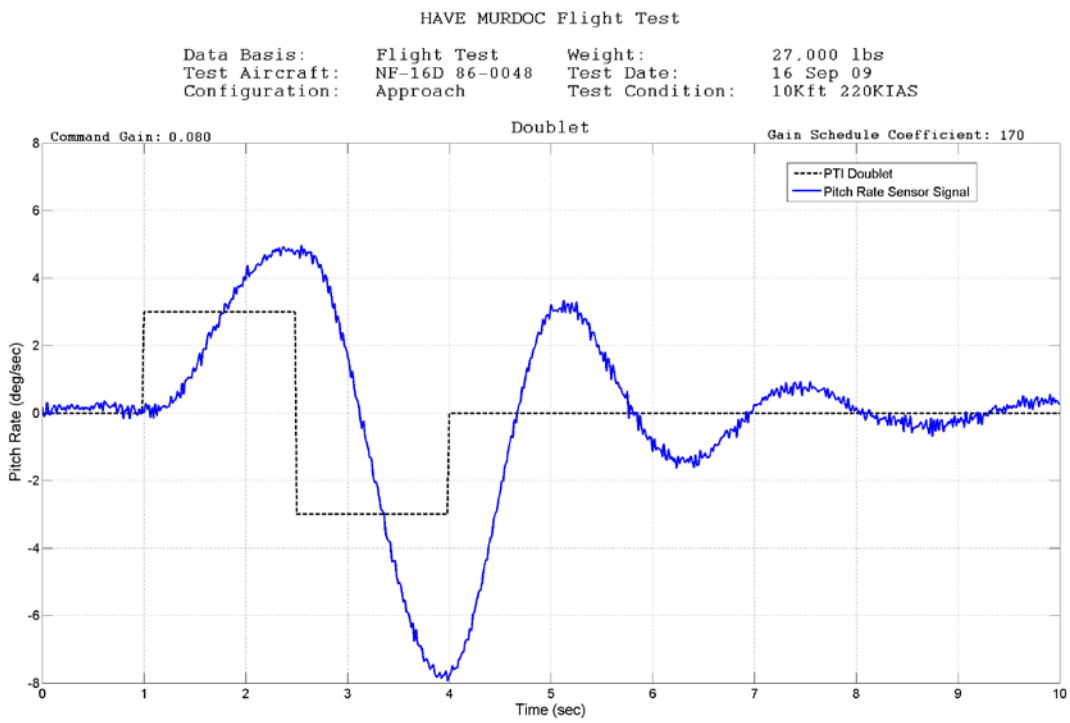

Figure 73: Doublet (10K, 220KIAS)

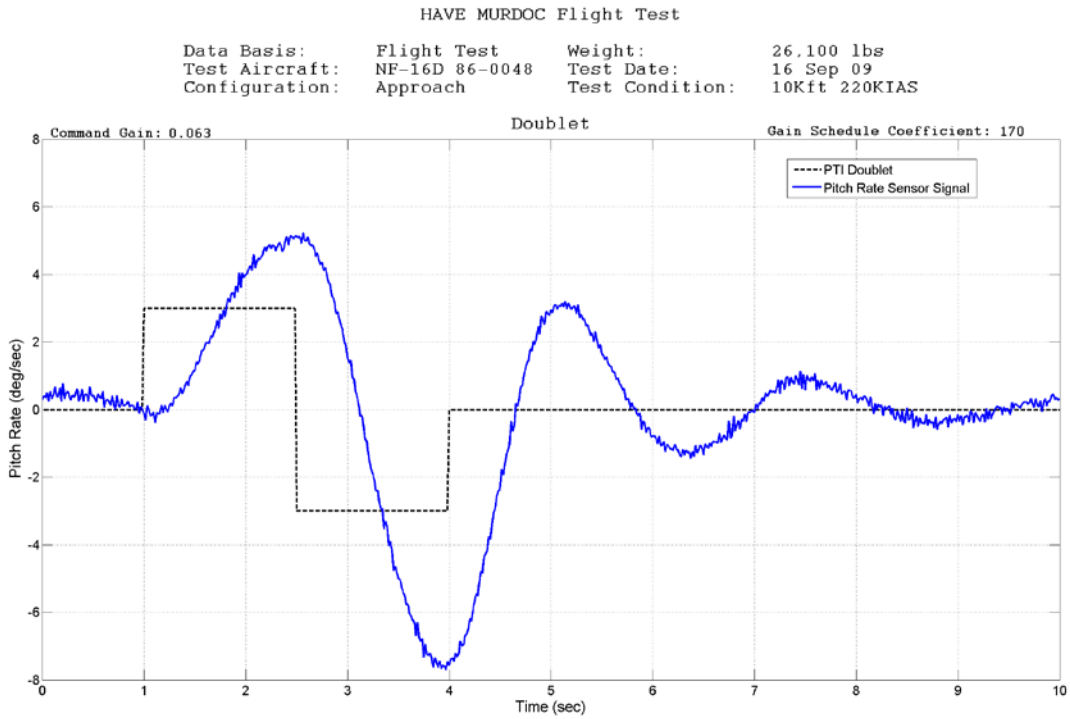

Figure 74: Doublet (10K, 220KIAS)

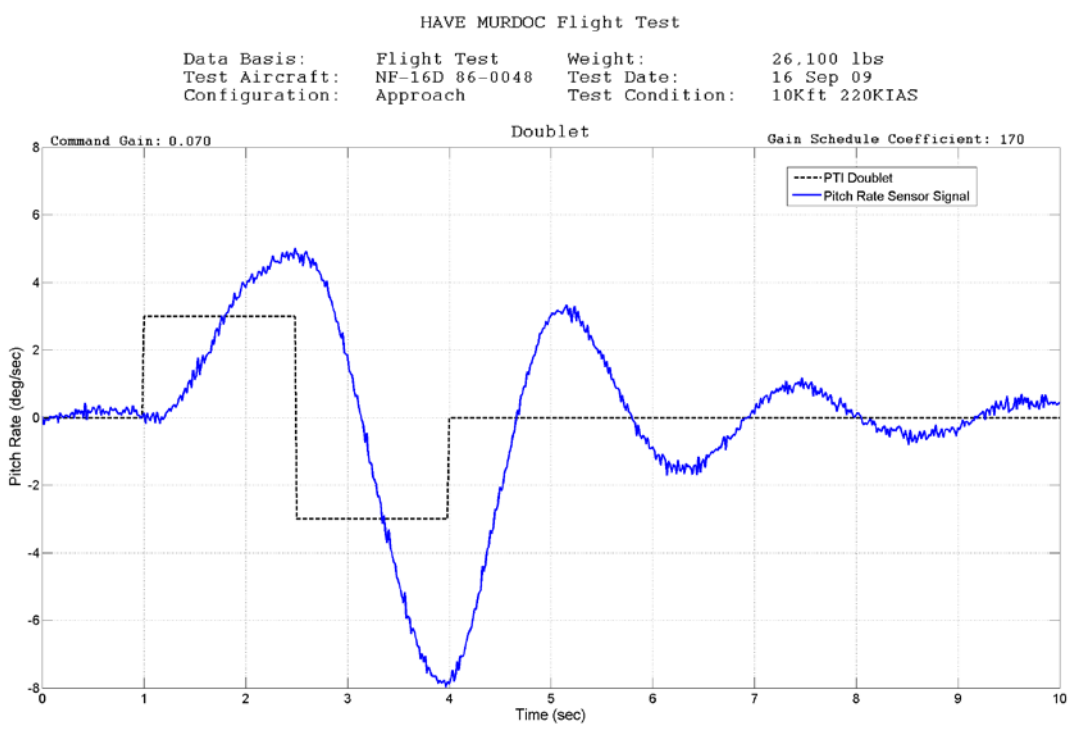

Figure 75: Doublet (10K, 220KIAS)

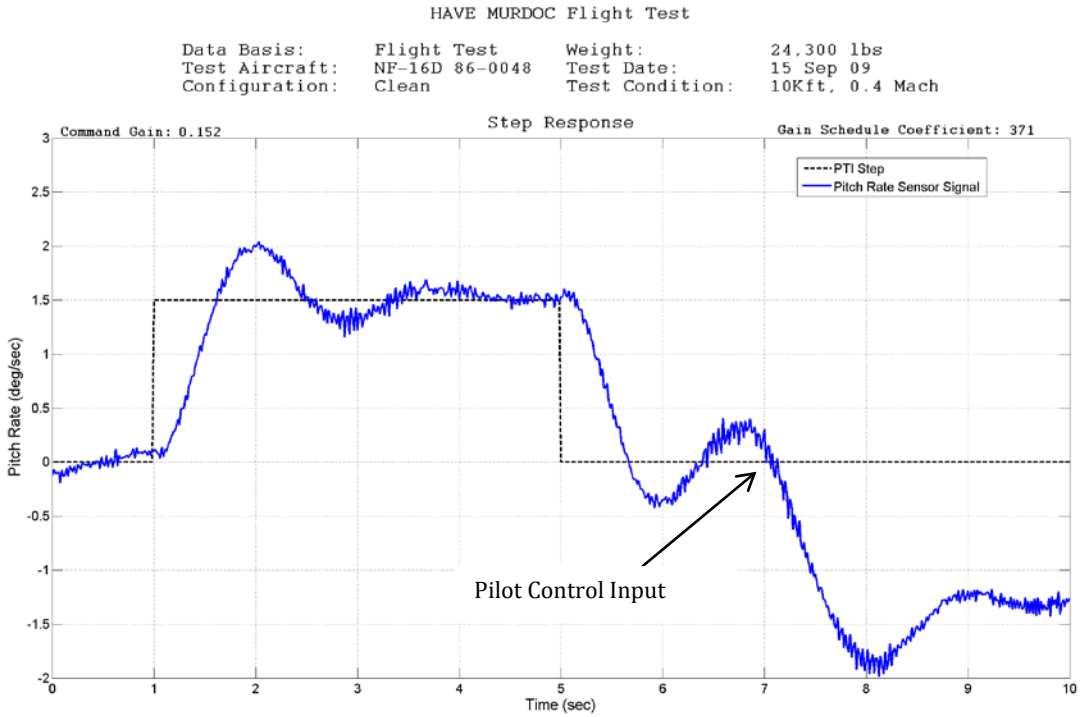

Figure 76: Step (10K, 0.4 Mach)

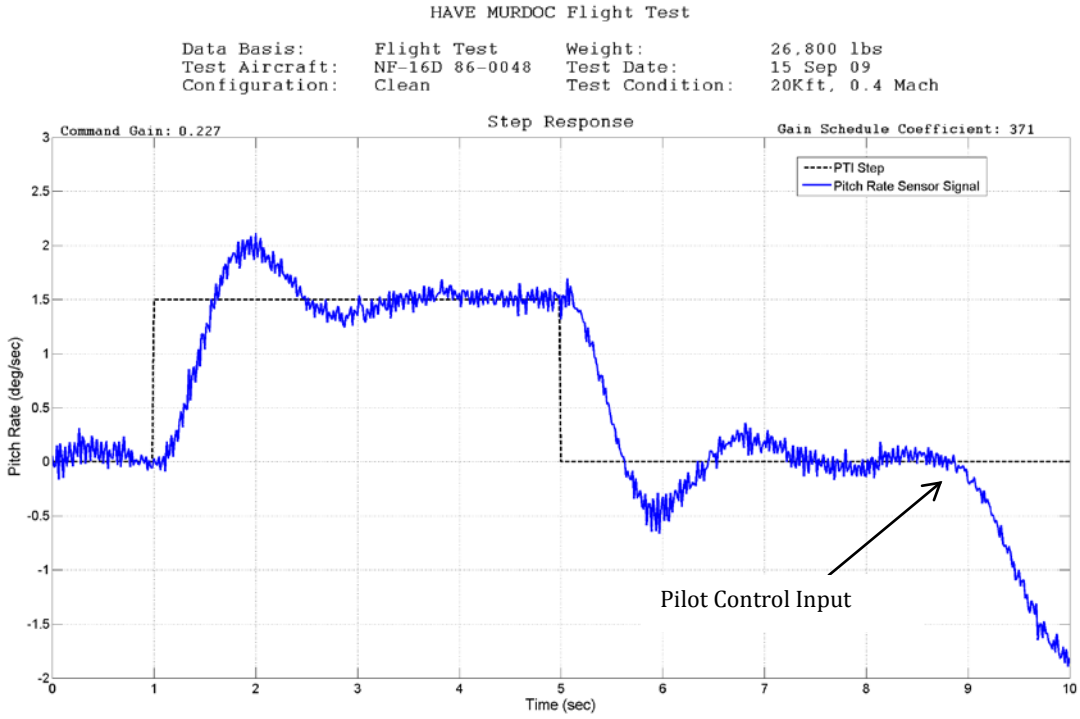

Figure 77: Step (20K, 0.4 Mach)

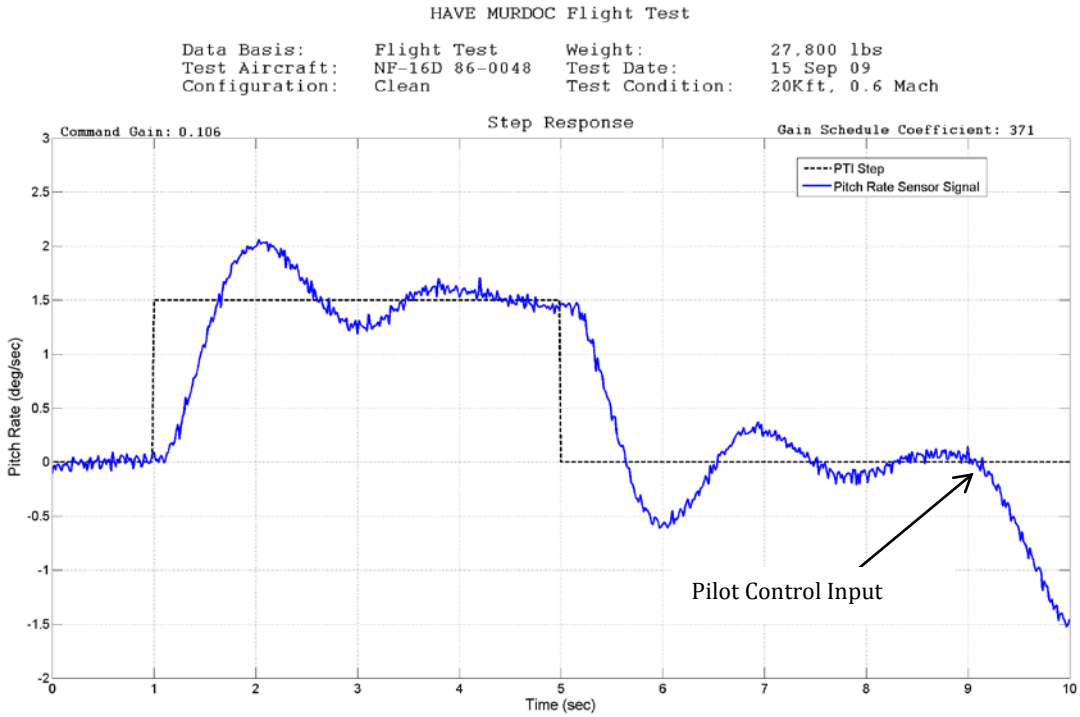

Figure 78: Step (20K, 0.6 Mach)

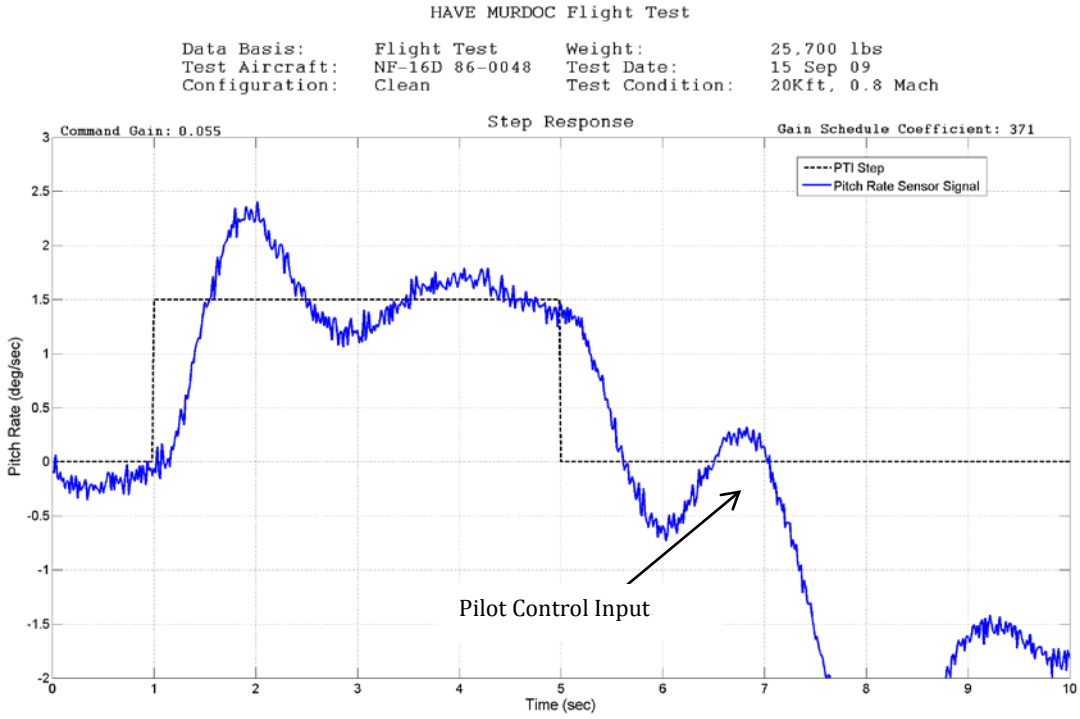

Figure 79: Step (20K, 0.8 Mach)

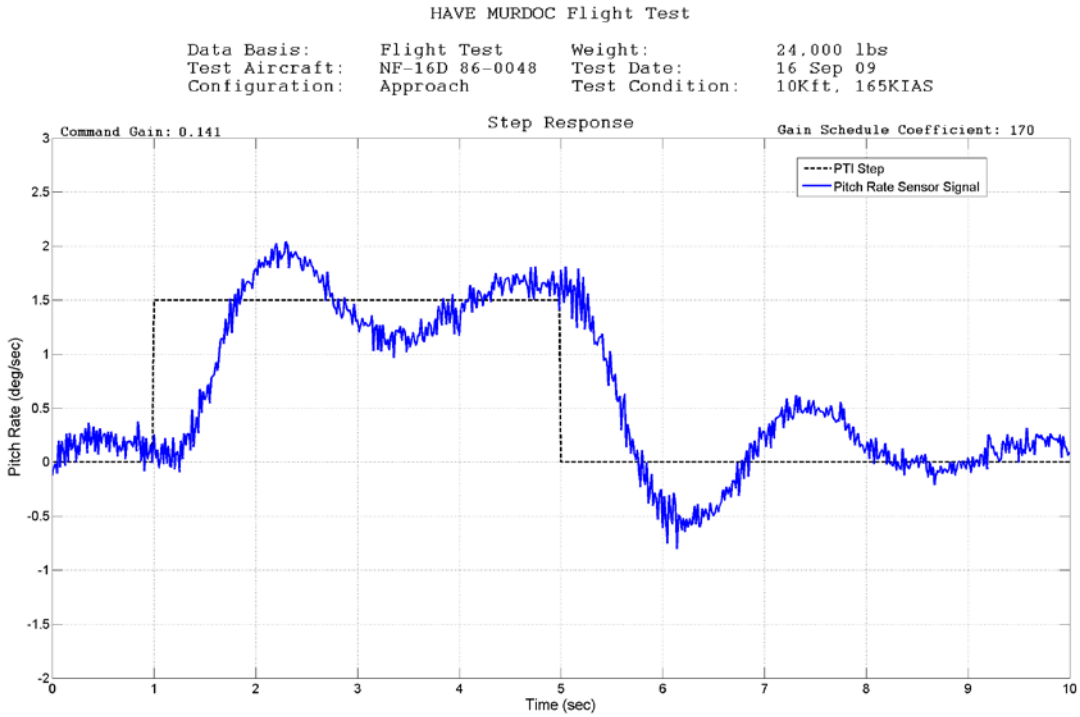

Figure 80: Step (10K, 165KIAS)

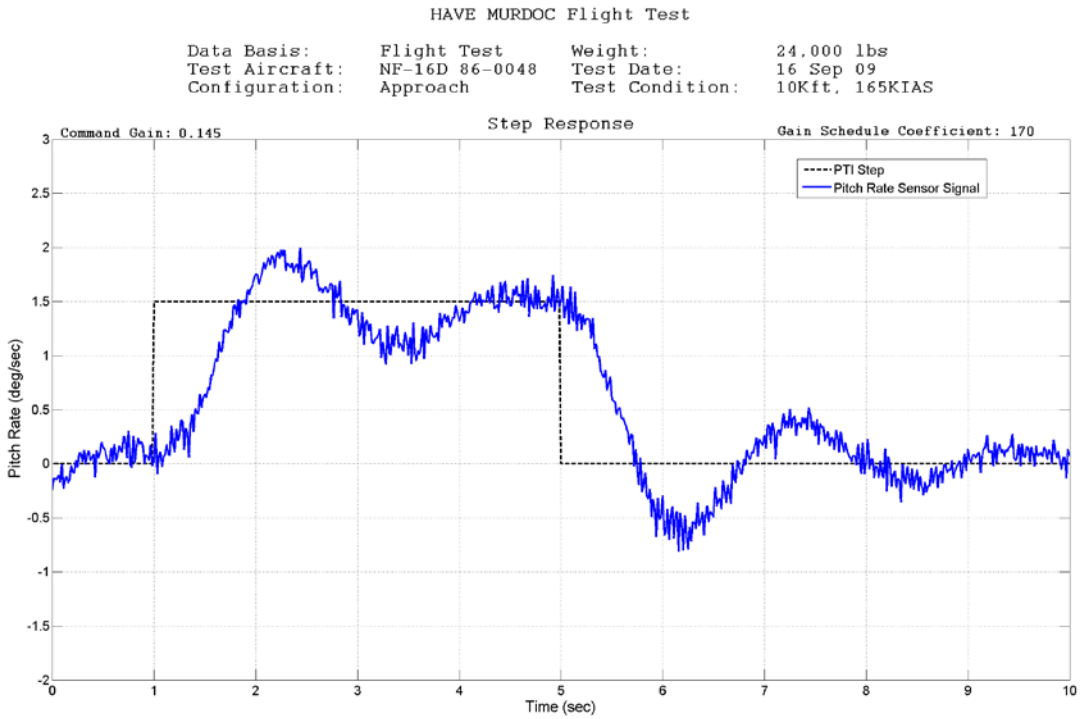

Figure 81: Step (10K, 165KIAS)

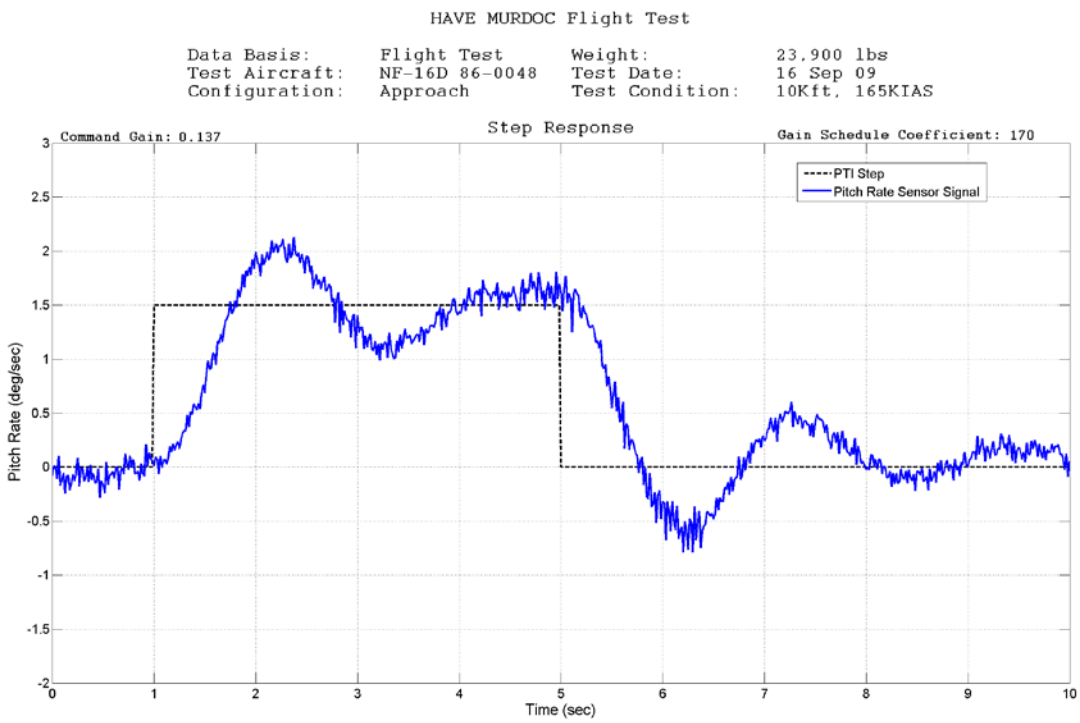

Figure 82: Step (10K, 165KIAS)

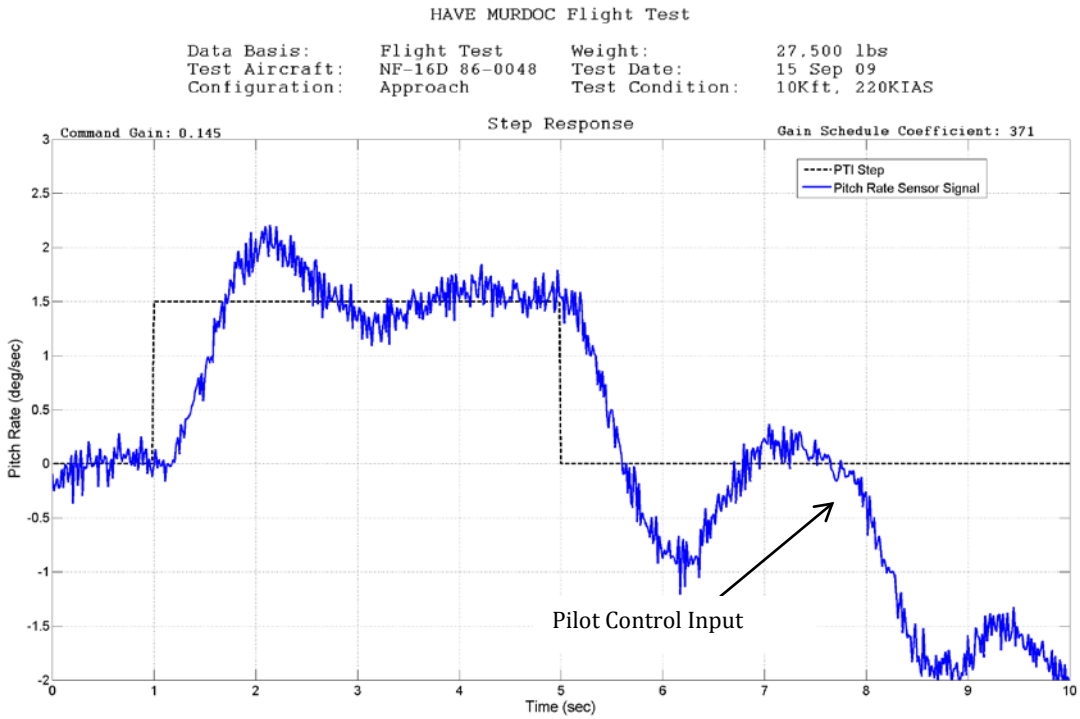

Figure 83: Step (10K, 220KIAS)

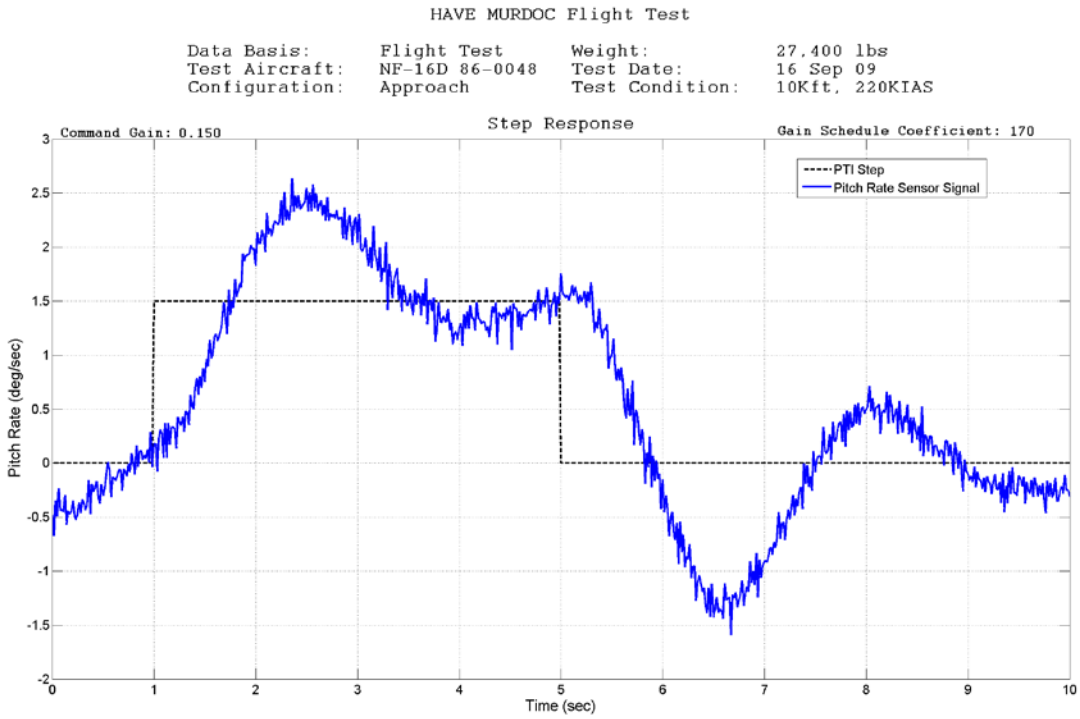

Figure 84: Step (10K, 220KIAS)

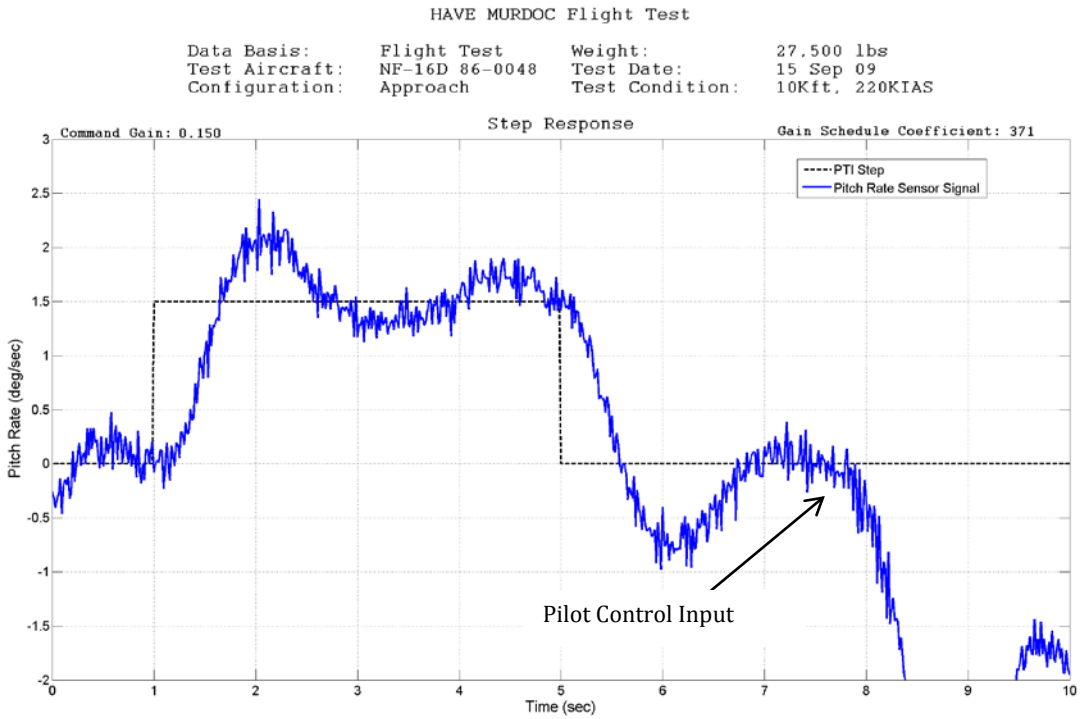

Figure 85: Step (10K, 220KIAS)

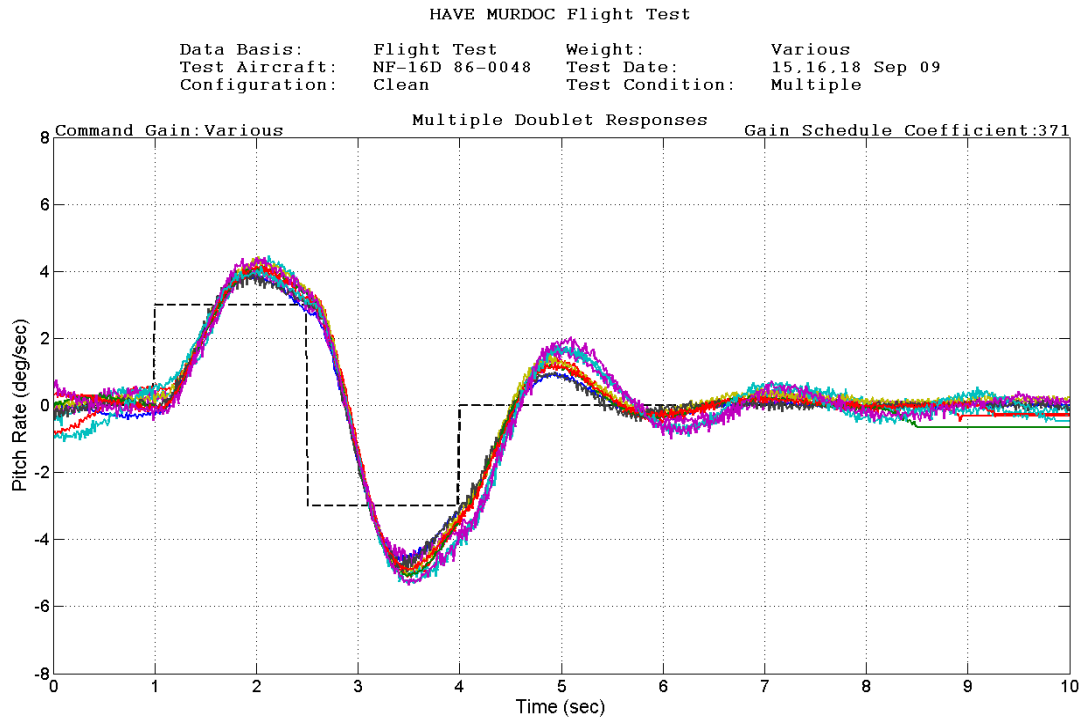

Figure 86: Doublet (Multiple Conditions)

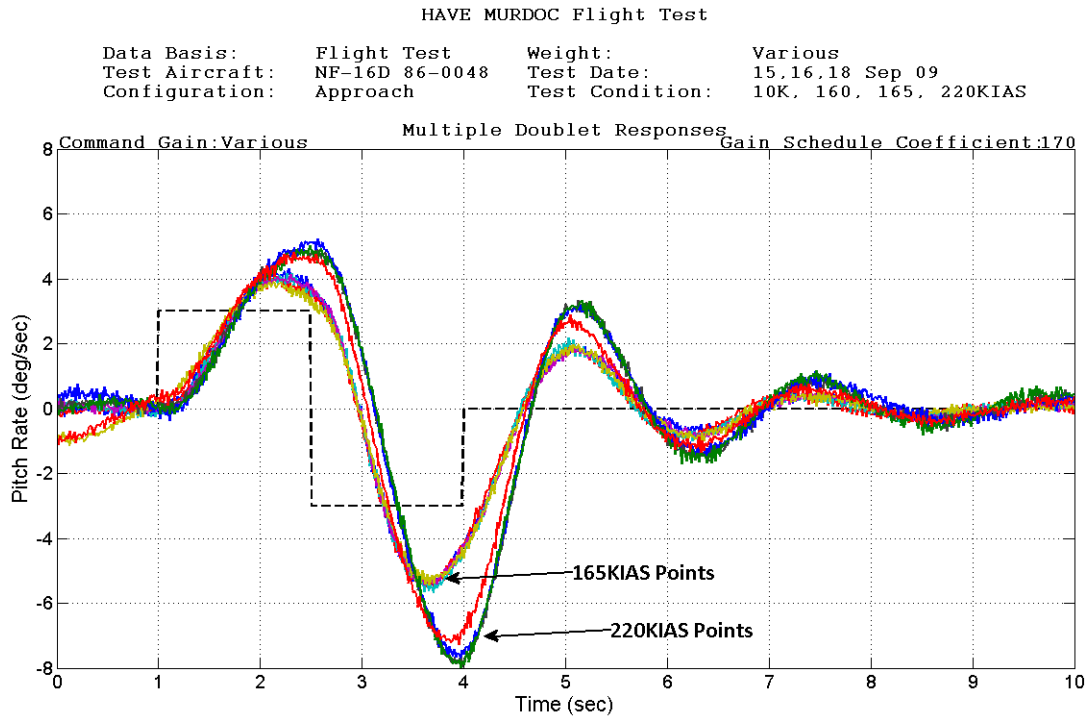

Figure 87: Doublet (Multiple Approach Configuration Plots)

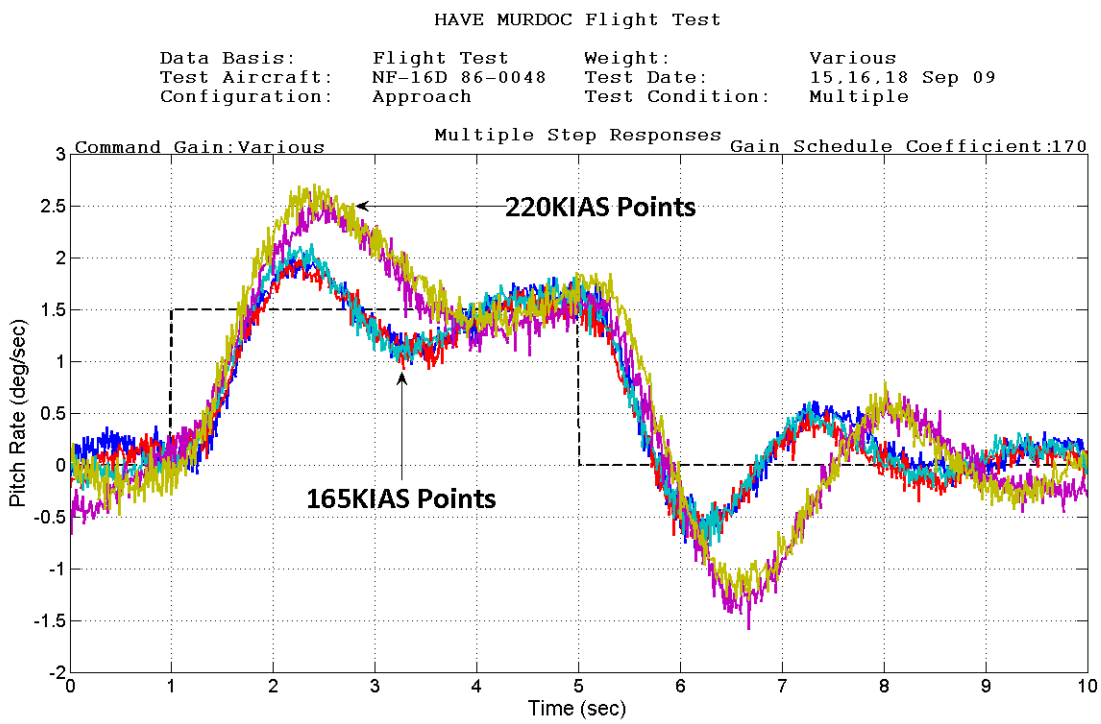

Figure 88: Step (Multiple Approach Configuration Plots)

REPORT DOCUMENTATION PAGE

Form Approved
OMB No. 074-0188

1. REPORT DATE *(DD-MM-YYYY)*	2. REPORT TYPE	3. DATES COVERED *(From – To)*
25-03-2010	Master's Thesis	Sept 2007 – March 2010

TITLE AND SUBTITLE

Disturbance Observer: Design and Flight Test of a Large Envelope Flight Controller

5a. CONTRACT NUMBER

5b. GRANT NUMBER

5c. PROGRAM ELEMENT NUMBER

6. AUTHOR(S)

Rein, Donevan A., Major, USAF

5d. PROJECT NUMBER
NA

5e. TASK NUMBER

5f. WORK UNIT NUMBER

7. PERFORMING ORGANIZATION NAMES(S) AND ADDRESS(S)
Air Force Institute of Technology
Graduate School of Engineering and Management (AFIT/ENY)
2950 Hobson Way, Building 640
WPAFB OH 45433-8865

8. PERFORMING ORGANIZATION REPORT NUMBER

AFIT/GAE/ ENY/10-M18

9. SPONSORING/MONITORING AGENCY NAME(S) AND ADDRESS(ES)
USAF TPS (attn: Bill.Gray@Edwards.af.mil)
220 S Wolfe Ave
Edwards CA 93524

10. SPONSOR/MONITOR'S ACRONYM(S)
USAF/TPS

11. SPONSOR/MONITOR'S REPORT NUMBER(S)

12. DISTRIBUTION/AVAILABILITY STATEMENT
APPROVED FOR PUBLIC RELEASE; DISTRIBUTION UNLIMITED.

13. SUPPLEMENTARY NOTES

14. ABSTRACT

A new flight controller was evaluated through piloted simulation and flight test conducted at the USAF Test Pilot School. The controller, commonly called a disturbance observer, uses inertial sensor feedback routed through a simple control architecture that acts to force the desired response while rejecting sensor noise and atmospheric disturbances. The investigation included both handling qualities testing in the Octonian simulator at the Air Force Research Laboratories Air Vehicle Directorate, and initial flight test conducted as part of a Test Management Project at the USAF TPS. Simulation produced positive results with desired performance throughout a wide flight envelope. In addition, the desired response of the aircraft was easily modified by changing variables within the controller. Flight test was conducted on the Variable-stability In-flight Simulator and Test Aircraft (VISTA). Twelve test sorties totaling 16.4 flight hours were conducted and culminated in multiple landings at Edwards AFB, CA. Time delay inherent in the VISTA resulted in the requirement to gain down the control surface command signal. Sensor noise was amplified and caused a control surface 'buzz." Flying qualities exhibited lower damping and frequency than 'desired' yet were consistent throughout a larger flight envelope. Post flight analysis resulted in the determination of ways to reduce the noise causing the 'buzz' and improve the flying qualities by adjusting the controller's 'desired dynamics.'

15. SUBJECT TERMS
Disturbance Observer, Feedback Flight Control, Flying Qualities Testing, Flight Test, Handling Qualities Testing

16. SECURITY CLASSIFICATION OF: Unclassified			17. LIMITATION OF ABSTRACT	18. NUMBER OF PAGES	19a. NAME OF RESPONSIBLE PERSON
a. REPORT	b. ABSTRACT	c. THIS PAGE			Paul A. Blue, Lt Col, USAF
U	U	U	UU	122	19b. TELEPHONE NUMBER *(Include area code)* paul.blue@stratcom.mil

Standard Form 298 (Rev. 8-98)
Prescribed by ANSI Std. Z39-18